

A Multiagent Socio-hydrologic Framework for Integrated Green Infrastructures and Water Resource Management at Various Spatial Scales

Mengxiang Zhang and Ting Fong May Chui

Department of Civil Engineering, The University of Hong Kong, Hong Kong SAR, China

Correspondence: T. F. M. Chui (maychui@hku.hk)

Abstract. Green infrastructures have been widely used to manage urban stormwater, especially in water-stressed regions. They also pose new challenges to urban and watershed water resources management. This paper focuses on the green infrastructure-induced dynamics of water sharing in a watershed from three spatial scales. A multiagent socio-hydrologic model framework is developed to provide an optimization-simulation method for city-, inter-city-and watershed-scale integrated green infrastructures and water resource management (IGWM) that comprehensively considers the watershed circumstances-, the urban water managers-and the watershed manager-urban water managers interactions. We apply the framework to conduct three simulating experiments in the Upper Mississippi River Basin, the US. Four patterns in city-scale IGWM are classified and two dynamics of cost and equity in inter-city- and watershed-scale IGWM are characterized through various sensitivity, scenario, and comparative analyses. The modeling results could advance our understanding of the role of green infrastructures [and the impact of water policy](#) in urban and watershed water resources management and assist water managers in making associated decisions.

1 Introduction

In recent decades, urban water scarcity worldwide caused by urbanization, population growth, and climate change necessitates new approaches to increase water supply (McDonald et al., 2014; Schewe et al., 2014). Green infrastructures (GIs), which are decentralized nature based measures for rainwater and stormwater capture and recharge, have prevailed in many countries, such as the United States, the United Kingdom, China, and Australia (Dietz, 2007; Coutts et al., 2013; Zhou, 2014; Li et al., 2017). GI systems, as demonstrated by many studies, are effective in increasing water availability and reducing urban flooding, which, to some extent, can supplement the centralized water services provided by grey infrastructure systems (Rozos et al., 2010; Jayasooriya and Ng, 2014). Therefore, ~~more and more cities start to take GIs into account as a component of an urban water system, that is, to generate a hybrid urban water system (HUWS) via combining GIs with the existing grey infrastructures (Daigger and Crawford, 2007; Sapkota et al., 2014). A HUWS includes two inter-dependent subsystems: centralized (i.e., grey infrastructures) and decentralized (i.e., GIs) systems (Dandy et al., 2019). In a centralized system, different types of water supply, storage, treatment and distribution facilities are constructed and maintained to provide various water supply, sanitation and drainage services to urban water users (Sitzenfrei et al., 2013). And, in decentralized systems, multiple GIs with different hydrologic performances, which~~ [an increasing number of cities are incorporating GIs into](#)

25 their urban water systems (Daigger and Crawford, 2007; Sapkota et al., 2014). However, the development of GIs in urban areas can transform socio-hydrologic dynamics within a watershed at various scales (See Fig. 1). At the city scale, the development of GIs, hydrologically, can increase urban water storage capacity (Askarizadeh et al., 2015), thus altering the urban water cycle (Meng, 2022). Socially, GIs provide alternative water sources that enhance water users' choices and reduce water use costs (Zhan and Chui, 2016), gradually changing their water use habits (Kallis, 2010) and shifting the original balance of water supply and demand. At the inter-city scale, the benefits of GIs can encourage an increase in the proportion of GIs systems in each urban area. The cumulative effect of these systems on the urban water cycle can increase (Palla and Gnecco, 2015), leading to local socio-hydrologic changes in each urban area that gradually affect the distribution of water resources within the watershed. This occurs because multiple urban areas along a river share water resources within the watershed. At the watershed scale, the over-development of GIs driven by self-interest in each urban area can result in an uneven distribution of water resources across the watershed (Glendenning et al., 2012), potentially causing conflicts between urban areas. These conflicts necessitate watershed-level water policies from higher authorities to mitigate. Therefore, the GIs-driven socio-hydrologic dynamics at various scales pose a series of challenges to urban and watershed water management. These challenges are managed by multiple interactive decision-makers with individual goals at different authority levels: Urban Water Manager (UWM), who is responsible for managing and maintaining the urban water system cost-effectively, and Watershed Managers (WM), who is responsible for ensuring equitable water resource distribution across the watershed through policy-setting. To simulate these GIs-driven socio-hydrologic dynamics at various scales and optimize the behavior of relevant decision-makers at different authority levels, it is essential to develop new water management frameworks. These frameworks should incorporate GIs development, rainfall utilization, and water resources management. This approach, termed Integrated GIs and Water Resources Management (IGWM), should be applied at various scales.

45 A city-scale IGWM framework involves the integration of urban land use and water management strategies, specifically focusing on decisions related to GIs construction and water supply portfolio choices. UWMs must plan the construction of diverse GIs with varying hydrologic performances within urban areas. These infrastructures should be designed to collect and store stormwater, thereby supplementing the urban water supply with stormwater resources. In general, GIs are divided into two groups depending on the desired flow regime; retention- and infiltration-based GIs (Fletcher et al., 2013); ~~are built in an urban area to manage rainwater and stormwater.~~ To be specific, the retention-based GIs, such as green roofs, cisterns, and rain barrels, can retain stormwater, which can be directly used for non-potable water uses, or with filtration and disinfection for potable water uses (McArdle et al., 2011). Furthermore, the infiltration-based GIs, e.g., rain gardens, porous pavements, and wetlands, can restore some aspects of pre-development flow regimes in receiving water through the recharging of subsurface flows and groundwater, which can be indirectly used by groundwater abstraction (Endreny and Collins, 2009). ~~In general, such a HUWS generally makes urban hydrologic regimes, water supply and demand more complicated (Sapkota et al., 2014; Goonrey et al., 2009), which poses a series of challenges to urban water management and watershed development. For example, such an increased complexity induced by HUWSs may lead to the failures of conventional water management approaches that cope with the issues of grey and green infrastructure systems separately (Poustie et al., 2015). To manage and operate a HUWS scientifically, therefore, it is necessary for an urban water manager (UWM) to develop new~~

60 urban water management frameworks considering GIs development and rainfall utilization, that is, integrated GIs and water resources management (IGWM) at a city scale.

For a city-scale IGWM framework, it is in fact a coupling urban land and water management regime, which refers to GIseconstruction decisions and water supply portfolios choices. Specifically, a UWM needs to supply water extracted from rivers and aquifers via grey infrastructure systems to satisfy ~~Meanwhile, It also needs to must determine optimal water supply~~ portfolios from both grey infrastructure systems, such as rivers and aquifers (Sitzenfrei et al., 2013), and from constructed GIs, including rainwater and stormwater harvesting systems, to meet various water demands ~~Meanwhile, it also plans to construct GI systems to collect, store and use rainwater resources to supplement (See Fig. 1 A). The increased complexity introduced by GIs development and the use of rainwater in the urban water supply. The whole process of a city-scale IGWM is interactive because a HUWS is a human-environment system (Sapkota et al., 2014). On the one hand, various external environmental factors , such as hydroclimatic, geographic, and socioeconomic conditions, can affect the system may render conventional urban water management approaches inadequate (Poustie et al., 2015) due to the involvement of more external socio-hydrologic factors in IGWM decision-making of IGWM~~. For example, the magnitude and frequency of upstream inflow and precipitation directly ~~determine the available amounts influence the availability~~ of surface water and stormwater ~~to a city; for an urban area. Additionally, the socioeconomic development level of a city-an urban area (e.g., residents' housing types and~~ water use habits) can ~~influence selections of affect the selection of GIs~~ types, sizes, and locations of GIs. IGWM decisions made by a UWM, on the other hand, can also change external socio-hydrologic circumstances in turn. Hydrologically, developing GIs within a urban area can increase the infiltration rate and rainwater harvesting capacity of the relevant land, which enables a city to retain and detain more water during a rainfall event, thereby changing (Chen et al., 2019). Therefore, it is crucial for a city-scale IGWM framework to address how to configure water resources drawn from grey infrastructure (i.e., surface water and groundwater) and from GIs (i.e., rainwater and stormwater), as well as to develop relevant plans for GIs construction. This approach aims to optimize the use of limited water supplies while minimizing costs.

At the inter-city scale, an IGWM framework must consider the cumulative effects of expanding GIs within urban areas. The increased rainwater storage capacity, enhanced groundwater recharge (Zhang and Chui, 2019), and elevated evapotranspiration (Ebrahimian et al., 2019) resulting from GIs development can significantly alter the urban water cycle. ~~Socially, alternative water sources driven by GIs enrich water users' choices and gradually change their water use habits (Kallis, 2010), which tips the original water supply and demand balance.~~

Besides, there are generally ~~Consequently, city-scale IGWM decisions made by UWMs can impact the broader hydrologic dynamics. In a watershed, multiple urban areas along a river and they typically share water resources within a watershed, all of which hope to access enough along a river, each striving to secure sufficient and affordable water for their maintenance and~~ development ~~In that watershed, the changes needs. The modifications~~ in the urban water cycle induced by a city-scale IGWM may shift ~~decisions can alter the inflow and outflow patterns of an urban area. The effects of such a regional hydrologic shift may expand gradually These regional hydrologic shifts can gradually propagate throughout the watershed because the river network closely connects urban areas. Since the relevant stakeholders share the common land and water resources due to the interconnected nature of the river network. Therefore, IGWM decisions made by an upstream UWM can influence those made~~

95 by downstream UWMs, highlighting the interdependence of urban water management within a watershed, ~~the decision-making of IGWM in an urban area might affect that in other areas.~~ Some studies demonstrated that over-development of GIs might decrease the river flow to downstream areas (Glendenning et al., 2012), which may be detrimental to stream health (Fletcher et al., 2007). In comparison, others showed that expansion of GIs might, to some extent, decline the variability of river flow, which is beneficial to downstream water supply (Golden and Hoghooghi, 2018). Under the circumstances, all UWM within a watershed make their own IGWM decisions rationally, not only depending on ~~natural hydrologic conditions~~ urban hydrologic states but also anthropogenic activities from upstream urban areas. ~~That is, the behavior of an upstream UWM can affect that of the subsequent downstream UWM because the water is transported along the river. Such~~ (See Fig. 1 B). Therefore, the interactive behavior among UWMs for IGWM will be bound together to form forms a unique sequential ~~multi-players interaction at an multi-player interaction at the~~ inter-city scale, ~~which can be characterized as the~~. This can be simulated by considering the hydrologic state of the first upstream urban area after implementing its own IGWM decisions, followed by the hydrologic state of the adjacent downstream urban area after its own IGWM decisions. These states transition sequentially along the river. This state transition process exhibits the Markov property (Frydenberg, 1990) ~~the future hydrologic regime in a~~ where the hydrologic state of an urban area depends on only on the hydrologic state of the only the current hydrologic regime partly influenced by the decision-makings of city-scale IGWM in the upstream area and that adjacent upstream area after making its IGWM decisions and the decisions of the urban area itself. ~~It~~ Such interactions might lead to unexpected watershed-level performance. ~~So~~ Therefore, it is ~~worthwhile to extend the scope of IGWM to a watershed level and explore the interactions among urban areas driven by multiple~~ essential for an inter-city scale IGWM framework to investigate the socio-hydrologic dynamics of interactions among multiple urban areas in relation to their city-scale IGWM decisions, ~~i.e., IGWM at an inter-city scale.~~

115 Understanding IGWM interactions at an inter-city scale is just one side of the picture, and the other side is how watershed water policies influence them. Since the interactive behavior of IGWM among multiple UWMs may significantly alter hydrological regimes and social circumstances in the entire watershed, it might offer a difficulty for a watershed manager (WM) who ~~continues to use traditional water policy approaches that generally ignore such interactions among~~ In general, optimal decision-making for city-scale IGWM can reduce the cost of accessing water resources for individual urban areas. ~~In general, an unordered IGWM at an~~ However, at the inter-city scale, uncoordinated IGWM efforts might lead to ~~an inequitable, costly, and unsustainable sharing of water resources in~~ inequitable and unsustainable water resource distribution within a watershed (Müller et al., 2017), potentially causing conflicts between upstream and downstream urban areas. For a watershed-scale IGWM framework, a WM must implement policies, such as streamflow penalty strategies, to regulate the decision-making of UWMs and achieve equitable water distribution within the watershed. A WM needs to prescribe various policies and strategies to regulate all

125 UWMs' decision-makings of city-scale IGWM to achieve set targets for watershed environments' health, stabilization, and sustainability. In the context, a In this context, the WM and multiple UWMs will construct form a bi-level system, ~~which follows a specific~~ based on their respective authority levels, following hierarchical decision rules for the leader ~~and the multiple followers. That is~~ (WM) and the followers (UWMs). Specifically, the WM at the upper level first set a water policy sets water policies at the watershed level, and ~~then the multiple UWMs at the lower level make their own~~ the UWMs subsequently make

130 ~~their~~ city-scale IGWM decisions with full knowledge of ~~the policy set by the WM ; the WM also can adjust its own policy~~
~~prescription these policies.~~ The WM can also adjust its policy prescriptions based on the rational ~~UWMs' reactions, responses~~
~~of the UWMs~~ (See Fig. 1 C). In economic theory, this hierarchical ~~interactive process between a WM and multiple UWMs~~
~~interaction process~~ is described as a Stackelberg game (Simaan and Cruz, 1973). ~~Hence, it is also important to introduce a~~
~~WM into the multi-UWMs system for~~ Given that uncoordinated interactions among multiple UWMs for IGWM can result in
135 inequitable water resource distribution within the entire watershed, a WM may face challenges when using traditional water
policy approaches that generally overlook such interactions. Therefore, it is crucial for a watershed-scale IGWM and discuss the
effect of various framework to consider the impact of water policies on the ~~dynamics of multiple city-scale IGWM decisions,~~
~~namely, IGWM at a watershed scale~~ socio-hydrologic dynamics of interactions among multiple urban areas.

Currently, there are rich studies related to city-scale IGWM, most of which focused on studying the following three critical
140 aspects: 1) integrating water management framework ~~for HUWS~~ with GIs, 2) assessing rainwater potential 3) modeling urban
water cycle of a ~~HUWS~~ urban water system incorporating GIs. The first aspect involves building an integrated water manage-
ment framework that combines conventional water supply systems with stormwater/rainwater harvesting schemes (Daigger,
2009). To determine the appropriate stormwater harvesting scheme option under different settings, Goonrey et al. (2009) de-
veloped a decision-making framework. To address on-site and catchment urban surface water issues, Ellis (2013) introduced
145 sustainable drainage systems into a GI framework. Dandy et al. (2019) presented an integrated framework to help UWMs
select and evaluate stormwater harvesting systems. The second aspect of the studies is mainly focused on the quantitative eval-
uation of rainwater/stormwater resources supply options in various urban areas. Kim et al. (2022) investigated the impact of
water management strategies, such as rainwater harvesting, on urban water demand in Filton Airfield, UK, using water demand
profiles and urban water cycle simulations. Kim et al. (2022) developed a framework to assess a variety of centralized and
150 decentralized water supply options, including rainwater harvesting and groundwater extraction via private wells, for meeting
urban water demand in southern India. Souto et al. (2022) studied the effects of a rainwater harvesting system in reducing the
demand for drinking water in the city of Goiânia by using two water balance models. Researches addressing the third aspect
has focused on developing models to simulate urban hydrologic regimes within a ~~HUWS~~ urban water system incorporating
GIs, such as the Aquacycle (Mitchell et al., 2001), Urban Cycle (Hardy et al., 2005), City Water Balance (Last, 2011), Ur-
155 banBEATS (Bach et al., 2015) and SUWMBA (Moravej et al., 2021). These models, to some extent, allow users to improve
their understanding of the impacts of various GIs options at different scales and to assess the comprehensive performance of
~~HUWSs~~ the urban water systems across the entire urban water cycle. Although there is a rich literature addressing issues of
city-scale IGWM, there is very little work that comprehensively considers the selection of centralized and decentralized water
supply options, as well as the decision-making associated with GIs construction plans within a ~~HUWS~~ urban water system in
160 changing environments. This has become a key issue of concern for UWMs. Therefore, more in-depth studies are needed to
develop a decision-making framework that can assist authorities in making effective decisions about IGWM at a city scale.

Besides, several studies associated with inter-city scale IGWM have attempted to investigate the issues of interactions be-
tween water users in a shared water resources system, especially in irrigation systems (Barreteau and Abrami, 2007; Berger
et al., 2007). To better understand the effects of water users or managers' behaviors and their interactions in a watershed-scale

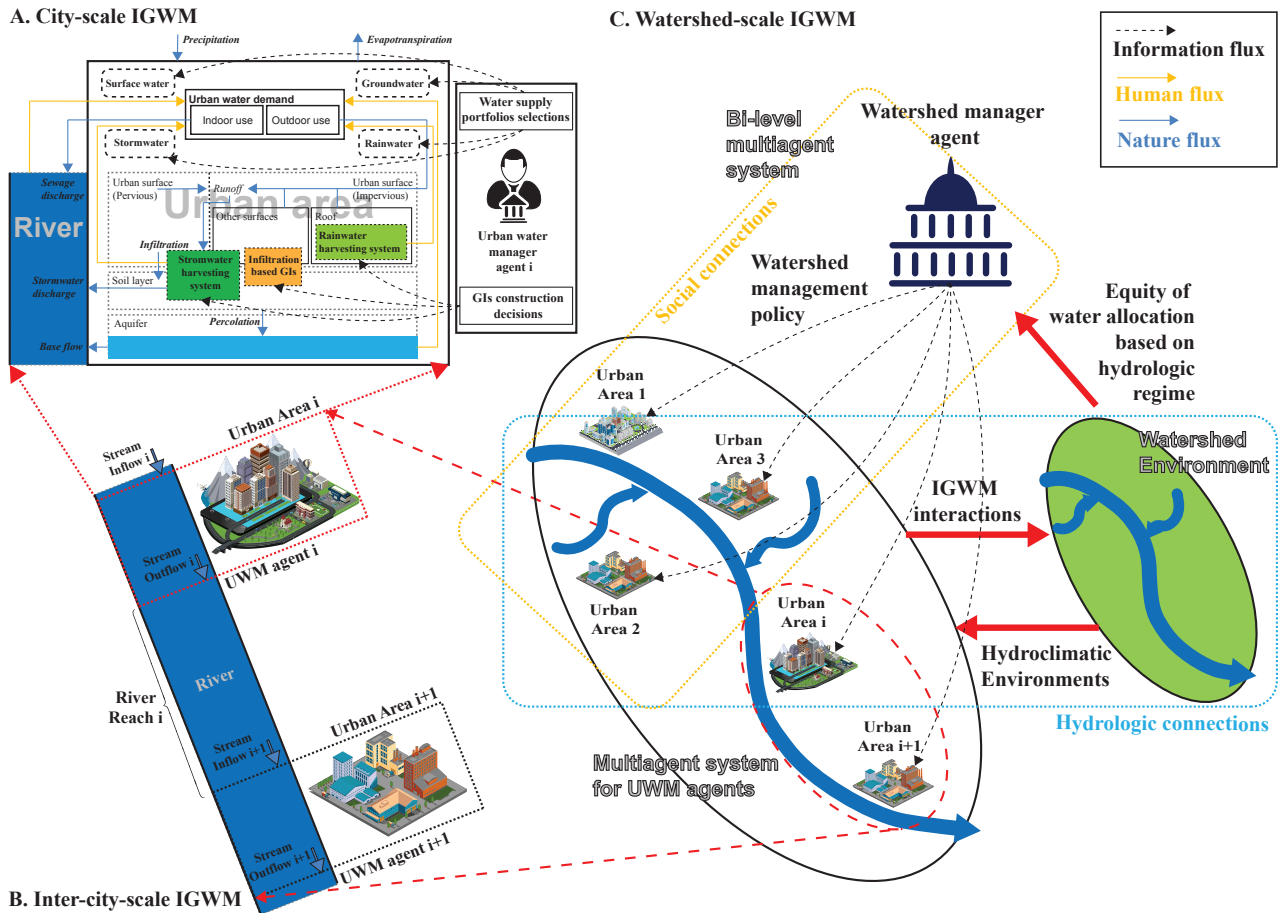


Figure 1. Schematic diagram of IGWM at three spatial scales. A) At the city scale, UWMs must consider the simultaneous construction of GIs and water supply portfolios to meet urban water demands cost-effectively. B) At the inter-city scale, IGWM decisions made in upstream areas can influence downstream areas due to hydrologic connections. C) At the watershed scale, a WM needs to establish water policies that regulate UWM decision-making regarding IGWM, based on socio-hydrologic interactions.

Note: UWM represents Urban Water Manager, GIs represents Green Infrastructures, IGWM represents Integrated GIs and Water Resources Management, and WM represents Watershed Manager.

165 water resource system, a diverse range of multi-agent systems (MAS) have been constructed and used studies have utilized agent-based models to simulate the actions and interactions of autonomous water users or managers within a water resources environment (Banks, 2002). These models are part of a broader computational framework known as multiagent systems, which consist of multiple interacting autonomous agents. The aim is to assess the collective effects of these interactions on the overall system (Barreteau and Abrami, 2007). Berglund (2015) reviewed an emerging area of research within water resources management that uses agent-based models and MAS multiagent systems to simulate the water resources allocation, and to predict the performance of infrastructure design. Yang et al. (2009) built a MAS, which includes multiple distributed land and water users

170

~~within a watershed, to mimic interaction schemes among water users in real-world watershed management problems.~~ Giuliani and Castelletti (2013) explored the effect of different levels of cooperation and information exchange among water users on the upstream-downstream water conflict in a large-scale water resources system through using a well-designed ~~MAS~~multiagent system. Some studies have also focused on interactions between water users and the watershed environment, coupling ~~MAS~~multiagent systems with watershed hydrologic models (He, 2019; Du et al., 2020). ~~Reeves and Zellner (2010) integrated an~~Montalto et al. (2013) constructed an agent-based ~~land-use model with MODFLOW to analyze the complexity inherent in~~land-use change and its effect on groundwater resources. ~~Montalto et al. (2013) constructed a agent-based~~ framework to analyze the effect of different spatiotemporal distributions of GIs determined by numerous household decision-makers on urban water cycle in South Philadelphia. ~~Du et al. (2020) coupled a rule-based~~Hung and Yang (2021) developed a reinforcement learning agent-based ~~model with a distributed hydrologic model, i.e., GSFLOW, to simulate spatial and temporal dynamics of~~human-hydrological interactions. ~~framework in which agricultural water users act as agents that learn and adjust their water demands based on interactions with the water systems.~~ Similarly, Motlaghzadeh et al. (2023) employed a three-game model to construct a hierarchical multi-agent decision-making framework for managing water and environmental resources under ~~the uncertain conditions of climate change and complex agent characteristics.~~ Additionally, Khorshidi et al. (2024) proposed ~~an agent-based model framework to evaluate the suitability of transitioning to modernized surface irrigation systems from~~traditional practices. While these studies can inspire this study, there are some common limitations for modeling IGWM at an inter-city scale. Firstly, the studies of interactions between water users tend to focus on agricultural regions rather than urban regions, and do not address the issues of interaction between urban areas driven by developing GIs and using rainwater sources within a watershed. Secondly, rule-based models have been widely used to simulate the behavior of water users or managers in a water resource system, but are unable to describe the complex decision processes of city-scale IGWM due to over-simplified decision rules.

In the field of research within IGWM at a watershed scale, several studies have focused on the evaluation or design of water policies to manage interactions or conflicts among multiple water users within a watershed via using various ~~MAS~~multiagent systems (Berger and Ringler, 2002; Akhbari and Grigg, 2013; Lin et al., 2020). For instance, Kock (2008) developed and applied two agent-based models of society and hydrology to test relations between different water policies in a watershed and the level of water conflict in that watershed. Kanta and Zechman (2014) built a ~~MAS~~multiagent system framework by integrating a urban water demand and a supply model and considering water users and managers as agents. A wide set of water policies, such as conservation strategies and interbasin transfer strategies, set by the water managers and the associated responses from the water users were simulated via using the framework. Darbandsari et al. (2020) proposed a new conflict resolution model to assess different water management policies through simulating the interactions of all water users' behaviors. A Stackelberg game theory-based model was used to describe the leader-follower interactions between water users and managers within a basin. Although these previous studies can provide guidance for IGWM at a watershed scale in an exploratory way, there is still a gap in building a sound and flexible watershed policy framework for the design and evaluation of various water strategies to allocate limited water resources to urban areas that develop GIs and use rainwater resources, as well as for the simulation of the complicated responses of water supply and GIs development in each urban area to these strategies.

This paper focuses on ~~integrated GIs and water resources management in a watershed that consists~~ IGWM within a watershed composed of multiple urban areas , which build green infrastructures and use rainwater , that implement GIs and utilize rainwater at three spatial scales .~~For the issue of IGWM at a~~ (See Fig. 1). At the city scale, we examine how ~~a UWM can make the best configuration for centralized (i.e., surface water and groundwater) and decentralized (i.e., rainwater and stormwater) water resources, as well as the relevant plan for GIs construction, in order to make optimal an UWM can optimally configure various water resources extracted from rivers, aquifers, stormwater, and rainwater harvesting systems, alongside planning for GI construction, to maximize the efficient use of limited water supplies with minimal cost; For the issue of IGWM at an~~ while minimizing costs. At the inter-city scale, we ~~also investigate how the behavior of city-scale IGWM determined by the upstream UWMs can affect that of the downstream UWMs in a watershed; Finally, for the issue of IGWM at a~~ investigate the effects of interactions among multiple urban areas on the socio-hydrologic dynamics of the watershed, stemming from their city-scale IGWM decisions. At the watershed scale, we explore how a watershed water policy—, ~~such as a stream-flow penalty strategy —set by WM can influence all UWMs’ behaviors of~~ set by a WM, can influence the behaviors of all UWMs regarding city-scale IGWM and their interactions with each other. ~~Therefore, we build~~ To address these issues, we develop a multiagent socio-hydrologic framework ~~to solve IGWM-related issues mentioned above. To be specific, it includes. Specifically, this framework includes:~~ 1) an agent-based model ~~of urban water manager (ABM-UWM), which is,~~ developed by coupling an ~~economic optimization model and agent-based model for UWM with~~ a hydrologic simulation model, to determine ~~the optimal decision-making of for~~ city-scale IGWM ~~for a UWM~~ in changing watershed settings; 2) a multiagent system ~~for multiple UWMs (MAS-UWM), which is constituted via integrating the above ABM-UWMs, created by integrating the aforementioned agent-based models~~ with a streamflow routing ~~models-model~~ based on the Markov property, to simulate interactions ~~among them~~ in inter-city-scale IGWM , and assess its impact on the ~~whole entire~~ watershed; and 3) a bi-level multiagent system ~~(BL-MAS), which is,~~ constructed by combining the ~~above MAS-UWM multiagent system~~ with an agent-based model ~~of watershed manager (ABM-WM) on account of the for WM based on~~ Stackelberg game theory, to mimic the interactions and ~~feedbacks~~ feedback between a WM and multiple UWMs driven by the implementation of a watershed water policy in watershed-scale IGWM, ~~thereby ultimately~~ designing an optimal watershed strategy. Besides, we also demonstrate our framework to conduct three numerical experiments based on a realistic basin - the Minneapolis-La Crosse section of the Upper Mississippi River, the US. The results obtained from these experiments allow us to characterize and classify the decision-making of city-scale IGWM for a UWM under different circumstances, to analyze the socio-hydrologic ~~dynamic of~~ dynamics of the watershed induced by inter-city-scale IGWM, and to assess the role of a water policy in watershed-scale IGWM.

The outline of this paper is as follows. ~~Section 2 presents a socio-hydrologic model framework which is established to simulate decision-makings of:~~ Section 2 introduces the multiagent model framework used to simulate city-scale IGWM ~~for UWM and decision-making by UWMs and the socio-hydrologic dynamics of inter-city- and watershed-scale IGWM resulting from interactions~~ 1) among UWMs hydrologically, and 2) between the , considering interactions both among UWMs and between UWMs and the WM ~~institutionally. In Section 3, we present. Section 3 details~~ three simulation experiments based on ~~a case of~~ the Upper Mississippi River basin to generate understanding and insight to the provide insights into IGWM at three spatial scales. ~~In Sections 4 we discuss and analyze~~ Section 4 discusses and analyzes the results of the simulation experiments.

The features of optimum IGWM for UWM are identified via sensitivity analysis, and the characteristics of UWM-UWM. It identifies optimal IGWM features for UWMs through sensitivity analysis and UWM-WM interactions in inter-city and watershed-scale IGWM are assessed and summarized by scenarios assesses interactions among multiple UWMs and the WM at inter-city and watershed scales using scenario and comparative analysis, respectively. Section 5 ends this. Section 5 concludes the paper with a conclusion summary of findings, limitations, and proposals for future research.

2 Methodology

This section proposes a multiagent socio-hydrologic framework for solving the issues mentioned above of the IGWM at three spatial scales. The framework includes

2.1 Overview of the multiagent system architecture

The framework considers UWMs and WMs within the watershed as individual agents. It includes: 1) ~~two~~ Two agent-based models (i.e., for urban water and watershed manager agents) to have a more realistic representation of city- and watershed-scale IGWM decision behavior, separately; to realistically represent UWM and WM decision-making processes. 2) ~~two multiagent systems to simulate the two types interactions (i.e., UWM-UWM)~~ Two hydrologic models: the Urban Water Balance Simulation Model (UWB-SM) and UWM-WM interactions) in inter-city and watershed-scale IGWM based on the geographic and social connections. Fig. 1 shows a watershed system for IGWM the Muskingum-Cunge routing model. The UWB-SM describes the dynamics of urban water balance induced by city-scale IGWM decisions, while the Muskingum-Cunge routing model simulates changes in streamflow in river reaches connecting adjacent urban areas. By integrating these components, we build an agent-based model and two multiagent systems to simulate GI-driven socio-hydrologic dynamics at three spatial scales. In the framework, an for addressing IGWM issues (See Fig. 1). Specifically: 1) An agent-based model for UWM is used to deal with the issue of IGWM at a city scale combines the UWM agent-based model with the UWB-SM to address city-scale IGWM (See Fig. 1 A). 2) A multiagent system for UWMs is used for IGWM at an integrates multiple UWM agent-based models with the Muskingum-Cunge routing models for inter-city scale IGWM (See Fig. 1 B), and a. 3) A bi-level multiagent system is built to simulate the dynamics of IGWM at a watershed scale.

Schematic diagram of IGWM at three spatial scales.

2.2 Agent-based model (ABM) for IGWM at a city scale

combines the multiagent system with the WM agent-based model to simulate watershed-scale IGWM dynamics (See Fig. 1 (A)) illustrates city-scale IGWM activities and resulting changes in urban hydrologic cycles. As shown (C). Detailed introductions to the model components and structure are provided in the following sections.

270 2.1.1 Two agent-based models

Agent-based models for UWM: As illustrated in Fig. 1(A), ~~an UWM needs to consider a UWM must simultaneously consider~~ GI construction and water supply portfolios ~~and GIs construction simultaneously to meet various to meet diverse~~ urban water demands cost-effectively. ~~In the water supply portfolios selection, four types of water sources, which are classified by water intake locations, can be chosen to withdraw, treat, divert water to~~ For GI construction, three types of GIs can be built to utilize ~~rainfall resources within~~ an urban area; 1) surface water, 2) groundwater, 3) rainwater, and 4) stormwater (Steffen et al., 2013). ~~Surface and groundwater, which are used for supplying potable and non-potable water, can be obtained from the river near an urban area and the aquifer beneath an urban area via grey infrastructure systems. Rainwater and stormwater can be collected from roofs and drains separately via specific GI systems. In the GIs construction decision, infiltration-based GIs to enhance groundwater recharge by altering infiltration rates of pervious surfaces, rainwater harvesting systems to collect rainwater from~~ roofs before it contacts the ground, and stormwater harvesting systems to collect stormwater draining off land areas, including ~~roofs and ground surfaces (Fielding et al., 2015). The water supply portfolios involve four types of water sources classified by intake locations: surface water from nearby rivers, groundwater from aquifers beneath urban areas, rainwater collected via rainwater harvesting systems, and stormwater collected via stormwater harvesting systems (Steffen et al., 2013). Potable water demand is satisfied by surface water and groundwater supplies, whereas all water resources can support non-potable demands.~~

285 The agent-based model for UWM aims to determine cost-effective annual construction areas for the three types of GIs— ~~infiltration-based GIs, rainwater, and stormwater harvesting systems—can be built to use rainfall resources within an urban area directly or indirectly. The infiltration-based GIs can change infiltration rates of pervious surfaces, which can enhance groundwater recharge. The rainwater and stormwater harvesting systems can collect and store rainfall, which provides non-potable water. To simulate UWM's behavior of city-scale IGWM, an~~ , considering urban land limitations, and determine least-cost ~~monthly water supply portfolios to meet urban water demands, subject to allowable source amounts. The objective function is to minimize the annual IGWM cost, which includes the costs of GI construction, water supply, and wastewater drainage. Constraints include the available construction areas for GIs, monthly water supply limits for each water source, and monthly water demand requirements for potable water, total water, and urban irrigation for GI maintenance. Detailed descriptions of the UWM agent-based model for UWM is developed via coupling the IGWM optimization model (IGWM-OM) and the~~

290 urban water balance simulation model (UWB-SM). In the model, monthly optimal IGWM decisions are represented by the ~~IGWM-OM, whereas changes in urban hydrologic processes induced by the decisions are simulated in the UWB-SM. model~~ are provided in Appendix B2.

Agent-based models for WM: As shown in Fig. 1(C), the WM sets a water policy, specifically a streamflow penalty strategy, to regulate the IGWM decisions of all UWMS within a watershed. This strategy is inspired by water withdrawal regulations ~~in regions like South Carolina (Nix and Rouhi Rad, 2022), where over-extraction of surface water can incur penalties. The~~ WM prescribes a series of low streamflow thresholds at checkpoints based on monthly hydrologic states; if the streamflow at ~~an urban area's outlet falls below its threshold, a penalty fee is imposed on the respective UWM. This approach encourages~~

300

UWMs to consider the externalities of their IGWM decisions, thereby adjusting their actions to account for potential costs (Baumol et al., 1988).

305 The WM agent-based model determines the monthly low streamflow thresholds at each checkpoint based on the hydrologic conditions of the corresponding river reach to influence UWM decisions effectively and achieve equitable water resource distribution in the watershed. The IGWM-OM interacts with the UWB-SM via a coupling strategy. Using this coupling strategy, we can use a simulation-based optimization approach to estimate and predict the UWMs' decision-making of IGWM and the induced urban hydrologic dynamic under different socioeconomic and hydroclimatic conditions.

310 The UWB-SM, objective function aims to minimize the water allocation Gini coefficient, as proposed by Hu et al. (2016) and Xu et al. (2019), which measures equity in watershed-scale IGWM by calculating the equitable sharing of the used water quantity for each unit of cost (See Fig. 2). Minimizing the Gini coefficient ensures maximal fairness in water resource distribution. The model includes streamflow constraints that set the allowable range for low streamflow thresholds at each checkpoint. Detailed descriptions of the agent-based model for WM are provided in Appendix B3.

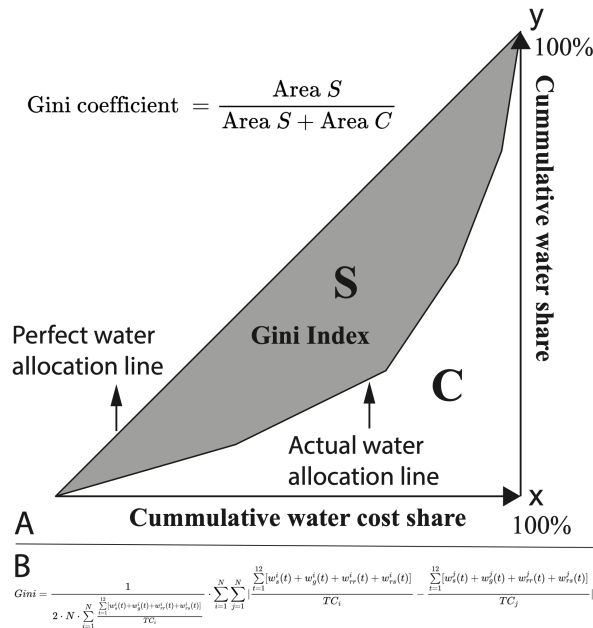


Figure 2. (a) Basic principle for calculating water allocation Gini coefficient, and (b) The objective function for agent-based model for WM.

Note: In Fig. 2 (B), relevant symbols are listed in Tab. B1 and B2 in Appendix B1.

315 2.1.2 Two hydrological models

Urban water balance simulation model (UWB-SM): We developed a lumped urban water system model, is developed to describe the dynamic dynamics of urban water balance induced by city-scale IGWM decisions decision-making. The model

includes 1) incorporates all urban water flows (natural and anthropogenic), 2) grey urban water systems, and 3) green infrastructures GI systems to simulate the interactions between the water supply-wastewater supply-wastewater discharge network, the rainfall-stormwater-rainfall-stormwater runoff network, and the three types of GIs-GI systems within an urban area. In the Figure 3(A) illustrates the urban water mass balance modeled in the UWB-SM, the urban water cycle receives input both showing water flow movements between seven storage units: roof, other surfaces, rainwater and stormwater harvesting systems, shallow soil layer, aquifer, and river. The UWB-SM receives input from rainfall and river inflow, which together pass through the pass through both grey and green infrastructures system and output in infrastructure systems, resulting in outputs in the form of evapotranspiration and river outflow. And water flows movement between Water moves between the seven storage units, with the amounts of water in these units representing their states. These states are used to measure the total water balance within an urban region—roof, other surfaces, rainwater, and stormwater harvesting systems, area and to calculate available amounts of four water resources: surface water and groundwater extracted from the river and aquifer storage units, and rainwater and stormwater collected by harvesting systems. Following Mitchell et al. (2001), indoor water use is divided into potable and non-potable demands, while outdoor water use is considered non-potable.

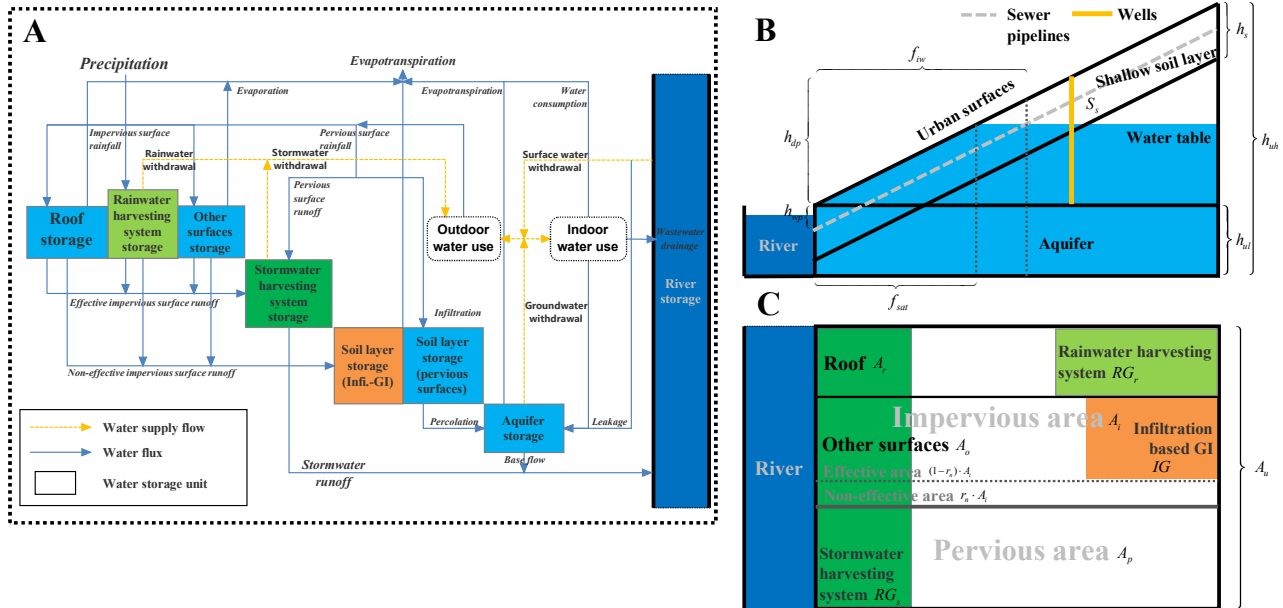


Figure 3. The structure of the UWB-SM.

Note: In Fig. 3 (B) and (C), relevant symbols are listed in Tab. C1, C2 and C4 in Appendix C1.

The vertical structure of the UWB-SM, illustrated in Fig. 3(B), consists of four components: urban surfaces, shallow soil layer, aquifer, and river. The state of model simulates water flux transfers between these storage units is used to measure the total water balance within an urban area, thereby calculating available amounts of water resources in a period. Hydrologically, based on the principle of water mass conservation, considering various surface-subsurface water interactions and pipe network

335 exfiltration and infiltration ~~are considered via simulating water fluxes transfers between these storage units on the basis of the~~
~~water mass conservation principle. Besides, the~~. On urban surfaces, there are four water storage units: roof, other surfaces,
rainwater, and stormwater harvesting systems (see Fig. 3(C)). The urban surface is divided into pervious and impervious
areas based on infiltration rates. Impervious surfaces, where infiltration is negligible, are further divided into effective and
non-effective areas. Effective areas directly drain runoff to the stormwater drainage system, while non-effective areas drain
340 onto adjacent pervious areas, with remaining water evaporating. Pervious areas infiltrate part of the runoff into the underground
soil layer, reducing runoff and enhancing groundwater recharge. Roofs and other surfaces, such as roads and paved areas, are
classified based on the construction conditions of different GIs. Rainwater harvesting systems are assumed to be built only on
roofs, while infiltration-based GIs (e.g., infiltration trenches and porous pavements) are constructed on non-roof impervious
areas, turning them into pervious areas. Runoff generated from roofs, rainwater harvesting systems, and other impervious
345 surfaces is managed through evaporation or rainwater extraction. Stormwater harvesting systems collect runoff from the entire
urban surface for stormwater supply. The UWB-SM ~~be set as that a UWM agent can supply surface water and groundwater by~~
~~extracting from the river and the aquifer storage units. It also can access rainwater and stormwater collected by rainwater and~~
~~stormwater harvesting systems. Details of the UWB-SM are formulated in Appendix C2.~~

~~The IGWM-OM is built to simulate optimal IGWM decisions for a UWM agent—it needs to determine cost-effective~~
350 ~~construction areas of~~ simplifies spatial features of the urban surface, focusing on the cumulative effects of three types of GIs
(i.e., infiltration-based GIs, rainwater, and stormwater harvesting systems) ~~to increase rainwater availability according to urban~~
~~land limitation and also to determine least-cost~~ on the urban water cycle and hydrological interactions.

The UWB-SM requires four types of input data: IGWM decision-making, urban water demand, hydroclimatic data, and
urban land and water characteristics. Specifically, IGWM decision data updates the monthly water supply portfolios (i.e.,
355 amounts of four water resources and the annual construction areas for three GI systems as determined by a UWM agent. Urban
water demand data includes monthly indoor and outdoor water demands, which can be estimated based on the urban population
and economic development levels. Hydroclimatic data comprises mean monthly river inflow, precipitation, and potential
evapotranspiration within an urban area. Urban land and water characteristics are described by calibrated and measured
parameters, which are listed in Tab C2. Measured parameters relate directly to physical catchment characteristics and can
360 be determined through measurement, observation, or local experience. The 12 calibration parameters, along with their units,
symbols, and ranges, are grouped according to land features such as surfaces, soil layer, aquifer, river, and urban water system,
as shown in Tab C3. These values are adjusted during calibration to optimize the selected objective function. Detailed governing
equations for the UWB-SM are provided in Appendix C2.

Muskingum-Cunge routing model: It simulates textcolorredupstream-downstream hydrologic interactions between UWM
365 agents in an associated river reach, as illustrated in Fig. 1(B). For example, the upstream inflow for UWM agent $i + 1$
in month t can be mathematically expressed as the outflow from UWM agent i in the same month and the next month
(Garbrecht and Brunner, 1991; Weinmann and Laurenson, 1979). The Muskingum-Cunge routing model, which is used to simulate
these interactions, is described in detail in Appendix C3.

2.2 Agent-based model for city-scale IGWM

Fig. 1(A) illustrates the decision-making process of city-scale IGWM by an UWM agent and the resulting changes in urban water cycles. To simulate the UWM's behavior in city-scale IGWM, an agent-based model is developed by coupling the agent-based model for UWM with the UWB-SM. In this model, annual decisions on GI construction made by the proportions of surface water, groundwater, rainwater, and stormwater supply) to satisfy urban, diverse water demand subjecting to associated allowable amounts of water sources. In the IGWM-OM, the objective function – to minimize the annual IGWM cost for the UWM agent – consists of the annual costs of GIs construction, water supply and wastewater drainage. The relevant constraint conditions include the GIs construction, water supply and demand constraints; GIs construction constraints restrict the are first used as inputs to the UWB-SM. Subsequently, monthly water supply portfolio selections are represented by the UWM agent, while the resulting changes in urban water cycles are simulated in the UWB-SM. The agent-based model for UWM interacts with the UWB-SM through a coupling strategy. This coupling strategy enables us to use a simulation-based optimization approach to estimate and predict the UWM's decision-making in city-scale IGWM and the resulting urban hydrologic dynamics under different socioeconomic and hydroclimatic conditions.

The data exchange between the UWB-SM and the agent-based model for UWM occurs in two phases to ensure feasible solutions (Fig. D1(B) in Appendix D2). In Phase 1, an annual data exchange generates feasible GI construction decision variables for the UWM agent and initializes the UWB-SM. Initial data, including urban water demand, land and water characteristics, and hydroclimatic data, are input into both models. Annually available construction areas for infiltration-based GIs, rainwater GI, rainwater, and stormwater harvesting systems within the urban region; Water supply constraints limit the available monthly water supply amounts for four types water sources – surface water, groundwater, rainwater are determined by GI construction constraints and used to update the urban land features in the UWB-SM. In Phase 2, a monthly data exchange generates feasible water supply decision variables for the UWM agent. Each month, the UWB-SM runs at least twice, exchanging data with the agent-based model for UWM. The UWB-SM updates the urban hydrologic state based on the storage levels of seven storage units from the previous month and computes available runoff for stormwater harvesting. This information, along with the storage levels of four storage units (river, aquifer, rainwater, and stormwater harvesting systems) from the previous month, is used by the agent-based model for UWM to generate feasible monthly water supply decision variables. These variables are then transferred back to the UWB-SM to simulate urban hydrologic variables for the current month. The updated hydrologic variables are sent back to the agent-based model for UWM to verify the feasibility of the decision variables. If the decision variables fail the check, they are regenerated by the agent-based model for UWM. If they pass, the relevant IGWM cost is calculated, and stormwater; Water demand constraints set three types of monthly water requirements the UWM agent need to meet, that is, potable water, total water and urban irrigation demand. The details of the IGWM-OM are illustrated in Appendix B2 the updated storage units' data are used to initialize the UWB-SM for the next month. This process continues until the termination criteria are satisfied, generating a feasible IGWM decision variable and associated annual cost.

In the ABM for UWM, The UWB-SM and IGWM-OM and the agent-based model for UWM are tightly coupled at the source code level, i.e., the with subroutines of the IGWM-OM are embedded into relevant subroutines of agent-based model embedded into the UWB-SM. The primary data exchanged and shared between the two models are (1) include water supply portfolios and GIs construction plan, and (2) hydrological conditions. Therefore, according to features of the model, GI construction plans, and hydrologic states. Given that some parameters of the IGWM-OM need to be agent-based model for UWM are computed by the UWB-SM, a simulation-based adaptive particle swarm optimization (S-APSO) is designed. Compared with particle initialization and evaluation for standard PSO, a coupling procedure proposed above for data exchange between IGWM-OM and UWB-SM is nested to make sure all particles feasible and measurable. Compared with the standard PSO updating mechanism, a Boltzmann selection operator and an evolutionary state-based parameter adaptation scheme are added to avoid premature convergence to improve algorithm performance; a simulation-based check & repair mechanism is introduced to guarantee all particles feasible during the particle updating process. These key features of the proposed S-APSO are explained corresponding solution approach is detailed in Appendix D2.

2.3 Multiagent system for **IGWM at an inter-city scale** IGWM

Fig. 1(B) illustrates the hydrologic connection between the two urban areas. Such hydrologic connection among all UWM agents within the watershed, which means river connections between urban areas, which significantly affect the impact of GIs on urban and watershed hydrology in terms of water resource allocation. These river connections mean that all UWM agents have to must share surface water resources with others, and IGWM activities of upstream agents may affect that of downstream. That is, an optimal decision-making of city-scale from a UWM agent may not be suitable for the whole watershed economically and hydrologically because of negative externalities, which affect IGWM decision behavior of the other UWM agents being linked with it socially or hydrologically (Glendenning et al., 2012). Therefore, urban areas, and the decisions made by upstream agents can affect downstream agents (Glendenning et al., 2012). A multiagent system is constituted by considering multiple urban areas and interconnected river networks can constitute a MAS-UWM (See Fig. 1 B). In the MAS-UWM, as shown in Fig. 1 (B), In this system, all UWM agents are linked with each other by a stream river network, and each UWM agent makes IGWM decisions by a river network. Each UWM agent independently makes city-scale IGWM decisions—such as water supply portfolios and GIs construction—independently, only—based on its urban hydrologic conditions as well as the current hydrologic states and upstream inflow, which is partly determined by the outflow of the upstream urban areas influenced by the IGWM decisions of the outflows from upstream areas and the decisions of associated UWM agents. Therefore, the UWM-UWM agent interactions in watershed-scale IGWM The interactions among multiple UWM agents can be depicted as a sequence of city-scale IGWM decisions along with river networks, which is a unique sequential decision process as the upstream UWM agent's IGWM decision affects the decision of the subsequent downstream agent because the as water is transported along the river; this interaction process can be regarded as downstream. This interaction process exhibits the Markov property (Frydenberg, 1990), where the hydrologic state of a downstream urban area depends only on the hydrologic state of the adjacent upstream area after making its own IGWM decisions and its own decisions. This state transition process continues sequentially along the river.

To simulate the up-and-downstream hydrologic interaction between UWM agent i and $i + 1$ in the associated river reach (See Fig. 1 B), a Muskingum-Cunge The multiagent system for inter-city scale IGWM is formulated by integrating the agent-based model for UWM (M-C) routing equation is used to simulate changes in streamflow in the river reach connected with two adjacent urban areas (Garbrecht and Brunner, 1991; Weinmann and Laurenson, 1979). That is, taking the UWM agent $i + 1$ in month t as an example (See Fig. 1 B), its upstream inflow in a month can be expressed mathematical by outflow of the UWM agent i in the month and the next month. In addition, it should be noted that the Muskingum-Cunge approach is also applicable in the case that there are branches in the main riverreach (See UWM agents 1,2 and 3 in Fig. 1 B), which can be solved by dividing the river reach into several sub-reaches based on intersections of the main river and associated branches, and then calculate them in sequence. The details of the Muskingum-Cunge routing equation are illustrated in Appendix C3.

Therefore, the MAS-UWM can be formulated by the integration of the ABM-UWM (Eq. B1) with the UWB-SM and the Muskingum-Cunge routing model (Eq. C10), depending on its feature of the leveraging its Markov property. A This system is modeled as a special type of multi-stage decision system is employed to model the MAS-UWM (Bellman, 1966) and (Bellman, 1966), where the sequence of decisions-makings decision-making for each UWM agent—city-scale IGWM—relies on associated—follows their spatial locations along with the river networks, which is in order from upstream to downstream. The hydrologic variable—upstream inflow of—, specifically the upstream inflow for each UWM agent—, is considered the state variable to describe interactions between UWM agents. It can be written as follows, that describes interactions between agents. This can be expressed as follows:

$$\begin{cases} \text{agent-based model for UWM } i + \text{UWB-SM}, & \forall i & (01) \\ \text{Muskingum-Cunge routing model } i \text{ in } t, & \forall i, t & (02) \\ q_{ri}^1(t) = Q_t^1, \text{ and } q_{ri}^i(0) = Q_0^i, & \forall i, t & (03) \end{cases} \quad (1)$$

where the third row of Eq. (1) are initial conditions for the MAS-UWM multiagent system for UWMs, and Q_t^1 and Q_0^i are the initial amounts of the upstream inflow for UWM agent 1 in month t and UWM agent i in month 0, respectively. The details of the MAS-UWM are illustrated in Appendix E2.

To solve the MAS-UWM, it is available to combine multiple S-APSO algorithms with the Muskingum-Cunge routing equation to simulate the dynamics of the MAS-UWM according to its Markovian property. That is, the optimal solutions for each UWM agent model are solved one by one in a specific order, which follows the sequence of the MAS-UWM via using the associated S-APSO. Notice in particular that the monthly outflow amounts for the optimal solution of each UWM agent model needs to be recorded during the S-APSO search process. They, as an input of the relevant Muskingum-Cunge equation, are used to calculate the monthly upstream inflow amounts in the associated downstream reach—an input data for the adjacent UWM agent model. In this way, the multi-S-APSO framework for simulation of the interactions of the MAS-UWM is developed. The details of the solution approach for MAS-UWM are illustrated in Appendix multiagent system and the corresponding solution approach are presented in Appendix sections E2 and E2.

2.4 Bi-level multiagent system for watershed-scale IGWM at a watershed scale In the MAS-UWM

In the described multiagent system, each UWM agent minimizes its own IGWM costs without ~~direct regard for directly~~ considering the external effects on ~~the other UWM agents' interests because of other UWMs due to~~ the Markov property of the system. ~~It may appear to be inequalities of water resources sharing where upstream water users might easily take up~~ This might lead to inequalities in water resource sharing, where upstream users might consume more surface water than downstream users ~~(Giuliani and Castelletti, 2013), which might increase IGWM costs of downstream agents. For a watershed manager, of interest is the ability of the water policy to address the inequality and encourage more,~~ potentially increasing the IGWM costs for downstream areas (Giuliani and Castelletti, 2013). To address this inequality and promote sustainable water use in watershed-scale IGWM ~~(See Fig. 1 C). Thus, we develop a ABM-WM and build a bi-level multiagent system via combining the ABM-WM with the MAS-UWM, which can simulate water policy-induced interactions between MW and UWM agents.~~

~~To achieve equitable surface water resources allocation in the MAS-UWM, the WM specifies limits for surface and groundwater withdrawal—prescribing the minimum storage levels of the river for each urban areas, and enacts a streamflow penalty strategy to regulate UWM agents' IGWM decision behavior—setting a series of low flow thresholds at each checkpoint; if the UWM has out-of-threshold surface water withdrawal, then penalties are imposed. In the study, an agent-based model for watershed manager (ABM-WM) is built to describe how a WM set a watershed management policy—a streamflow penalty strategy—to regulate all UWM agents' behaviors of IGWM in a watershed. That is, a WM limits water abstraction decisions of each UWM agent in the period via prescribing a series of low streamflow thresholds in associated hydrological stations based on hydrologic conditions; If streamflow in outlet for an urban area is below its threshold, a penalty fee will be imposed on the UWM agent. The strategy, in theory, can force UWM agents to recognize one or more of the externalities caused by IGWM, thereby adjusting their IGWM decisions because it can, to some extent, determine the cost of IGWM (Baumol et al., 1988).~~

~~The WM can share fair water resources among urban areas in a watershed by setting a rational,~~ a WM can implement policies such as a streamflow penalty strategy ~~that affects all UWMs' decisions. The details of the ABM-WM are illustrated in Appendix B3.~~

~~Under the policy intervention from a WM~~ such policy interventions, each UWM agent ~~needs to make reasonable IGWM decisions to trade off the previous three types of costs (i.e.,~~ must balance the costs of GIs construction, water supply, ~~wastewater drainage) and the possible penalty fee set by a WM to minimize their own total IGWM costs under the~~ and wastewater drainage with the potential penalty fees imposed by the WM for not meeting specified low streamflow thresholds. ~~Therefore, the above ABM-UWM will be extended—its~~ Consequently, the agent-based model for UWM is extended to include these penalty fees in the annual IGWM cost function ~~is converted as the sum of GIs construction, water supply, wastewater drainage costs, and penalty fees. The details of the model are shown.~~ Details of this model extension are provided in Appendix F1.

~~As mentioned above illustrated in Fig. 1(C), a streamflow penalty strategy prescribed by a WM agent might change some UWM agents' decisions of IGWM—may prompt~~ upstream UWM agents ~~might have to adjust their IGWM decisions to increase outflow to avoid over high penalty fees for costs minimization, which is beneficial to the,~~ thereby minimizing penalty fees and benefiting downstream agents. ~~Such changes in UWM agents' behavior can, to some extent, These adjustments can~~ shift the interactions ~~in the MAS-UWM, which might have a potential impact on the watershed environment that can be measured by the assessment index (i.e.,~~ within the multiagent system, impacting water resource distribution within the

watershed, which can be quantified using the water allocation Gini coefficient) set by the MW (See Fig. 1 C). Therefore, a WM-agent WM. The WM can assess the effects of the policy policy's effects on the watershed via checking the given index that reflects feedbacks of the MAS-UWM and then gradually adjusts it by evaluating this metric and iteratively adjusting the policy to find the optimal onesolution. This process is a WM-UWM-agent interaction represents an interaction between the WM and UWMs in watershed-scale IGWM under a water policy. Fig. 1 (C) illustrates that the WM-UWM-agent interaction is no longer determined only streamflow penalty strategy. This interaction is not solely determined by the WM or the UWMs, and both of them try; both parties aim to optimize their objectives (i.e., equity vs. cost objectives for WM and equity for the WM and cost minimization for UWMs) under the associated constraints (i.e., steamflow vs. respective constraints (streamflow for the WM and GI construction, water supply, and demand constraints) and for the UWMs) and the reactions of the other party. Therefore, they follow a specific decision rule. That is, the WM-agent first makes a This decision-making process follows the Stackelberg game theory (Von Stackelberg, 2010), where the WM makes the initial decision, and then each UWM-agent specifies a decision UWMs respond to optimize their own objectives with full knowledge of the WM's decision; the WM also optimizes its own. The WM then optimizes its objective based on the rational UWMs' reactions. In economic theory, this process the WM-UWM-agent interaction is a Stackelberg game (Von Stackelberg, 2010) reactions of the UWMs.

Based on the features of the WM-UWM-agent interaction, it can follow a hierarchical decision rule for the leader the WM-agent and the multiple followers the UWM-agents (Dempe, 2002). Besides, for the followers, the UWM-agents form a MAS-UWM (Eq. 1) that has a Markov property, which involves a special multi-stage decision-making process (Bellman, 1966). By integrating the ABM-UWM, the ABM-WM and the MAS-UWM (Eq. C10) mentioned above, a BL-MAS for IGWM at a watershed scale can be developed to describe the Stackelberg game between the WM and multiple UWM-agents, and unique multi-stage system constructed to reflect the state transitions for the multiple WM-UWM-agents, which Leveraging the Stackelberg game framework (Dempe, 2002), we construct a bi-level multiagent system by combining the agent-based model for WM with the multiagent system comprising multiple extended agent-based models for UWMs and the relevant hydrologic models. This system can be formulated as follows:

$$\left\{ \begin{array}{l} \text{agent-based model for WM;} \\ \text{where } W_i, GI_i \text{ solves} \\ \left\{ \begin{array}{ll} \text{extended agent-based model for UWM } i + \text{UWB-SM,} & \forall i \\ \text{Muskingum-Cunge routing model } i \text{ in } t, & \forall i, t \\ q_{ri}^1(t) = Q_t^1, \text{ and } q_{ri}^i(0) = Q_0^i. & \forall i, t \end{array} \right. \end{array} \right. \quad (2)$$

where $[-]_*$ represents that the parameter is from simulating calculation of the UWB-SM. W_i and GI_i represent the decision variables of water supply portfolios and GIs construction for UWM agent i . The details of the BL-MAS bi-level multiagent system and the pertaining solution approach are illustrated in Appendix F2 -

To solve the BL-MAS (Eq. F3), the proposed S-APSO is also applied in the BL-MAS, only the fitness function for particles needs to be adjusted. Besides, the above multi-S-APSO framework is also available in simulating the interactions among all UWM-agents in the BL-MAS under a given streamflow penalty strategy because of the features of its hydrologic connections

530 ~~—Markovian property. For the ABM-WM, the above S-APSO framework without the simulation-based initialization and the check & repair mechanism is available to look for the optimal solution due to its simple constraint conditions. However, there is a critical factor in the simulation of the BL-MAS that is how to deal with the special decision rule between the WM and the UWN agents—a Stackelberg game, i.e., the WM agents’ best response is based on the associated reactions of all UWN agents (Von Stackelberg, 2010). In fact, it is challenging to obtain a Stackelberg solution to the BL-MAS using general solution~~
 535 ~~methods because the bi-level model is an NP-hard problem, even in its simplest linear case (Dempe, 2002). To deal with the specific bi-level model decision rules, the study nests the multi-S-APSO framework for the MAS-UWN mentioned before into the particle performance measurement of the S-APSO for the WM agent, which can simulate the responses of the MAS-UWN to a given streamflow penalty strategy prescribed by the WM agent, thereby assessing the policies’ effects accurately. By the nested structure, therefore, a nested S-APSO framework is proposed for searching for the optimal WM-UWN interactions in~~
 540 ~~the BL-MAS under a streamflow penalty strategy. The details of the nested S-APSO is shown in Appendix [and](#) F3.~~

3 Case study and experimental design

In this section, the proposed multiagent socio-hydrologic framework is utilized in a case study on the Minneapolis-La Crosse section of the Upper Mississippi River, United States, and three numerical experiments are designed to ~~demonstrate its effectiveness and efficiency and to characterize the decision-making~~ characterize the decision-makings of IGWM at ~~a city and~~
 545 ~~watershed scale~~ three spatial scales.

3.1 Overview of the study area

As Fig. 4 shows, the Upper Mississippi River basin ranges in latitude from 47° N to 37° N, and its flows roughly 2,092 km, from Lake Itasca (northern Minnesota) to the Ohio River (southern Illinois), which covers seven states of the US, such as Illinois, Iowa, Minnesota and Wisconsin, and has a watershed area of 489,508 km². The main river and its tributaries have
 550 an average annual discharge of 3,576 m³/s, which has three high- (late April, late June, and October) and two low-flow (midsummer and late winter) periods as a result of varied rain and snow conditions (Baldwin and Lall, 1999).

~~Schematic diagram of the study area. Notice that the base map and metropolis and city group maps in the bottom right of the figure are from Esri (2012) and U.S. Census Bureau (2018), respectively; the US states boundary map and the Upper Mississippi River Basin map in the bottom left of the figure are from U.S. Census Bureau (2018) and U.S. Geological Survey (2021), respectively.~~
 555 ~~;~~

In the watershed, more than 70% of the area is used for agriculture and animal husbandry. Only 5% of the site has been converted to urban areas. However, it has a population of about 24 million, especially in the metropolitan high-density regions (> 100,000 people/km²), such as Minneapolis-St. Paul, Minnesota and La Crosse, Wisconsin. It is estimated that over 5.3 million m³ of water are withdrawn from the Upper Mississippi River each day in the 60 counties for municipal and public
 560 supplies. ~~Although the basin is-~~

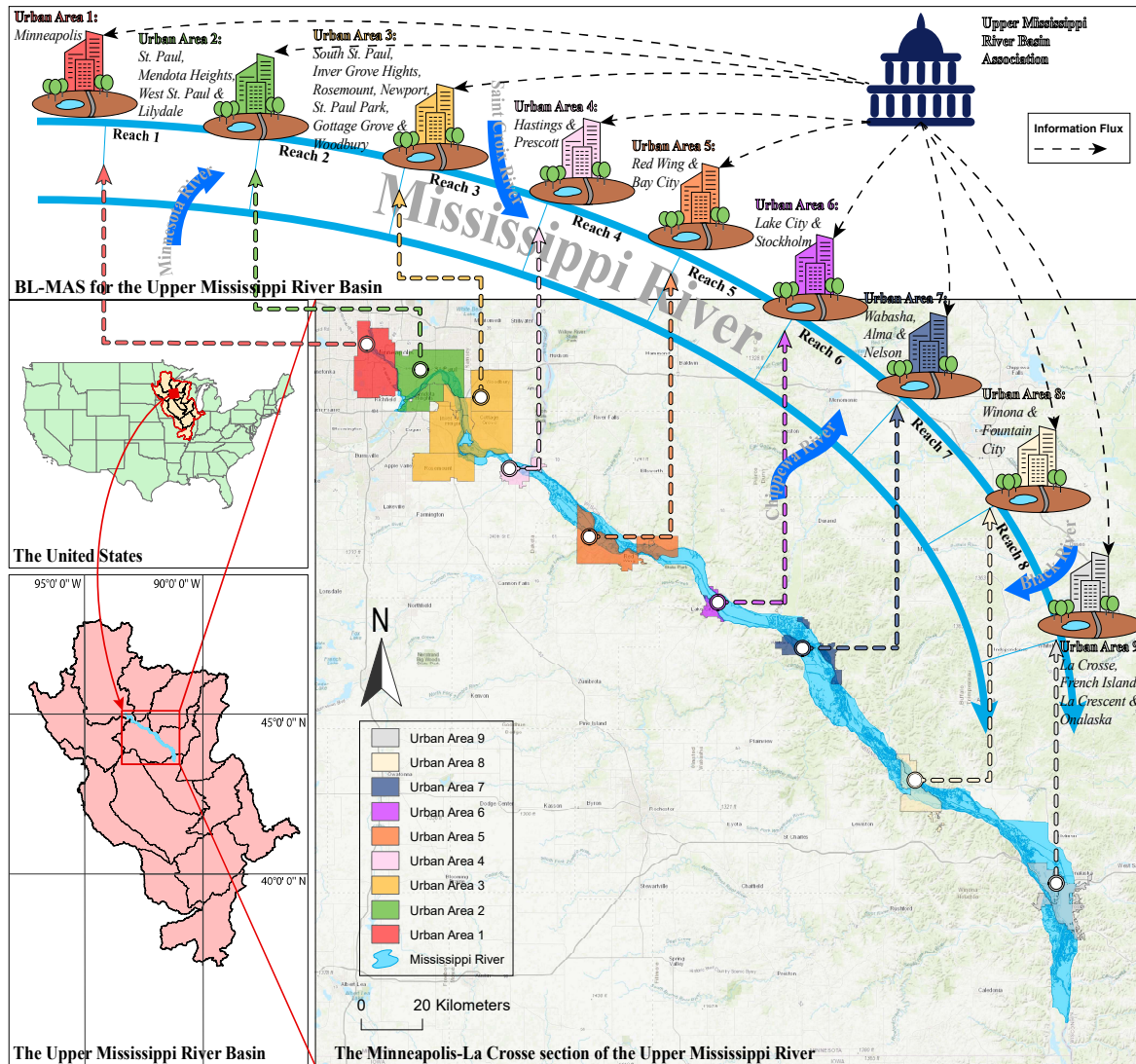


Figure 4. Schematic diagram of the study area. Notice that the base map and metropolis and city group maps in the bottom right of the figure are from Esri (2012) and U.S. Census Bureau (2018), respectively; the US states boundary map and the Upper Mississippi River Basin map in the bottom left of the figure are from U.S. Census Bureau (2018) and U.S. Geological Survey (2021), respectively.

There are three primary reasons for selecting the Upper Mississippi River Basin as the case study for conducting numerical experiments. First, although the widespread use of GIs for rainwater harvesting is not prevalent in the United States, the study (Ennenbach et al., 2018) has demonstrated the potential for rainwater harvesting in this watershed, attributed to its humid climate and abundant annual precipitation. However, this study also indicates that seasonal variations in water demand necessitate a deeper exploration of rainwater harvesting potential. Applying the socio-hydrologic framework to the basin can

provide valuable insights into this potential. Second, despite being a water-rich basin, water sharing among the riparian urban areas is still a remains a significant concern due to the high water demands for the environment and agriculture, the demands for environmental and agricultural purposes, strict water level regulations for navigation, and the high-density urbanization. Groundwater is also a crucial source of water that is Climate change is expected to drastically alter the probability distribution of streamflow, increasing the frequency and magnitude of both high and low streamflow extremes. Consequently, even high-flow river basins also might face nonstationary drought risks (Dierauer and Zhu, 2020). The study have simulated that climate change could result in streamflow decreases in all seasons except winter within the basin (Lu et al., 2010). Third, there are notable similarities between the actual case and the simulated case by the proposed model. For instance, in fact, the Upper Mississippi River Basin Association as WM aims to implement a water level management policy (Reed et al., 2020), which mirrors the multi-player management structure assumed in the proposed model. Additionally, surface water and groundwater are crucial sources of water widely used by the partial-urban areas, and green infrastructures are continually-gradually encouraged and expanded to manage urban stormwater by the local communities and authorities (Askew-Merwin, 2020). Therefore, it is appropriate to analyze the watershed-scale IGWM in the Upper Mississippi River basin. (Askew-Merwin, 2020; Guo, 2023)

In this study, the Minneapolis-La Crosse section - approximately 236 km long - of the Upper Mississippi River basin, a high-density urban area, is considered as the study area. (See Fig. 4). Notice that the study only focuses on the urban water use and allocation, which perhaps is a small percentage of the basin water resource in the study region. Fig. 4 indicates that there are nine main riparian urban areas along the section; i.e., $i = 1, 2, \dots, 9$. Some are metropolises with a large population for these urban areas, such as Minneapolis, St. Paul, and La Crosse. The others are city groups that consist of multiple small cities, such as Red Wing and Bay City. In short, the basic features of urban areas in the study site is shown in Tab. 1.

Table 1. The basic features of urban areas in the study site.

| No. of urban area | Urban names | Urban types | Population | Urban area A_u (km^2) | Ratio of impervious surface area (%) |
|-------------------|--|-------------|------------|-----------------------------|--------------------------------------|
| 1 | Minneapolis city; | metropolis | 2,914,866 | 139.86 | 65 |
| 2 | St. Paul, West St. Paul, Mendota Heights, and Lilydale; | metropolis | 350,167 | 172.26 | 63 |
| 3 | South St. Paul, InverGrove Hights, Rosemount, Newport, St. Paul Park, Gottage Grove, and Woodbury; | city group | 230,277 | 367.41 | 60 |
| 4 | Hastings and Prescott; | city group | 71,870 | 33.37 | 61 |
| 5 | Red Wing and Bay City; | city group | 49,167 | 91.75 | 64 |
| 6 | Lake City and Stockholm; | city group | 12,405 | 51.40 | 62 |
| 7 | Wabasha, Alma, and Nelson; | city group | 12,265 | 38.48 | 61 |
| 8 | Winona and Fountain City; | city group | 26,757 | 60.62 | 59 |
| 9 | La Crosse, LaCrescent, French Island, and Onalaska; | metropolis | 80,601 | 96.93 | 66 |

3.2 Experimental design

Given the background of the study area, all urban area - metropolises or city groups - is assumed as a UWM agent that makes city-scale IGWM decisions individually, which can be formulated by Eq. (B1) and the Upper Mississippi River Basin Association (~~UMRBA~~) is regarded as the WM agent that regulates these urban areas, and the associated interactions among UWMs and between WM and UWMs are formulated by Eq. (E1) and (F3), respectively. In the case study, we ~~examine the potential properties address the above issues~~ of IGWM at three spatial scales through observing and comparing the results of the ~~decision makings of~~ WM and UWM agents' ~~behaviors and their~~, and interactions in IGWM simulated by the proposed model under different socio-hydrologic settings. Therefore, three numerical experiments to IGWM at city, inter-city and watershed-scales are designed in the following:

~~Experiment 1 of IGWM at a city scale:- The experiment is designed-~~

3.2.1 Experiment 1 of IGWM at a city scale

~~The experiment aims to identify and classify the behavioral characteristics of characteristics of optimal decision-making for city-scale IGWM for UWM by UWM agents under different hydroclimatic settings, thereby investigating how watershed hydroclimatic circumstances affect the decision-making of city-scale IGWM. In this experience. Firstly,~~ a sensitivity analysis ~~to the ABM-UWM of the agent-based model for city-scale IGWM (see Section 2.2) is performed. All urban areas within the studied region are considered as study objects, and the associated ABM-UWMs are run many. The associated agent-based models for city-scale IGWM are run multiple times under different combinations of upstream inflow and precipitation, which are the model's input parameters, to calculate associated optimal decision-makings of city-scale IGWM. The combined effects of upstream inflow and precipitation on the city-scale IGWM in the study area is discussed to characterize the city-scale IGWM patterns of UWMs in changing environments. The baselines of the associated optimal decision-making scenarios. The baseline values for~~ these two hydroclimatic parameters are obtained from the USGS, and six ~~situations are set via scenarios are created by~~ decreasing and increasing the baselines by 25%, 50%, and 75%, respectively. ~~A, covering high and low streamflow and rainfall extremes. Secondly, based on the optimal decision-making scenarios of city-scale IGWM under mixed hydroclimatic conditions, a k-means clustering method (Likas et al., 2003) is employed to classify all UWMs' decision-making of IGWM -water supply portfolios and GIs construction- under mixed hydroclimatic conditions. By categorizing the responses of UWMs to different environments, we summarized the similarities of strategies. This classification characterizes the patterns of city-scale IGWM in changing environments by summarizing the similarities in UWMs' decision behavior, which can be used to indicate the features of city-scale IGWM patterns of UWMs under specific hydroclimatic conditions.~~

~~Experiment 2 of IGWM at an inter-city scale:-~~

3.2.2 Experiment 2 of IGWM at an inter-city scale

The experiment is ~~set for examining how a UWM agent affects other UWM agents in~~ designed to examine the impacts of inter-city scale IGWM ~~and assessing the impacts of the MAS-UWM interactions on the watershed. In this experience on~~

the socio-hydrologic dynamics of the watershed and investigate how watershed hydroclimatic and socioeconomic conditions affect these interactions. For the first objective, two scenarios are simulated by the MAS-UWM model using the multiagent system for inter-city-scale IGWM (see Section 2.3). The first scenario, as an experiment group, is conducted taking serving as the experimental group, includes GIs construction decisions into account, while the second one, as a control group, is configured without GIs development via setting r_{imax} , r_{rmax} and $r_{smax} = 0$ in the UWM agent model excludes GIs development and rainwater and stormwater usage by setting the maximum available areas for constructing three types of GIs to zero in all agent-based models for UWM. By comparing the results of the these two groups, we identify the possible impacts of the IGWM decisions in upstream urban areas on the downstream urban areas and quantify the relative attribution of GI in the impacts. Also, we conduct potential impacts of inter-city scale IGWM on water use cost, equity of water resource allocation, and available surface water distribution within the watershed, thereby quantifying the relative contribution of GIs to these impacts.

For the second objective, a sensitivity analysis to the experiment group to analyze the effects of different watershed settings on the UWM-UWM interactions economically. There are various of the experimental group is conducted. Various combinations of watershed settings (i.e., watershed upstream inflow, the precipitation, precipitation, and urban water demands) to be are considered. The scenario of the MAS with GIs was including GIs development and rainwater and stormwater usage is set as the baseline in the experiment. Similar to the Experiment 1, monthly precipitation and watershed upstream inflow were proportionally changed are proportionally varied from 25% to 175% based on the baselines, to simulate the hydroclimatic watershed dynamics; of the baseline to simulate hydroclimatic dynamics. Additionally, monthly urban water demands, including the encompassing both indoor and outdoor demands, were used to represent the socioeconomic changes of the watershed, which were appropriately shifted are adjusted from 25% to 175% according to the baseline of the baseline to represent socioeconomic changes in the watershed.

Experiment 3 of IGWM at a watershed scale: This experiment will be devised

3.2.3 Experiment 3 of IGWM at a watershed scale

This experiment is designed to investigate the influence of the a streamflow penalty strategy set by a WM agent on IGWM at a watershed scale. A policy simulation to the BL-MAS is conducted. According to on the features of the BL-MAS—Stackelberg game between the WM and the UWM agents, the optimal solutions of the BL-MAS is socio-hydrologic dynamics of the watershed within the context of IGWM and to examine the impacts of different hydroclimatic and institutional conditions on the interactions of watershed-scale IGWM. For the first objective, a policy simulation of the bi-level multiagent system for watershed-scale IGWM (see Section 2.4) is conducted. The optimal solution of this bi-level system can be defined as Stackelberg equilibrium points (Dempe, 2002)—equilibrium—equilibria between the WM and UWMs in the watershed-scale IGWM that none of them have where no party has an incentive to alter their decisions. In theory, there are likely to be multiple equilibrium points in a bi-level system (Dempe, 2002). Therefore, all equilibrium of the BL-MAS Multiple equilibrium points are likely in such a system (Dempe, 2002); hence, all equilibria need to be identified and analyzed to assess the possible effects of the water policies prescribed by the WM on the UWM agents' decision behavior of the watershed-scale

IGWM. In the experiment, the streamflow penalty strategy. The baseline penalty rate is specified as $0.005 \text{ \$/m}^3$. Notice that the penalty This rate is artificial due to no penalty strategy to the absence of an existing penalty strategy in the study area in reality. We have to choose a reasonable rate that might. The baseline rate is determined by referencing an actual water withdrawal regulation in South Carolina, US (Nix and Rouhi Rad, 2022), and through comprehensive parameter analysis (Parsapour-Moghaddam et al., 2015; Rosegrant et al., 2000) to ensure it can affect all UWMs' decision-behavior decision-making in the study area through a comprehensive parameter analysis (Parsapour-Moghaddam et al., 2015; Rosegrant et al., 2000). By comparing with the results of the results with those from Experiment 2, we evaluate the water policy-induced changes in the interactions in the MAS-UWM and the watershed hydrologic regime. Furthermore, we summarize the effect of the optimal potential impacts of the streamflow penalty strategy on watershed-scale IGWM in changing watershed institutional and hydroclimatic conditions through conducting water use cost, equity of water resource allocation, and surface water distribution within the watershed.

For the second objective, a sensitivity analysis under different parameters mixture is conducted under varying conditions of the penalty rate, the watershed upstream inflow, and the precipitation. precipitation. The aforementioned policy simulation scenario is set as the baseline. Monthly precipitation and watershed upstream inflow are proportionally varied from 50% to 150% of the baseline to simulate hydroclimatic dynamics. Six penalty rates— $0.002 \text{ \$/m}^3$, $0.004 \text{ \$/m}^3$, $0.005 \text{ \$/m}^3$ (baseline), $0.006 \text{ \$/m}^3$, $0.008 \text{ \$/m}^3$, and $0.010 \text{ \$/m}^3$ —are set to represent different institutional conditions. In cases with multiple equilibria in the bi-level multiagent system, we consider only the equilibrium with the lowest mean cost per unit of water as the corresponding result for watershed-scale IGWM.

3.3 Data collection and processing

In the proposed framework to the case study, some parameters of the ABM-UWM and ABM-WM, as shown in Tab. C1, C2 and B2 in Appendix D1 and ??, two agent-based models and two hydrological models need to be determined by collecting, processing and estimating actual data from diverse sources.

For the parameters of UWB-SM, as detailed in Table C1 of Appendix B, the urban water demand data (36×9) were measured based on the associated derived from urban populations and layouts via the Last (2011) method using the method of Last (2011). The hydroclimatic data inputs (27×9) were obtained estimated using raw data on streamflow, precipitation, and temperature from the USGS Current Water Data for the Nation (<https://waterdata.usgs.gov/nwis/rt>) and the NOAA (-) databases. Global Historical Climatology Network daily (GHCNd) databases (<https://www.ncei.noaa.gov/>). Specifically, upstream inflow data were identified from GIS maps of urban areas and estimated using the map correlation method (Archfield and Vogel, 2010) with monthly streamflow observations from USGS stations, because of the location difference between the urban area's inlet and the associated USGS stations. Evaporation and evapotranspiration data were calculated using the method of Ravazzani et al. (2012) with temperature data from the GHCNd database. The urban area data (1×9) were obtained sourced from the U.S. Census Bureau (<http://www.census.gov/>), and the urban land features data (4×9) were calculated through analyzing the derived from remote sensing images (Last, 2011). Also, we used different databases and methods to obtain the urban, as shown in Table C2 of Appendix B. Urban depth-related data . To be specific, the mean depths of the urban aquifer at the low topographic point

were obtained using various methods: mean aquifer depths at low topographic points (1×9) were assumed ~~as to be~~ ten meters plus ~~the mean depth of the riverbed obtained riverbed depths~~ from the National Elevation Dataset (NED, <http://ned.usgs.gov>), because of lack of relevant data about the aquifer. Moreover, they were also used to calculate the associated aquifer mean depth at the high point while aquifer depths at high points (1×9) by using a linear fitting method were calculated using linear fitting to urban hypsometric curves (Sharma et al., 2013). Notice that we believe that the rough assumptions might have little impact on the results of the three experiments because the study area is within a water-rich watershed, and the surface water is the primary source of urban water supply. The mean depths of wells These assumptions are believed to have minimal impact due to the region's abundant water supply. Mean well depths for groundwater withdrawal (1×9) were measured via averaging adjacent wells' depths from the USGS database. Besides, the maximum ratios of the averaged from nearby wells in the USGS Groundwater Data for the Nation database (<https://waterdata.usgs.gov/nwis/gw>). Maximum ratios for constructed areas of rain-water, stormwater harvesting systems, and infiltration-based GIs to the relevant surface green infrastructure (3×9) were set as at 50%. Notice that we want to test the maximum potential for to test maximum urban rainfall utilization in the study area. However, the actual ratios of GIs areas might be much smaller than these ratios. All of the mean depths of the shallow soil layer potential, though actual ratios may be lower. Mean depths for shallow soil layers (1×9) and the wastewater pipe networks (1×9) were set as at 3 ~~m~~ meters and 2 ~~m~~ meters, respectively, based on similar settings (Frost et al., 2016). The mean Mean effective porosity (1×9) was estimated as at 10% based on the Prior et al. (1953) report due to lack of related accurate information from the report by Prior et al. (1953). Storage capacity data (4×9) were determined based on urban layouts using the method of Frost et al. (2016).

For the parameters of IGWM-OM, the agent-based model for UWM, as shown in Table B2 in Appendix C, the construction cost data for three types of GIs construction cost data green infrastructure (GIs) (3×9) were estimated based on the relevant GIs cost databases in the EPA websites EPA cost databases (<https://www.epa.gov/>) through the Houle et al. (2013) approach. And the following the method of Houle et al. (2013). The associated cost scaling coefficients (3×9) were obtained using a linear fitting method to these cost data. Some parameters related to the cost of surface, groundwater supply, and wastewater drainage (8×9) and the urban water supply capacities derived using a non-linear fitting method (Marquardt, 1963). Cost-related parameters for surface water and groundwater supply (4×9) were set according to the recommendations by Kirshen et al. (2004), while those for stormwater and rainwater harvesting (2×9) followed the recommendations of Dallman et al. (2016). Parameters for sewage drainage costs (2×9) were collected, processed, and calculated from various open materials on the websites of the associated water agencies. According to the existing hydrologic regimes and water use framework in the study sites, there are various other water users with different purposes in addition to the chosen urban areas to share water resources, such as agricultural irrigation, commercial navigation, and ecological conservation. Therefore, we set set based on Guo et al. (2014). Due to a lack of specific data for each urban area, these cost parameters were uniformly applied. Water availability-related parameters (24×9) were determined by setting the minimum storage levels for surface and groundwater withdrawals (24×9) water withdrawals based on the minimum monthly historical streamflow from the USGS datasets using the above same method. Minimum storage levels for groundwater withdrawals were set based on the various materials and databases related to the water level regulation, water use, and streamflow. In addition, the mean depths of wells. Water supply capacity-related parameters

(2×9) were set equal to the corresponding maximum monthly indoor water demand. The ratio of soil moisture for plant demand (1×9) was uniformly set at 0.31 based on Mitchell et al. (2001) recommendations. Additionally, for the parameters of agent-based model for WM, as shown in Table B3 in Appendix C, minimum and maximum historical streamflow data (24×9) ~~the parameters of the WM agent~~ were obtained from the USGS datasets using the above same method.

725 3.4 Model and algorithm setup

In the framework, the other parameters of the UWB-SM and the Muskingum-Cunge routing model were evaluated ~~by model calibration to hydrologic data (See Tab. C3 and C6 in Appendix D1 and ??).~~ through model calibration and validation using estimated historical streamflow data via the above same method.

For the calibration parameters of UWB-SM~~(13 × 9), they~~, as detailed in Table C3 in Appendix C, these were obtained by
730 calibrating and validating the UWB-SM against ~~the monthly outflow of an urban area, which is estimated. Notice that the outflow of an urban area was estimated via using a map correlation method (Archfield and Vogel, 2010) to available monthly streamflow observations from the associated USGS stations in the study system because of the location difference between the urban area's outlet and the associated USGS stations. In this study, time series of observed and simulated outflow at each urban area are analyzed for both calibration (1996–2020) and validation (1971–1995) periods. In the process of the estimated~~
735 historical monthly outflow data derived from USGS datasets. The calibration process utilized estimated monthly inflow from USGS databases, and monthly rainfall data from NOAA databases as inputs for the UWB-SM~~calibration, the GI construction and the relevant~~. During calibration, rainwater and stormwater ~~supply decisions are not considered, and monthly surface and groundwater withdrawals are set as actual water use data. Model calibration is performed using the proposed S-APSO framework to solve a specified single objective optimization – maximization of the modified Kling-Gupta Efficiency (He, 2019)~~
740 ~~Similar to the~~ supplies were excluded, and urban water demands (both indoor and outdoor) were assumed to be met solely through surface water and groundwater supplies, with a set ratio of 1:1. Monthly surface water and groundwater supply amounts were determined based on this setting. The simulated monthly outflow data from the UWB-SM ~~, the parameters of the were then compared with the estimated outflow data for calibration and validation. Detailed calibration and validation results are presented in Tab 2.~~

745 For the calibration parameters of the Muskingum-Cunge ~~equations were also calibrated based on the estimated monthly outflows.~~ routing model, as shown in Table C6 in Appendix C, these were obtained by calibrating and validating the model using estimated historical monthly outflow data from the upstream urban area and inflow data for the adjacent downstream urban area. Detailed calibration and validation results for the Muskingum-Cunge routing model are also provided in Tab 2.

Furthermore, to guarantee the proposed algorithm's effectiveness, there are also algorithm parameters to be calibrated in
750 this case. For the S-APSO, only population size and iteration number need to be determined due to the use of the adaptive parameter scheme. They were calibrated based on the results of a trial-and-error algorithm parameter calibration procedure that was carried out to observe the behavior of the algorithm at different parameter settings (Beielstein et al., 2002). Therefore, the calibrated parameters for the S-APSO were selected as follows: the population size and the iteration number are set as 50 and 200, respectively. Three numerical experiments mentioned above were conducted and run on an 8-Core Intel Core i7,

Table 2. Details and representative results of calibration and validation for two hydrologic models

Note: * represents the representative results for the two hydrologic models for urban area 1. KGE, NSE, R and B represents four types of performance metrics - the Kling-Gupta Efficiency (Kling et al., 2012), the Nash-Sutcliffe coefficient of efficiency (Nash and Sutcliffe, 1970), the correlation coefficient between simulated and observed streamflow and the percent bias (Gupta et al., 1999), respectively.

| Model | UWB-SM | Muskingum-Cunge routing model |
|-----------------------|--|--------------------------------------|
| Calibration parameter | See Tab. C3 | See Tab. C6 |
| Dimensions | 12×9 | 3×9 |
| Calibration data | Estimated monthly outflow; | Estimated monthly inflow and outflow |
| Data periods | Calibration (1996-2020) and Validation (1971-1995) | |
| Data sources | USGS Current Water Data for the Nation database | |
| Calibration objective | Maximization of the KGE (Kling et al., 2012) | |
| Calibration algorithm | S-APSO framework (See Appendix D2) | |
| Validation results* | KGE=0.66, NSE=0.46, R=0.8, B=4.1%; | KGE=0.78, NSE=0.51, R=0.82, B=3.8% |

755 **4 Results and discussion**

The results of these experiments and the associated analysis are discussed as follows.

4.1 Characteristics of city-scale IGWM in changing environments

The classified results of UWMs’ decisions of IGWM to different environments are illustrated in Fig. 5 (a). As Fig. 5 (a) shows, there are four IGWM patterns for UWMs in response to the different combinations of upstream inflow and rainfall inputs. The light blue dots region is defined as pattern 1, which represents the similar reactions of UWMs in the decision-making of IGWM to the high upstream inflow and rainfall inputs. The green dots region indicates pattern 2, indicating the consistent behavior of IGWM for UWMs to the low upstream inflow and high precipitation settings. Similarly, patterns 3 and 4 are set in the dark blue and yellow dots region, which denotes the analogous decision-makings of IGWM for UWMs in the study site under high (low) inflow and low (low) rainfall conditions respectively. The result indicates the homogeneous behavior of city-scale IGWM for all UWMs in the relatively extreme hydroclimatic conditions in the study region. ~~This phenomenon might be that most urban areas in the study area have similar costs of accessing the four types of water sources, mainly because they are located in the same states, Minnesota and Wisconsin. Economically, the similar costs of water resources lead to similar responses of UWMs in IGWM under given hydrologic conditions (Loueks and Van Beek, 2017). In addition, the grey dots region is a transition area in which UWMs may make different IGWM decisions to minimize water use costs under some hydroclimatic settings. This might be because of the physical differences among urban areas in the study area, such as impervious ratios, locations, urban landscape, and water demands, which affect available amounts of different water resources, thereby changing IGWM decisions under some specific environments.~~

~~Characteristics of four city-scale IGWM in changing environments. **Note:** -In Fig. 5 (e), Ratio of system water output to input is used to measure the overall balance in an urban area, which is calculated as; the system water output divided by the system water input, where system water output is equal to the sum of monthly evapotranspiration, water consumption and outflow, and system water input is the sum of monthly upstream inflow and rainfall; Ratio of rainfall harvesting is set as the~~

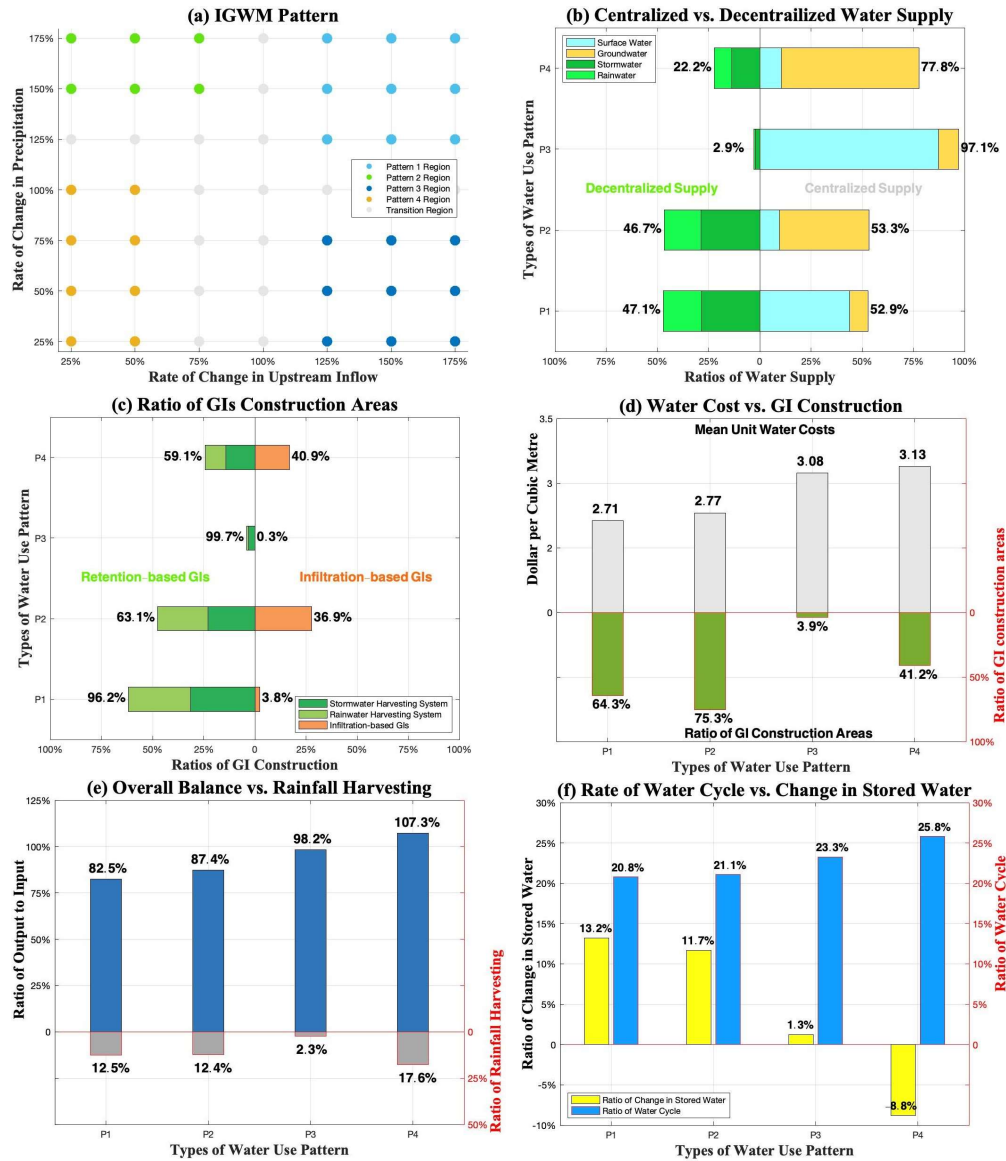


Figure 5. The classified results of city-scale IGWM in different environments. a) Four IGWM patterns can be classified based on four color dots. b) - d) Different ratios of water supply portfolios and GIs construction and the costs of water use are shown in the four patterns. e) - f) Four patterns significantly influence the urban water cycle.

Note: - In Fig. 5 (e), the *Ratio of system water output to input* measures urban water balance, calculated as the sum of monthly evapotranspiration, consumption, and outflow (output) divided by the sum of monthly upstream inflow and rainfall (input). The *Ratio of rainfall harvesting* is the ratio of combined stormwater and rainwater supply to total rainfall. - In Fig. 5 (f), the *Ratio of water cycle* is the annual ratio of total water supply (surface water, groundwater, stormwater, and rainwater) to total urban stored water (sum of monthly storage across seven units: roof, other surfaces, rainwater, stormwater, soil layer, aquifer, and river). The *Ratio of change in stored water* is the difference between stored water in the last and first months, divided by stored water in the first month.

ratio of the sum of stormwater and rainwater supply to total rainfall. - In Fig. 5 (f), *Ratio of water cycle* is set as the ratio of the total amounts of water supply to the total amounts of urban stored water in a year, where the total amounts of water supply is

780 set as the sum of the amounts of surface water, groundwater, stormwater and rainwater supply, and the total amounts of urban stored water is defined as the sum of the monthly amounts of water storage of seven well-defined water storage units – roof, other surfaces, rainwater, stormwater, soil layer, aquifer and river; *Ratio of change in stored water* is calculated as follows; the difference between the amounts of urban stored water in the last and first months divided by that in the first month, where the amounts of urban stored water in the first and last months are equal to the sum of the amounts of water storage of seven well-defined water storage units in the first and last months.

785 The characteristics of the four IGWM patterns mentioned above are shown in Fig 5 (b) - (f). The ratios of water supply portfolios and GIs construction in the four patterns are illustrated in Fig 5 (b) - (d). There are large distinctions in the IGWM between the four patterns; In pattern 1, centralized and decentralized water account for 52.9% and 47.1% of total water supply, respectively, which means that stormwater and rainwater are widely utilized. More than 80.0% of centralized water supply is from surface water. In the aspects of GI construction, over three-fifths of available urban areas are used to develop stormwater and rainwater harvesting systems, which accounts for 96.2% of total GIs construction areas. These results show the features responses of IGWM to the high upstream inflow and rainfall inputs - UWMs prefer to use stormwater and rainwater directly to meet urban non-potable water demand by stormwater and rainwater harvesting systems for the sake of cost, and to supply surface water to meet potable water demand. In pattern 2, similar to pattern 1, stormwater and rainwater are also heavily used directly to satisfy non-potable demand. At the same time, groundwater is the main potable water resource due to the low upstream inflow input. Accordingly, over 75% of available areas are utilized for GIs development, and 35.9% of which, unlike 795 pattern 1, is for infiltration-based GIs for groundwater recharge. In pattern 3, stormwater and rainwater are hardly used (only 2.9% of total water supply), and the construction of the associated GIs (only 3.9% of available urban areas) is also limited due to the scarcity of precipitation. The surface water resource is dominant in urban water supply, accounting for 87.2% of total water withdrawals because of the high upstream flow inputs. In comparison, stormwater and rainwater are partially used (22.2% of 800 total water supply) directly or indirectly by constructing GIs at a moderate level (41.2% of available urban areas) in pattern 4. This might be because UWMs have to collect and use all kinds of available water resources as much as possible when system water inputs - rainfall and upstream inflow - are low. Hence, the groundwater is supplied more extensively for maintaining water supply steadily. It is worth mentioning that infiltration-based GIs, which account for 16% of total GI construction areas, are, to a great extent, built to enhance aquifer recharge for reducing the costs of groundwater abstraction. Besides, Fig 5 (d) 805 also illustrates the mean IGWM costs per unit of water in the four patterns. Undoubtedly, the costs of the pattern under high system water inputs conditions are lower than those under low water inputs.

~~Also, we investigate the impacts of the four IGWM patterns on the urban hydrologic regime.~~ Fig. 5 (e) and (d) illustrates the four indexes used to measure urban water cycle defined by Kenway et al. (2011) under these patterns, which show that the impacts of the four IGWM patterns on the urban water cycle. As Fig. 5 (e) shows, the ratios of system water output to input and rainfall harvesting vary from pattern to pattern. Except pattern 4, the ratio of system water output to input of the rest of the patterns are smaller than one, which means that the relevant IGWM patterns can increase water storage in an urban system, especially the pattern 1 and 2 with relatively large areas of GIs - 17.5% and 12.6% of water inputs are stored, respectively, which, to some extent, decrease the outflow of the urban catchment. The result is consistent with the Glendenning et al. (2012)

results. However, in contrast to the other patterns, the ratio of system water output to input of the pattern 4 indicates the decreases in urban water storage. ~~This might be because of the over-exploitation of groundwater under low upstream inflow and precipitation conditions.~~ In this circumstance, to build a small range of infiltration-based GIs (i.e., The ratio of rainfall harvesting = 17.6%) to increase groundwater recharge is limited. Besides, as shown in Fig. 5 (f), the ratios of water cycle increase orderly from the pattern 1 to 4, and the associated ratios of change in stored water have an opposite shift. These results also are consistent with the above results in Fig. 5 (e).

~~All in all, these results show the interactions and feedbacks between the urban areas and the corresponding~~ Our simulation study demonstrates the reasonable responses of UWM agents to different hydroclimatic settings in city-scale IGWM. Specifically, the hydroclimatic environment determines the ~~available amounts~~ availability of the four types of water sources, thereby ~~affecting UWMs' selections~~ influencing UWMs' selection of IGWM patterns from an economic perspective. ~~Also, Furthermore,~~ the IGWM patterns chosen by UWMs can ~~change urban hydrologic regimes, which can alter the urban water cycle, which,~~ in turn, ~~shifts the watershed environment.~~ In addition, these results demonstrate that the proposed model can simulate the UWMs' decision-making of IGWM in changing settings affects the hydrologic environment of the watershed.

4.2 Characteristics of inter-city-scale IGWM in changing environments

The results of the inter-city-scale IGWM in the two cases are shown in Tab. 3. The ratios of water supply portfolios of all urban ~~areas~~ area in the two scenarios are shown in the 2nd-5th and 9th-10th rows of Tab. 3. In the case without GIs - a control group, surface water use fractions gradually decrease from the upstream to the downstream areas. For example, the ratios of surface water in the urban area 1, 5, and 9 are 0.85, 0.79, and 0.73, respectively. ~~There is~~ It might be because of a trend that the available amounts of surface water gradually decrease along with the river (See the blue line in Fig. 6 a). These results indicate the adverse impacts of upstream water users on the downstream water users in surface water withdrawals. That is, water extraction from a stream in the upstream areas reduces the available amounts of surface water in the downstream regions, which would increase the costs of surface water withdrawal for the downstream urban areas, thereby forcing them to substitute other water resources, such as groundwater. In contrast, in the case with GIs - an experiment group, the fractions of surface water use appear to be independent of the study area locations due to stormwater and rainwater use via GIs. However, it might aggravate the adverse impacts - ~~up-and-downstream~~ upstream-downstream imbalance of available surface water. For example, the ratios of surface water use markedly decrease in the downstream urban areas, especially in urban areas 6, 8, and 9, which have adopted the IGWM pattern 4 - the high ratio of groundwater use. This may be because the upstream UWMs prefer to use stormwater and rainwater resources through developing GIs, such as the IGWM pattern 1 and 2, to minimize the costs of water use (Cooley et al., 2019). However, as mentioned before, the IGWM pattern 1 and 2 can reduce the outflow of urban subcatchment (See Fig. 5 e), which might worsen the decrease of available surface water in the downstream region (See the red line in Fig. 6 a). Besides, the 8th and 12th rows of Tab. 3 also shows the Gini coefficients (Eq. F1) in the two scenarios - 0.0129 and 0.0169, indicating that the GIs construction to use stormwater and rainwater intensifies the imbalance in water use in the study area.

Table 3. Results of the inter-city-scale IGWM in the two scenarios

| 01 | Scenarios | Urban Area i | | $i = 1$ | $i = 2$ | $i = 3$ | $i = 4$ | $i = 5$ | $i = 6$ | $i = 7$ | $i = 8$ | $i = 9$ | |
|----|-----------------------------------|--|---------------|---------|---------|---------|---------|---------|---------|---------|---------|---------|--|
| 02 | multiagent systems with GIs | Ratio of water supply portfolios | Surface water | 0.39 | 0.81 | 0.38 | 0.72 | 0.11 | 0.09 | 0.55 | 0.13 | 0.12 | |
| 03 | | | Groundwater | 0.13 | 0.14 | 0.12 | 0.17 | 0.46 | 0.68 | 0.27 | 0.66 | 0.63 | |
| 04 | | | Stormwater | 0.28 | 0.01 | 0.32 | 0.09 | 0.25 | 0.15 | 0.11 | 0.13 | 0.18 | |
| 05 | | | Rainwater | 0.19 | 0.04 | 0.19 | 0.05 | 0.19 | 0.08 | 0.08 | 0.08 | 0.07 | |
| 06 | | Water use pattern | | P1 | P3 | P1 | P3 | P2 | P4 | P3 | P4 | P4 | |
| 07 | | Mean unit water costs | | 2.89 | 2.91 | 2.96 | 3.07 | 3.03 | 3.11 | 3.09 | 3.15 | 3.12 | |
| 08 | | Gini coefficient | | 0.0129 | | | | | | | | | |
| 09 | | Ratio of water supply portfolios | Surface water | 0.85 | 0.87 | 0.83 | 0.81 | 0.79 | 0.70 | 0.75 | 0.72 | 0.73 | |
| 10 | Groundwater | | 0.15 | 0.13 | 0.17 | 0.19 | 0.22 | 0.30 | 0.25 | 0.28 | 0.27 | | |
| 11 | | Mean unit water costs | | 2.98 | 2.96 | 3.03 | 3.10 | 3.09 | 3.14 | 3.11 | 3.18 | 3.14 | |
| 12 | | Gini coefficient | | 0.0169 | | | | | | | | | |

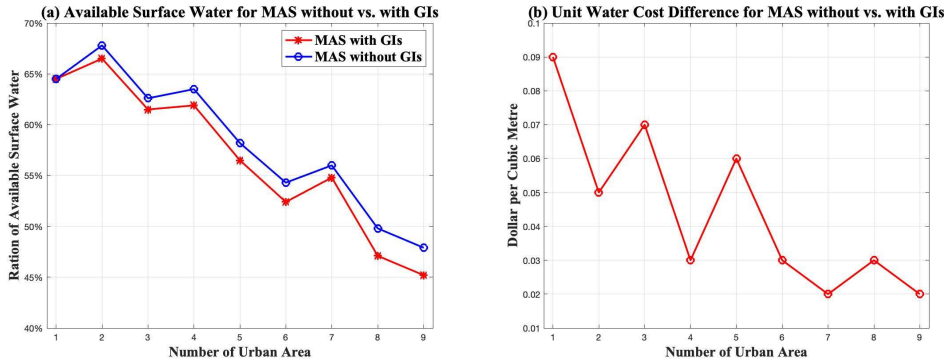
Note: · *Ratio of water supply portfolios* for urban area i is calculated as follows; The amounts of a type of water source supply divided by the total amounts of water supply in the urban area i .

· *Mean unit water costs* for urban area i is obtained as follows; The total IGWM costs divided by the total amounts of water supply in the urban area i .

The 7th and 11th rows of Tab. 3 illustrate the IGWM cost per unit of water for each urban area in the two scenarios. There is a trend that the unit water costs constantly increase from the upstream to the downstream region, indicating the adverse impacts of the ~~up-and-downstream-upstream-downstream~~ imbalance of the surface water on the cost of water use for the downstream urban areas. In comparison, the costs of water use in the ~~MAS-multiagent systems~~ with GIs are smaller than those without no GIs for all urban ~~areasarea~~. In contrast, the differences in these costs between the two scenarios continuously decrease from the urban area 1 to 9 (See ~~the red line in~~ Fig. 6 b). The reasons behind these results might be that there are two main factors - upstream inflow and GIs - affecting the costs of water use in the ~~MAS-UWMmultiagent system for UWMs~~, especially for the downstream UWM agents. In general, the upstream inflow reduction can decrease the amounts of surface water, thereby increasing the cost of water use for the downstream UWMs. On the contrary, rainwater and stormwater use via GIs can increase the available amounts of water resources and decrease water supply costs. In the ~~MAS-UWMmultiagent system for UWMs~~, especially for the downstream UWM agents, the cumulative effect of the upstream IGWM decision behavior on streamflow gradually amplifies along the river. In contrast, the impact of the GIs on rainfall resource use generally remains stable due to the limitations of climatic, physical, socioeconomic conditions. Therefore, the combination of the two effects might lead to a gradual decrease in the impact of GIs on the cost of water use along with the river.

~~Our results illustrate the effects of inter-city-scale IGWM on the cost of water use and the equity of water resource distribution across urban areas. Specifically, 1) there is a trend of upstream-downstream imbalance in accessing water resources, which may be exacerbated by the development of GIs; 2) On a city scale, the development of GIs can reduce the cost of water use. However, on a watershed scale, it may also exacerbate inequity in water resource allocation among urban areas.~~

~~Next, we explored the influences of various social and hydroclimatic settings on the dynamics of the MAS-UWM in a watershed-scale IGWM. A sensitivity analysis of the MAS-UWM model in the study case was run.~~



Available surface water and unit

water cost difference in the two scenarios **Note:** –In Fig. 6 (a), Ratio of available surface water for urban area is set as the average of the ratio of the available monthly storage levels of river for water withdraw to the maximum theoretical that levels in an urban area. –In Fig. 6 (b), Unit water cost difference for urban area calculated as follows; The difference of the mean unit IGWM costs in the urban area in the scenarios of the MAS without and with GIs.

Figure 6. Available surface water and unit water cost difference in the two scenarios. a) There is a trend that the available amounts of surface water gradually decrease along with the river, and GIs development might worsen the trend. b) There is a trend that costs between the two scenarios continuously decrease along with river.

Note: · In Fig. 6 (a), Ratio of available surface water for urban area is set as the average of the ratio of the available monthly storage levels of river for water withdraw to the maximum theoretical that levels in an urban area.

· In Fig. 6 (b), Unit water cost difference for urban area calculated as follows; The difference of the mean unit IGWM costs in the urban area in the scenarios of the multiagent systems without and with GIs.

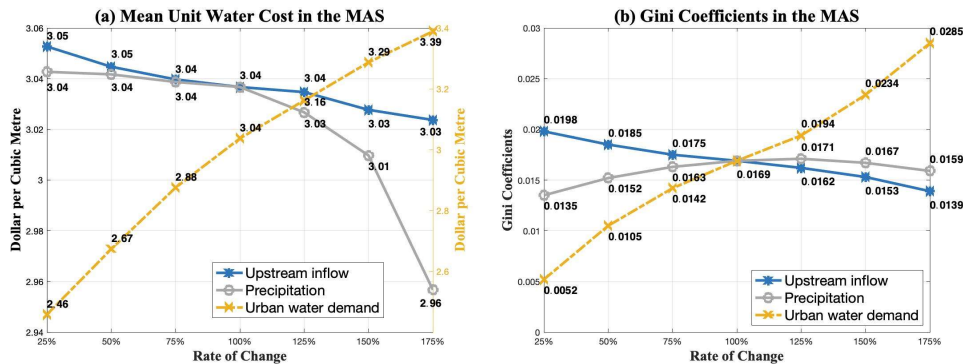


Figure 7. Changes in unit water costs and Gini coefficients under different social and hydroclimatic settings. a) These is a non-linear inverse relationship between the cost of water use and the system water inputs. b) There is an inverted U-shaped curve for the Gini coefficient when the precipitation increases

· **Note:** In Fig. 7 (a), Mean unit water costs in the multiagent system is obtained as; The total IGWM cost divided by the total amounts of water supply in the multiagent system.

The mean unit costs and the Gini coefficients in the MAS-UWM multiagent system for UWMs under different precipitation, upstream inflow, and urban water inputs are illustrated in Fig. 7 (a) and (b).

Changes in unit water costs and Gini coefficients under different social and hydroclimatic settings. -- **Note:** In Fig. 7 (a), Mean unit water costs in the MAS is obtained as; The total IGWM cost divided by the total amounts of water supply in the MAS.

, which shows the influences of different social and hydroclimatic settings on the socio-hydrologic dynamics of the watershed in the context of inter-city-scale IGWM. In Fig. 7 (a), the blue and grey lines represent the changes in the mean costs per unit of water use in the MAS-UWM-all urban area under different precipitation and upstream inflow inputs. It shows a non-linear inverse relationship between the cost of water use and the system water inputs - the mean cost of water use in a watershed-scale IGWM decreases with the increases in both watershed upstream inflow and rainfall. Notice that the cost of water use in the MAS-UWM-multiagent system for UWMs is more sensitive to the precipitation than upstream inflow. Notably, the mean cost of water use decreases from 3.01 $\$/m^3$ to 2.96 $\$/m^3$ when the rainfall increases from 150% to 175%. It appears that rainfall inputs, when it goes beyond a certain threshold, might have a profound effect on the IGWM cost of the MAS-UWM-multiagent system for UWMs. This might be due to that more and more UWMs can switch IGWM patterns from Pattern 3 or Pattern 4 to Pattern 1 or Pattern 2, with the available rainfall exceeding a given threshold, leading to a significant decline in water use costs. These results are consistent with the results in Fig. 5 (d). In comparison, as the yellow line in Fig. 7 (a) shows, the cost of water use in the MAS-UWM-all urban area is highly sensitive to the urban water demands. The increases in urban water demands are equivalent to the decreases in available water resources within an urban area, which greatly adds to the costs of water use.

Fig. 7 (b) shows the changes in the equity level of water use in the MAS-UWM-all urban area under different hydroclimatic and socioeconomic settings. The blue and grey lines in Fig. 7 (b) represent the trends of Gini coefficients in the MAS-UWM under mixed precipitation and upstream inflow conditions - the Gini coefficient curve it tends to proportionally decrease as the upstream inflow increases, while there is an inverted U-shaped curve for the Gini coefficient when the precipitation increases; it reached a peak (0.0171) when the ratio of the rainfall to the baseline is equal to 125%. On the side of the upstream inflow, these results show that the reduction in watershed upstream inflow harms the equity levels of water use in watershed-scale IGWM. The possible reason is that the Markov property of the MAS-UWM-multiagent system for UWMs has a cumulative effect on the reduction in surface water availability along with the river. It can, to some extent, amplify the surface water conflicts between the up-and-downstream-upstream-downstream urban areas as the watershed upstream inflow decreases. On the side of the precipitation, the impact of rainfall on the equity of water use in the MAS-UWM-resources distributions among urban areas is more complicated. The reasons for the increase in the Gini coefficient as the precipitation increase slightly might be that the water use costs for the upstream UWMs decrease remarkably by substituting stormwater and rainwater for surface and groundwater water as the rainfall increases. In contrast, in the downstream regions, the reduction in the relevant costs is limited because the cumulative effect of upstream inflow mentioned above limits the intention of the corresponding UWMs to switch IGWM patterns to use more rainfall resources economically. However, as the precipitation increases significantly, the abundant rainfall encourages the downstream UWMs to use stormwater and rainwater via GIs cost-effectively, reducing water use costs sharply, thereby making the watershed-scale IGWM more equitable. In comparison, the Gini coefficient in the MAS-UWM-all urban area is more sensitive to upstream inflow than rainfall. This is because the cumulative effect of upstream inflow might offset the impact of rainfall due to the Markov property of the MAS-UWM-multiagent system for UWMs.

~~In short, these results illustrate~~ Our results highlight the impact of different social and hydrologic settings on ~~IGWM at watershed scale; Hydrologically, the change in rainfall is~~ inter-city-scale IGWM. Hydrologically, changes in rainfall are more likely to influence the cost of water use in the study basin due to the relatively low cost of stormwater and rainwater resources. ~~Yet, the shift~~ Conversely, shifts in watershed upstream inflow ~~easily affects the equity level of water use in the MAS-UWM significantly affect the equity of water resource distribution among urban areas~~ because of the Markov property of the ~~MAS-UWM~~ multiagent system for UWMs. Socially, ~~the change in the~~ changes in urban water demands ~~has a profound effect on~~ have a profound impact on both the cost and equity of water ~~use in MAS-UWM because it is equivalent to resources in~~ inter-city-scale IGWM. These findings suggest that WM must pay closer attention to issues of upstream-downstream imbalance in accessing water resources, particularly in the context of GIs development and the combined effects of rainfall and upstream inflow, use of stormwater and rainwater in each urban area. This is especially critical under climate change conditions that drastically alter the probability distribution of streamflow.

915 4.3 Impacts of water policy on watershed-scale IGWM

~~The results of the policy simulation to the BL-MAS are shown in Tab. 4.~~

Table 4. Results of watershed-scale IGWM in the ~~BL-MAS~~ bi-level multiagent system.

| 01 | Equilibriums | Urban Area i | | $i = 1$ | $i = 2$ | $i = 3$ | $i = 4$ | $i = 5$ | $i = 6$ | $i = 7$ | $i = 8$ | $i = 9$ |
|----|---|----------------------------------|---------------|---------|---------|---------|---------|---------|---------|---------|---------|---------|
| 02 | Equilibrium 1 in the bi-level multiagent system | Ratio of water supply portfolios | Surface water | 0.50 | 0.72 | 0.64 | 0.61 | 0.40 | 0.14 | 0.55 | 0.62 | 0.31 |
| 03 | | | Groundwater | 0.14 | 0.18 | 0.16 | 0.20 | 0.30 | 0.59 | 0.24 | 0.15 | 0.47 |
| 03 | | | Stormwater | 0.19 | 0.03 | 0.09 | 0.13 | 0.14 | 0.16 | 0.12 | 0.14 | 0.16 |
| 05 | | | Rainwater | 0.17 | 0.07 | 0.11 | 0.06 | 0.16 | 0.11 | 0.10 | 0.09 | 0.07 |
| 06 | Equilibrium 2 in the bi-level multiagent system | Water use pattern | | P1 | P3 | P3 | P3 | P1 | P2 | P3 | P3 | P4 |
| 07 | | Mean unit water costs | | 3.05 | 3.06 | 3.06 | 3.07 | 3.06 | 3.07 | 3.06 | 3.07 | 3.07 |
| 08 | | Mean unit penalty fee | | 0.11 | 0.10 | 0.07 | 0.02 | 0.03 | 0.01 | 0.03 | 0.01 | 0.00 |
| 09 | | Gini coefficient | | 0.0011 | | | | | | | | |
| 10 | Equilibrium 1 in the bi-level multiagent system | Ratio of water supply portfolios | Surface water | 0.36 | 0.30 | 0.39 | 0.30 | 0.19 | 0.23 | 0.14 | 0.15 | 0.08 |
| 11 | | | Groundwater | 0.39 | 0.33 | 0.41 | 0.37 | 0.50 | 0.49 | 0.51 | 0.50 | 0.68 |
| 12 | | | Stormwater | 0.15 | 0.21 | 0.10 | 0.20 | 0.16 | 0.14 | 0.22 | 0.18 | 0.14 |
| 13 | | | Rainwater | 0.11 | 0.16 | 0.11 | 0.13 | 0.15 | 0.14 | 0.13 | 0.17 | 0.10 |
| 14 | Equilibrium 2 in the bi-level multiagent system | Water use pattern | | P4 | P2 | P4 | P2 | P4 | P2 | P4 | P2 | P4 |
| 15 | | Mean unit water costs | | 3.22 | 3.24 | 3.22 | 3.21 | 3.22 | 3.23 | 3.22 | 3.22 | 3.23 |
| 16 | | Mean unit penalty fee | | 0.28 | 0.29 | 0.19 | 0.13 | 0.14 | 0.09 | 0.09 | 0.03 | 0.05 |
| 17 | | Gini coefficient | | 0.0011 | | | | | | | | |

Note: · Mean unit penalty fee for urban area i is obtained as follows; The penalty fees divided by the total amounts of water supply in the urban area i .

The results of the policy simulation to the bi-level multiagent system are shown in Tab. 4. As Tab. 4 shows, there are ~~the~~ two Stackelberg equilibrium situations in the ~~BL-MAS~~ bi-level multiagent system, which means the two possible designs of the streamflow penalty strategies for the WM agent can achieve the minimum equity objective in the study region. An illustration of the water supply portfolios and the relevant water use patterns in all urban ~~areas~~ area under the two equilibrium situations is in the 2nd-6th and 10th-14th rows of Tab. 4. A spatial homogeneity in the UWMs' responses to the water policy can be

observed based on the associated ratios of water supply portfolios. For example, whether it is Equilibrium 1 or 2, most UWM agents prefer to adopt a similar IGWM pattern, such as Pattern 3 in Equilibrium 1 and the Pattern 2 and 4 in Equilibrium 2, in contrast to the case without the water policy (See the 6th row of Tab. 3). This might be because the streamflow penalty strategy has a similar effect on altering the IGWM cost of all urban ~~areas-area~~ in the study watershed, forcing some UWMs to change their water supply portfolio selections to a specific IGWM pattern to increase outflows of urban systems for avoiding high penalty fees. These findings can also be supported by the curves of the fractions of available surface water in each urban area (See in Fig. 8 a). As Fig. 8 (a) illustrates, the available amounts of surface water withdrawal for each urban area in the two equilibriums (i.e., the blue and green lines) are larger than that in the scenario without the water strategy (i.e., the red line).

The costs and equity levels in the ~~BL-MAS-study area~~ are shown in the 7th-9th and 15th-17th rows of Tab. 4. In the aspects of cost, to compare with the no policy case (See the 7th rows of Tab. 3), the mean costs per unit of water use of the ~~BL-MAS the study area~~ in the two equilibriums ($3.06 \text{ \$/m}^3$ and $3.22 \text{ \$/m}^3$) are higher than the cost in the no policy case ($3.04 \text{ \$/m}^3$). This is because some urban areas pay penalty fees, such as urban areas 1 and 2, and others switch IGWM patterns, such as urban area 3, which increases the water use cost. These results demonstrate the reactions of the UWMs to the water strategy set by the WM in IGWM at a watershed scale; the intervention of the water policy to the ~~MAS-UWM-multiagent system for UWMs~~ can force UWM agents to make a trade-off between the penalty fee and the IGWM cost in a city-scale IGWM. ~~That is, UWM agents have to alter urban water supply portfolios and GIs construction to reduce water storage and economically increase outflow, especially for the upstream UWM agents.~~ In the aspects of equity, undoubtedly, the Gini coefficients in the two equilibriums (0.0011) are the same, which are lower than that in the no policy case (0.0169, See the 8th rows of Tab. 3). It means that the two policy designs can mitigate the inequity of water sharing in the study region to some extent.

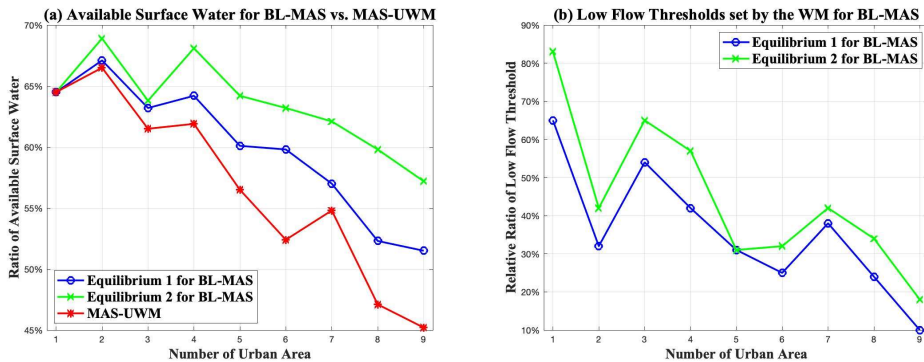


Figure 8. Available surface water and low flow threshold in the ~~BL-MASbi-level multiagent system~~.

Note: · In Fig. 8 (b), *Relative ratio of low flow threshold* for urban area calculated as follows; The average of the ratio of the monthly low flow threshold set by WM agent to the maximum theoretical that threshold in an urban area.

~~Next, we assessed the two equilibriums – the designs of the streamflow penalty strategy – by comparing them with their effects on watershed-scale IGWM. Hydrologically, as shown in the The 6th and 14th rows in Tab. 3 show that different effects of two streamflow penalty strategies on the decision makings of UWM agents for city-scale IGWM. That is, most UWM~~

agents prefer to select the IGWM pattern 3 - to withdraw more surface water - in equilibrium 1. In contrast, the UWM agents
 945 in equilibrium 2 incline to choose the Pattern 4, i.e., to extract more groundwater, which is easy to increase the outflows of
 urban subcatchment (See Fig. 5 e) to avoid the penalty fees. These results are consistent with the curves of the fraction of
 available surface water (See the blue and green lines in Fig. 8 a); The available amounts of surface water in the study area in
 the equilibrium 2 are higher than that in the equilibrium 1. Economically, the IGWM costs and the penalty fees per unit of
 water use in equilibrium 2 are greater than those in equilibrium 1. These results can be explained in part by the curves of the
 950 relative ratio of low flow thresholds in the two equilibriums (See Fig. 8 b); the low flow thresholds in the equilibrium 2 (i.e.,
 the green line) are higher than those in the equilibrium 1 (i.e., the blue line), which means that the policy in the equilibrium 2
 is more stringent than that in the equilibrium 1. As a result, the UWMs in equilibrium 2 have to further change IGWM patterns
 - over the withdrawal of groundwater and reduction in rainfall capture - to increase the outflow of the urban subcatchments
 to avoid the harsh penalty policy. It may cause over-reactions of the UWM agents in IGWM to the watershed water policy,
 955 thereby leading to the unnecessary costs of water use as well as the unreasonable water supply portfolios in the watershed.
 Therefore, the policy design in equilibrium 1 is regarded as a good watershed policy, but equilibrium 2 is not in the study area.

Lastly, we discussed the impacts of different hydroclimatic and institutional circumstances on the dynamics of the BL-MAS
 in a watershed-scale IGWM. Similar to Experiment 2, a sensitivity analysis of the BL-MAS model in the study region was
 conducted. In the experiment, the above equilibrium 1 of the BL-MAS was assumed as the baseline. As before, the changes
 960 in the hydroclimatic settings were simulated by using different ratios (i.e., from 50% to 150%) of mean total precipitation and
 watershed upstream inflow to the baseline. And six penalty rates—0.002 $\$/m^3$, 0.004 $\$/m^3$, 0.005 $\$/m^3$ (baseline), 0.006
 $\$/m^3$, 0.008 $\$/m^3$ and 0.010 $\$/m^3$ —were set to indicate the different institutional circumstances. Notice that we would select
 the equilibrium with the lowest mean cost per unit of water to represent the result of the BL-MAS in watershed-scale IGWM
 if there are several equilibriums of the BL-MAS under the same conditions.

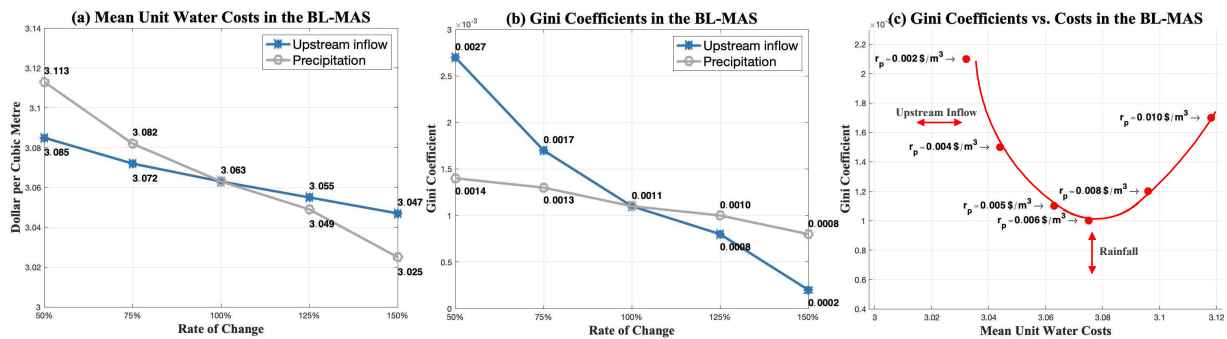


Figure 9. Changes in unit water costs and Gini coefficients under different institutional and hydroclimatic settings.

965 Fig. 9 (a) and (b) illustrate the mean unit water costs and the Gini coefficients of the BL-MAS study area under different
 upstream inflow and precipitation conditions, respectively. As Fig. 9 (a) and (b) show, both the costs of water use and the Gini
 coefficients of the BL-MAS study area decrease as the upstream inflow and the precipitation increase. This might be because

the increases in the upstream inflow and the precipitation not only enable the UWM agents to have more choices to make IGWM decisions to reduce the costs of water use but also mitigate the water conflicts among urban areas in the study site, encouraging the WM agent to loosen the water penalty policy. Besides, the cost of water use is more sensitive to the rainfall, while the Gini coefficient, in contrast, is easily affected by the alteration in upstream inflow, which ties in with the results in Fig. 7 (a) and (b).

The water use costs and the Gini coefficients of the equilibrium situations in the BL-MAS bi-level multiagent system under different penalty rates settings are illustrated in Fig. 9 (c). As Fig. 9 (c) shows, the costs of water use of the BL-MAS study area increase as the penalty rate increases, as expected. To avoid over-high penalty fees, the UWM agents have to alter the IGWM pattern further to increase the outflows of urban systems, thereby increasing water use costs. However, there is a U-shaped curve for the Gini coefficients when the penalty rate increases; the Gini coefficient reaches a nadir (0.001) when the penalty rate is $r_p = 0.006 \text{ \$/m}^3$. The possible reasons for these results are that the impact of the water strategy is too weak to affect UWMs' decision behavior of IGWM as the penalty rate is too low, whereas, over-high penalty rate might force UWMs to make unreasonable IGWM decisions, both of which fail to mitigate water conflicts between urban areas. Therefore, a suitable penalty rate is crucial in achieving equity in watershed-scale IGWM under a specific socio-hydrologic environment. For example, in the study, the reasonable penalty rate is set as $0.006 \text{ \$/m}^3$ by comparison with other alternative penalty rates.

5 Conclusions, limitations and future research

In this study, we focus on the issues of IGWM at three spatial scales. We developed a multiagent socio-hydrologic framework and the associated algorithm systems for simulating various dynamics of decision-makings of city-, inter-city- and Our results illustrate the impact of the streamflow penalty strategy prescribed by a WM agent on the cost of water use and the equity of water sharing in watershed-scale IGWM for UWMs and WM under changing socioeconomic and hydroclimatic circumstances. To be specific, 1) an ABM-UWM, which is made by coupling IGWM-OM and UWB-SM, is developed to optimize water supply portfolios and GIs construction simultaneously – city-scale IGWM – for UWM, and it can be solved by the improved PSO algorithm – S-APSO; 2) A MAS-UWM, which is made up of the multiple ABM-UWMs and the Muskingum-Cunge routing equations, is constructed to simulate watershed-scale IGWM via the interactions among UWMs in a river network – the Markov property, and it can be calculated via a multi-S-APSO framework. 3) A BL-MAS, which consists of the MAS-UWM and the WM agent model, is built to simulate dynamics of watershed-scale IGWM under a-. This strategy can increase the equity of water resource distribution, but it may also raise the cost of water use for some urban areas, particularly upstream areas. A well-designed streamflow penalty strategy can simultaneously reduce the cost of water use and enhance equity in water sharing compared to poorly designed strategies, which heavily depend on the penalty rate settings. These findings suggest that WM must develop effective watershed policies to regulate the decision-making of UWMs, particularly in upstream areas, to achieve equitable water sharing. Appropriate penalty rate settings are crucial to enhance policy effectiveness and prevent policy failure.

1000 4.1 Concluding remarks

To summarize the results and findings, we can draw the following concluding remarks:

- The cost-effectiveness of developing GIs to use rainwater in urban areas is highly dependent on the hydroclimatic conditions of the watershed.
- On a city scale, the development of GIs to use rainwater can reduce the cost of water use. However, on a watershed scale, it may exacerbate the inequity of water sharing among urban areas due to the Markov property of the multiagent system in inter-city-scale IGWM.
- The streamflow penalty strategy ~~through the interactions between UWMs and WM—Stackelberg game, which is dealt with via using a nested S-APSO structure.~~ set by WM to mitigate inequity in water sharing among urban areas is effective under suitable penalty rate settings. However, due to the bi-level multiagent system property in watershed-scale IGWM (i.e., Stackelberg game), there is a risk of policy failure.
- The proposed framework is flexible and can be adapted to other basins with different socio-hydrologic settings by adjusting parameters and model settings for various model components. For example, different water policies, such as water trading schemes, can be simulated within this framework by improving the agent-based model for WM.

1015 ~~The combination of the model and the algorithm framework allows us to examine how the hydrological and social settings affect IGWM at different spatial scales and policy effectiveness in a watershed via the UWM–urban environment, –UWM and –WM interactions, meanwhile, to observe how the decisions of IGWM affects the watershed environment. For an illustrative purpose, the multiagent framework is–~~

5 Conclusions, limitations and future research

1020 This study addresses three critical issues of IGWM at three spatial scales. We developed a multiagent socio-hydrologic framework that integrates two agent-based models for UWMs and WM, along with two hydrologic models. By integrating these components, we constructed agent-based models and multiagent systems to simulate decision-making processes for city-, inter-city-, and watershed-scale IGWM under varying socioeconomic and hydroclimatic conditions, thereby modeling the GIs-driven socio-hydrologic dynamics at three spatial scales. The framework was applied to the Minneapolis - La Crosse section of the Upper Mississippi River Basin, the ~~30 million people watershed in the US. Three simulating experiments to US.~~

1025 We designed three simulation experiments: the UWM agents model, the ~~MAS-UWM and the BL-MAS, are designed to test the framework's functionalities and capabilities for city and watershed-scale IGWM in the watershed. Through multiagent system for UWMs, and the bi-level multiagent system, to address the IGWM issues at the three spatial scales through various sensitivity, scenario, and comparison analyses, the results from the UWM agents model demonstrate the nonlinear relationships between city-scale IGWM decisions and hydroclimatic conditions. Even more importantly, they can capture the homogeneity~~

1030 in-UWMs' responses of IGWM to the similar hydrologic settings to characterize the city-scale IGWM in changing environment
via using a k-means clustering technique; Four. Results from Experiment 1 identified four types of city-scale IGWM patterns;
i.e., 1) the surface water and surface water-dominant, 2) the groundwater-rainwater hybrid, 3) the surface water, and 4) the
groundwater dominance, under the groundwater-dominant, under different upstream inflow and rainfall inputs are identified.
Also, the results from the MAS-UWM show the different impacts of rainfall and upstream inflow on conditions. Experiment 2
1035 demonstrated the effects of inter-city-scale IGWM on the cost of water use and the equity of water sharing among urban areas
under different social and hydroclimatic settings. Finally, Experiment 3 evaluated the impact of the streamflow penalty strategy
in watershed-scale IGWM; the change in rainfall is apt to affect the water use cost for the UWM agents, while the shift in
upstream inflow is more likely to affect the equity in water use in the study basin. Finally, the results from the BL-MAS display
the various available designs of the, highlighting the role of penalty rates in mitigating water conflicts between upstream and
1040 downstream urban areas. Insights from these results are informative for both WM and UWM in managing IGWM at three
spatial scales.

In short, 1) This study explored the role of GIs in urban and watershed water resource management, analyzing the potentials
and effects of rainwater and stormwater harvesting and usage in a watershed with multiple urban areas sharing and competing
for water resources. The findings reveal both positive and negative effects of GIs in IGWM across three spatial scales. On a
1045 city scale, the development of GIs to use rainwater can reduce the cost of water use. However, on a watershed scale, it may
exacerbate the inequity of water sharing among urban areas. 2) The study also investigated the impact of a streamflow penalty
strategy, all of which can achieve the minimum equity objective for the WM agent. Nevertheless, they can result in different
as an environmental economic-incentive policy in watershed-scale IGWM. The findings indicate that an effective balance of
water use cost and equity in water sharing can be achieved under suitable penalty rate settings. However, there is also a risk of
1050 policy failure, which could result in high water use costs for the UWM agents. The role of the penalty rate in mitigating water
conflict is also revealed in the BL-MAS. Insights from these results are informative for identifying effective watershed water
policies, such as setting a reasonable penalty rate and designing a good policy based on least-cost equilibrium and low equity
levels in the watershed. 3) The study developed a multiagent socio-hydrologic framework based on the core idea of describing
different types of interactions between agents and the environment in IGWM. This framework can model various types of
1055 social and hydrologic connections between multiple stakeholders, enabling the simulation of socio-hydrologic dynamics of
GIs-driven water resource systems at different scales. Therefore, the multiagent socio-hydrologic framework is flexible and
can address various IGWM-related issues in different basins with varying socioeconomic, hydroclimatic, and institutional
circumstances by incorporating new model components (e.g., new agent-based or hydrologic models) or adjusting settings for
existing components.

1060 This paper still has some limitations that can be addressed in future work. For example, in the UWM agent model, we
develop a 1) One limitation is that it only considers river connections between urban areas. The development of GIs can
also affect various hydrologic connections, such as groundwater interactions. By only considering river connections, we
may underestimate the effects of GIs on urban and watershed hydrology. Future research should integrate a groundwater
model, such as MODFLOW (Langevin et al., 2017), into the socio-hydrologic framework to simulate GIs-driven groundwater

connections between urban areas. 2) Another limitation is the use of a coarse time-resolution lumped urban hydrologic model (UWB-SM) to simulate the to simulate urban water cycle processes in the context of the combinations of water supply portfolios and GIs construction, which could lead to simulating results that are not accurate enough result in less accurate simulations. Future work can couple a should couple a fine time-resolution distributed urban water balance model, such as SUWMBA (Moravej et al., 2021), with the IGWM-OM to make water supply portfolio and GIs construction decisions more accurate and detailed for UWM. (Moravej et al., 2021), with the agent-based model for UWMs to enhance simulation accuracy. 3) The study area selected—a water-rich watershed in the US—presents another limitation. The widespread use of GIs for rainwater harvesting is not yet common in the US, and the proposed framework may also be suitable for addressing IGWM issues in water-stressed watersheds. These areas face serious water conflicts and may have more incentive to develop GIs for rainwater use. Future research should focus on applying the socio-hydrologic framework to a water-stressed basin.

Data availability. The data of the case study examined in this study have been obtained from the United States Geological Survey (USGS), the National Oceanic and Atmospheric Administration (NOAA), the United States Census Bureau, and the United States Environmental Protection Agency (U.S. EPA) databases. All of the data used to generate the figures in this paper are available publicly at: https://github.com/suoyuexh/Multiagent_IGWM.git.

Appendix A: ~~Details of agent-based model for IGWM at a city scale~~ Acronyms

- IGWM: Integrated green infrastructures and water resource management
- GIs: Green infrastructures
- UWM: Urban water manager
- WM: Watershed manager
- UWB-SM: Urban water balance simulation model

Appendix B: Details of two agent-based models

This appendix comprehensively elucidates the details of the two agent-based model at the city scale models for UWM and WM. It is meticulously described from various aspects including the notation, urban water balance simulation model, and the IGWM optimization model, along with the relevant solution approaches pertaining to this model the agent-based model for UWM and the agent-based model for WM.

B1 Notations

To facilitate the model presentation, some of the important notations used hereafter are summarized in Table B1 - ~~Table B2~~ B3.

Table B1. Decision variables of the UWM and WM agent.

| <i>Subscripts</i> | |
|--|--|
| t | Index of month for the IGWM, where $t = 1, 2, \dots, 12$; |
| i | Index of the UWM agent and the associated checkpoint, where $i = 1, 2, \dots, N$; |
| <i>Decision variables for the UWM agents</i> | |
| $w_s^i(t), W_s^i(t)$ | Monthly surface water supply of the UWM agent i in month t [m^3, mm]; |
| $w_g^i(t), W_g^i(t)$ | Monthly groundwater supply of the UWM agent i in month t [m^3, mm]; |
| $w_{rr}^i(t), W_{rr}^i(t)$ | Monthly rainwater supply of the UWM agent i in month t [m^3, mm]; |
| $w_{rs}^i(t), W_{rs}^i(t)$ | Monthly stormwater supply of the UWM agent i in month t [m^3, mm]; |
| IG^i | Area constructed infiltration-based GIs of the UWM agent i [km^2]; |
| RG_s^i | Area constructed stormwater harvesting systems of the UWM agent i [km^2]; |
| RG_r^i | Area constructed rainwater harvesting systems of the UWM agent i [km^2]; |
| <i>Decision variables for the WM agent</i> | |
| $S_q^i(t)$ | Low flow thresholds in month t at checkpoint i [m^3]. |

Table B2. Variables and parameters of the agent-based model for UWM

| <u><i>Cost-related parameters of GI systems</i></u> | |
|---|---|
| <u>c_{ig}, c_{rg}, c_{sg}</u> | <u>Mean annual construction cost of unit area for infiltration-based GIs and rainwater and stormwater harvesting systems [$\\$/km^2$];</u> |
| <u>e_{ig}, e_{rg}, e_{sg}</u> | <u>Cost scaling coefficient for infiltration-based GIs and rainwater and stormwater harvesting systems [<i>dimensionless</i>];</u> |
| <u><i>Cost-related parameters of water supply and sewage drainage</i></u> | |
| <u>c_{ri}, e_{ri}</u> | <u>Mean cost and associated scaling coefficient of unit surface water supply [$\\$/m^3, -$];</u> |
| <u>c_{gi}, e_{gi}</u> | <u>Mean cost and associated scaling coefficient of unit groundwater supply [$\\$/m^3, -$];</u> |
| <u>c_{rw}, c_{sw}</u> | <u>Mean cost of unit rainwater and stormwater supply [$\\$/m^3$];</u> |
| <u>c_{wd}, e_{wd}</u> | <u>Mean cost and associated scaling coefficient of unit wastewater drainage [$\\$/m^3, -$];</u> |
| <u><i>Water availability-related parameters</i></u> | |
| <u>S_{mina}, S_{minr}</u> | <u>Minimum storage level of aquifer and river for water withdraw [mm];</u> |
| <u><i>Water supply capacity-related parameters</i></u> | |
| <u>WC_a, WC_{ri}</u> | <u>Aquifer and River water supply capacity of grey infrastructure systems [mm];</u> |
| <u><i>Auxiliary variables of systems</i></u> | |
| <u>f_{sm}</u> | <u>Ratio of soil moisture for plant demand to saturated soil moisture [%];</u> |
| <u>C_{gi}, C_{si}, C_{wi}</u> | <u>Total annual costs of GIs development, water supply and wastewater drainage for the UWM agent i [$\\$];</u> |
| <u>TC_i</u> | <u>Total cost of IGWM of the UWM agent i [$\\$].</u> |
| <u>Note: $[-]$ represents dimensionless.</u> | |

B2 Agent-based model for UWM

Before model construction, the fundamental assumptions are given.

ASSUMPTION 1. Three types of GIs can only be built in specific urban areas.

Table B3. Parameters of the agent-based model for WM

| | |
|---------------------------------------|---|
| <i>Objective-related parameters</i> | |
| $Gini$ | Water allocation Gini coefficient index ; |
| r_p | Penalty rate in the watershed, [\$/m ³]; |
| P_i | Total annual penalty fees for the UWM agent i [\$/]; |
| <i>Constraints-related parameters</i> | |
| $SQ_{min}^i(t), SQ_{max}^i(t)$ | Minimum and maximum historical streamflow at checkpoint i in month t [m ³]. |

1095 ASSUMPTION 2. Four types of urban water demand need to be met via four types of water supply.

ASSUMPTION 3. All water resources for supply can only be withdrawn or collected in urban areas.

ASSUMPTION 4. The combined sewer system is considered in the urban system.

1100 Some of these assumptions are imposed for the simplicity of the model. Assumption 1 describes urban land features and the space limitations for the development of three types of GIs, which is consistent with corresponding settings of the UWB-SM (See Fig. 3 C). Assumption 2 is coherent with the associated hypothesis of the UWB-SM. Meanwhile, the irrigation demand of urban green space is also considered here. Assumption 3 indicates that inter-watershed water transfer schemes are not considered in the model for simplicity. Assumption 4 represents that the model would take the sum of stormwater and wastewater into account in the calculation of urban wastewater drainage cost. The relevant decision variables and parameters of the agent-based model for UWM are listed in Tab. B1 and B2, separately. Based on the above assumptions, using the UWM agent i as an example, the agent-based model for UWM model is formulated as a non-linear programming as follows:

$$\min_{W, GI} TC_i = C_{gi} + C_{si} + C_{wi} \quad (B1a)$$

$$s.t. \begin{cases} C_{gi} = c_{ig} \cdot (IG^i)^{e_{ig}} + c_{rg} \cdot (RG_r^i)^{e_{rg}} + c_{sg} \cdot (RG_s^i)^{e_{sg}}, & (01) \\ C_{si} = \sum_{t=1}^{12} [c_{ri} \cdot w_s^i(t)^{e_{ri}} + c_{gi} \cdot w_g^i(t)^{e_{gi}} + c_{rw} \cdot w_{rr}^i(t) + c_{sw} \cdot w_{rs}^i(t)], & (02) \\ C_{wi} = \sum_{t=1}^{12} c_{wd} \cdot [q_r(t) + q_{wd}(t)]^{e_{wd}}, & (03) \\ w_s^i(t) = 1000 \cdot A_u^i \cdot W_s^i(t), w_g^i(t) = 1000 \cdot A_u^i \cdot W_g^i(t), & \forall t \quad (04) \\ w_{rr}^i(t) = 1000 \cdot A_u^i \cdot W_{rr}^i(t), w_{rs}^i(t) = 1000 \cdot A_u^i \cdot W_{rs}^i(t), & \forall t \quad (05) \\ q_r(t) = 1000 \cdot A_u^i \cdot [Q_r(t)]^*, q_{wd}(t) = 1000 \cdot A_u^i \cdot [Q_{wd}(t)]^*, & \forall t \quad (06) \\ 0 \leq IG^i \leq r_{imax} \cdot A_o, 0 \leq RG_r^i \leq r_{rmax} \cdot A_r, 0 \leq RG_s^i \leq r_{smax} \cdot A_u, & (07) \\ 0 \leq W_s^i(t) \leq \max[0, \min([S_{ri}(t-1)]^* + Q_{ri}(t) - S_{minr}, WC_{ri})], & \forall t \quad (08) \\ 0 \leq W_g^i(t) \leq \max[0, \min([S_a(t-1)]^* - S_{mina}, WC_a)], & \forall t \quad (09) \\ 0 \leq W_{rr}^i(t) \leq [S_{gr}(t-1)]^* + \frac{RG_r^i}{A_u} \cdot P_g(t), & \forall t \quad (10) \\ 0 \leq W_{rs}^i(t) \leq [S_{gs}(t-1)]^* + \frac{RG_s^i}{A_u} \cdot [Q_{ru}(t)]^*, & \forall t \quad (11) \\ (1 - r_{dl}) \cdot [w_s^i(t) + w_g^i(t)] \geq D_{id}(t), & \forall t \quad (12) \\ (1 - r_{dl}) \cdot [w_s^i(t) + w_g^i(t)] + w_{rr}^i(t) + w_{rs}^i(t) \geq D_{id}(t) + D_{in}(t) + D_o(t), & \forall t \quad (13) \\ f_{sm} \cdot (1 - [f_{sat}(t)]^*) \cdot S_{smax} \leq [S_s(t)]^*, & \forall t \quad (14) \end{cases} \quad (B1b)$$

where $[-]^*$ represents that the parameter is from simulation results of the UWB-SM. Equation (C10) represents the objective function of the model, which aims to minimize the annual IGWM cost for the UWM agent. This cost is comprised of GI construction (C_{gi}), water supply (C_{si}), and wastewater drainage costs (C_{wi}). The calculation methods for these three costs are presented in the first to third rows of Equation (B1b). The fourth to sixth rows of Eq. B1b indicate the unit conversion

1110 process from millimeters ($[mm]$) to cubic meters ($[m^3]$), which is essential for coupling the UWB-SM (using the unit $[mm]$)
with the agent-based model for UWM (using the unit $[m^3]$). The seventh row of Eq. (B1b) establishes the constraints for GI
construction. Meanwhile, the eighth to eleventh rows describe the water supply constraints for surface water, groundwater,
rainwater, and stormwater withdrawals, respectively. Lastly, the twelfth to fourteenth rows of the equation outline the water
1115 demand constraints concerning potable water demand, total water demand, and irrigation water demand. Notice that irrigation
demand within urban areas only refers to the water needed for maintaining vegetation in both large-scale and small-scale
infiltration-based GIs. Large-scale GIs include street trees, urban green spaces, parks, and gardens etc., while small-scale GIs
encompass green roofs, rain gardens, and bioretention systems etc. It can be estimated via using the minimum storage level of
shallow soil layer for meeting basic water demands of plant.

B3 Agent-based model for WM

1120 The agent-based model for WM is discussed in detail in the following. The relevant hypotheses for constructing the model are
given.

ASSUMPTION 1. The flow of each urban catchment at the outlet is checked.

ASSUMPTION 2. Water withdrawal limit is not considered in the model.

Assumption 1 simplifies our models as WM set low flow thresholds of each urban area at the outlet. For Assumption
1125 2, computational complexity may be high in optimization of policy portfolio (setting water withdrawal limits and low flow
thresholds) for a WM agent model, especially when it is integrated into the multiagent system for UWMs. Also, a policy
limiting the water withdrawal of urban areas, as a mandatory regulation, generally relies on other water users' activities within a
watershed, such as agriculture sectors, which is beyond the scope of this study. Therefore, this paper considers water withdrawal
limits (i.e., the minimum storage levels of aquifer and river) as UWM agent models' specific parameters (See the 8th and 9th
1130 rows of Eq. B1b).

As demonstrated in the above assumptions, a WM agent model is used to describe how a WM set a watershed management
policy - a streamflow penalty strategy - to regulate all UWM agents' decision behavior of IGWM in a watershed. That is, a
WM limits water abstraction decisions of each UWM agent in the period via prescribing a series of low streamflow thresholds
in associated hydrological stations based on hydrologic states; If streamflow in outlet for an urban area is below its threshold,
1135 a penalty fee will be imposed on the UWM agent. The strategy, in theory, can force UWM agents to recognize one or more
of the externalities caused by IGWM, thereby adjusting their IGWM decisions because it can, to some extent, determine the
cost of IGWM (Baumol et al., 1988). The WM can share fair water resources among urban areas in a watershed by setting a
rational streamflow penalty strategy that affects all UWMs' decisions. Therefore, And details of the objective and constraints
of the agent-based model for WM are illustrated as follows.

1140 **Equity objective:** The Gini coefficient is widely used to assess resource allocation inequality (Gini, 1921; Nishi et al., 2015)
. Therefore, the WM agent model uses a water allocation Gini coefficient index proposed by Hu et al. (2016) and Xu et al. (2019)
- the equitable sharing of the used water quantity for each unit of cost - to measure equity of water sharing in watershed-scale
IGWM. Based on the definition of the index, to minimize the Gini coefficient means maximal fairness of water resources

1145 distributions in a watershed; accordingly, the minimization of the equity objective for the WM can be expressed mathematically as follows.

$$\min_{S_q^i} Gini = \frac{1}{2 \cdot N \cdot \sum_{i=1}^N \frac{\sum_{t=1}^{12} [w_s^i(t) + w_g^i(t) + w_{rr}^i(t) + w_{rs}^i(t)]}{TC_i}} \cdot \sum_{i=1}^N \sum_{j=1}^N \left| \frac{\sum_{t=1}^{12} [w_s^i(t) + w_g^i(t) + w_{rr}^i(t) + w_{rs}^i(t)]}{TC_i} - \frac{\sum_{t=1}^{12} [w_s^j(t) + w_g^j(t) + w_{rr}^j(t) + w_{rs}^j(t)]}{TC_j} \right|. \quad (B2)$$

Streamflow constraints: The WM specifies the low streamflow thresholds at each checkpoint, which should adapt to actual hydrologic states. Therefore, the low streamflow thresholds at each checkpoint cannot exceed the associated maximal historical streamflow and cannot be below the minimal one in each month:

$$SQ_{min}^i(t) \leq S_q^i \leq SQ_{max}^i(t). \quad \forall t, i \quad (B3)$$

In short, the WM agent model is represented as follows:

$$\min_{S_q^i} Gini = \frac{1}{2 \cdot N \cdot \sum_{i=1}^N \frac{\sum_{t=1}^{12} [w_s^i(t) + w_g^i(t) + w_{rr}^i(t) + w_{rs}^i(t)]}{TC_i}} \cdot \sum_{i=1}^N \sum_{j=1}^N \left| \frac{\sum_{t=1}^{12} [w_s^i(t) + w_g^i(t) + w_{rr}^i(t) + w_{rs}^i(t)]}{TC_i} - \frac{\sum_{t=1}^{12} [w_s^j(t) + w_g^j(t) + w_{rr}^j(t) + w_{rs}^j(t)]}{TC_j} \right| \quad (B4a)$$

$$s.t. \left\{ \begin{array}{l} SQ_{min}^i(t) \leq S_q^i(t) \leq SQ_{max}^i(t), \quad \forall t, i \end{array} \right. \quad (B4b)$$

1150 Appendix C: Details of two hydrologic models

This appendix comprehensively elucidates the details of two hydrologic models - UWB-SM and Muskingum-Cunge routing model. It is described from various aspects including the notation, the UWB-SM and the Muskingum-Cunge routing model.

C1 Notations

To facilitate the model presentation, some of the important notations used hereafter are summarized in Table C1 - C6.

Table C1. Urban water demand and the hydroclimatic input parameters of the UWB-SM.

| | |
|--|---|
| <i>Input parameters for the urban water demand</i> | |
| $D_{id}(t), D_{in}(t)$ | Monthly indoor potable and non-potable water demand for in month t [m^3]; |
| $D_o(t)$ | Monthly outdoor water demand in month t [m^3]; |
| <i>Input parameters for the hydroclimatic data</i> | |
| $P_g(t)$ | Precipitation on the land cover in month t [mm]; |
| $Q_{ri}(t)$ | Upstream river inflow in month t [mm]; |
| E_p, ET_p | Mean potential evaporation and evapotranspiration on the impervious and pervious surfaces [mm]; |
| E_{imax} | Maximum interception evaporation on the pervious surfaces [mm]. |

Table C2. Measured parameters of the UWB-SM.

| | |
|--|--|
| <i>Urban area-related parameters</i> | |
| A_u, A_p | Urban total and the associated pervious surfaces area [km^2]; |
| r_n | Ratio of non-effective impervious surfaces area to total impervious surfaces area [%]; |
| r_r | Ratio of roof surfaces area to effective impervious surfaces area [%]; |
| r_c | Ratio of canopy cover area to pervious surfaces area [%]; |
| r_{rmax}, r_{smax} | Maximum ratios of the area constructed rainwater and stormwater harvesting systems to relevant surfaces [%]; |
| r_{imax} | Maximum ratio of the area constructed infiltration-based GIs to relevant surface [%]; |
| <i>Urban depth-related parameters</i> | |
| h_{ul}, h_{uh} | Mean depth of urban aquifer at the low and high topographic point [m]; |
| h_s | Mean depth of urban shallow soil layer [m]; |
| h_{wp} | Mean depth of wastewater pipe network [m]; |
| h_{dp} | Mean depth of wells for groundwater withdraw [m]; |
| n | Mean effective porosity [%]; |
| <i>Storage capacity-related parameters</i> | |
| S_{rmax}, S_{omax} | Maximum storage capacity of impervious roof and other surfaces [mm]; |
| S_{grmax}, S_{gsmax} | Maximum storage capacity of rainwater and stormwater harvesting systems [mm]; |
| <i>Water use-related parameters</i> | |
| r_{wc} | Water consumption rate for indoor water use [%]. |

1155 **C2 Urban water balance simulation model**

Fig. 3 (A) exhibits how the urban water mass balance is modeled in the UWB-SM; arrows illustrate how IGWM-driven water flows movement between seven storage units within an urban region – roof, other surfaces, rainwater, and stormwater harvesting systems, shallow soil layer, aquifer, and river. The state of these storage units is used to measure the total water balance within an urban area, thereby calculating available amounts of water resources in a period. As shown in Fig. 3 (A), [Details of the governing equations for the UWB-SM](#) assumes that the urban water cycle receives input both from rainfall and river inflow, which together pass through the grey and green infrastructures system and output in the form of evapotranspiration and river outflow. The vertical structure of the UWB-SM is illustrated in Fig. 3 (B), which consists of four components; urban surfaces, shallow soil layer, aquifer, and river. Hydrologically, various surface-subsurface water interactions and pipe network exfiltration and infiltration are considered via simulating water fluxes transfers between these storage units on the basis of the water mass conservation principle. [are shown as follows:](#)

1165 The structure of the UWB-SM. **Note:** In Fig. 3 (B) and (C), relevant symbols are listed in Tab. C1, C2 and C4 in Appendix D1.

The UWB-SM requires four types of input data; IGWM decision, urban water demand, hydroclimatic, and urban land and water characteristic data. To the specific, IGWM decision data is used to update the amounts of four types of water monthly (i.e., water supply portfolios) and the areas to construct three types of GIs systems determined by a UWM agent. Urban water demand data refers to the monthly indoor and outdoor water demands, which can be estimated based on the associated

1170

Table C3. Calibration parameters of the UWB-SM.

| | |
|---|---|
| <i>Hydrologic parameters for urban surfaces</i> | |
| E_{ismax} | Maximum evaporation on impervious surfaces when the associated storage level is saturated [mm]; |
| r_{ie} | Ratio of average evaporation to rainfall per unit canopy cover [%]; |
| IF | Infiltration factor [dimensionless]; |
| I_{pmax} | Maximum infiltration on pervious surfaces when the associated storage level is empty [mm]; |
| <i>Hydrologic parameters for shallow soil layer</i> | |
| F_{set} | Soil evapotranspiration scaling factor corresponding to the unlimited soil water supply [dimensionless]; |
| k_s | Saturated hydrologic conductivity of shallow soil layer [mm/month] |
| <i>Hydrologic parameters for aquifer and river</i> | |
| k_r | Retention factor of aquifer [%] |
| k_{rd} | Routing delay factor of river [dimensionless] |
| <i>Parameters for urban watet system</i> | |
| r_{dl}, r_{wl} | Leakage rate of supply and wastewater pipe networks [%]; |
| I_{gi} | Mean groundwater infiltration into wastewater pipe networks [mm]; |
| F_{gi} | Groundwater infiltration scaling factor when wastewater pipe network is totally submerged by groundwater [dimensionless]. |

urban population and economic development levels in a study area. Mean monthly river inflow, precipitation, and potential evapotranspiration within a study region are required as hydroclimatic data. The urban land and water characteristics of the study area are described by the calibrated and measured parameters. Each measured parameter relates directly to a physical catchment characteristic; an appropriate value can be determined through measurement, observation, or local experience. A list of measured parameters is given in Tab. C2. The 13 calibration parameters, along with the associated units, symbols, and ranges listed in Tab. C3, are grouped according to their land features; surfaces, soil layer, aquifer, river, and urban water system. These values are adjusted during the calibration to optimize the selected objective function.

There are four water storage units – roof, other surfaces, rainwater, and stormwater harvesting systems – to be set on the urban surfaces (See Fig. 3 C). In Fig. 3 (C), the urban surface consists of the pervious and impervious areas based on their infiltration rates. The impervious surfaces on which the infiltration process is ignored, are divided into effective and non-effective areas. The effective area is used to represent the portion of impervious surface runoff that directly drains to the stormwater drainage system. It is assumed that runoff on the non-effective part drains onto adjacent pervious areas, and the remaining water is evaporated. Unlike impervious surfaces, the pervious area can infiltrate a part of runoff into the underground soil layer, decreasing the runoff and increasing groundwater recharge. In the effective impervious area, roofs and other surfaces (e.g., roads and paved areas) are classified by the construction conditions of different types of GIs. It is assumed that rainwater harvesting systems are only allowed to be built on the roof area, and infiltration-based GIs (e.g., infiltration trenches and porous pavements) are required to construct on the non-roof impervious area (i.e., Other surfaces), which turns it into the

Table C4. Urban surface-related variables and parameters of the UWB-SM

| | |
|--|--|
| <i>Urban area-related parameters</i> | |
| A_i | Impervious surfaces area [km^2]; |
| A_r, A_o | Impervious roof and other surfaces area [km^2]; |
| <i>State variables of storage systems</i> | |
| $S_r(t), S_o(t)$ | Store levels of impervious roof and other surfaces in month t [mm]; |
| $S_{gr}(t), S_{gs}(t)$ | Store levels of rainwater and stormwater harvesting systems in month t [mm]; |
| $S_s(t), S_a(t)$ | Store levels of shallow soil layer and aquifer in month t [mm]; |
| <i>Evaporation-related variables of systems</i> | |
| E_{ir}, E_{io} | Evaporation on the impervious roof and other surfaces [mm]; |
| E_{in} | Evaporation on the non-effective impervious surfaces [mm]; |
| E_{pi} | Interception evaporation on the pervious surfaces [mm]; |
| <i>Runoff-related variables of systems</i> | |
| Q_{rir}, Q_{rio} | Runoff on the impervious roof and the other surfaces [mm]; |
| Q_{rrr} | Runoff on the rainwater harvesting systems [mm]; |
| Q_{rin}, Q_{rp} | Runoff on the non-effective impervious and the pervious surfaces [mm]; |
| Q_{ru} | Runoff on the urban surfaces before stormwater harvesting [mm]; |
| Q_r, q_r | Runoff on the urban surfaces after stormwater harvesting [mm, m^3]; |
| <i>Infiltration-related variables of systems</i> | |
| I_p | Infiltration on the pervious surfaces [mm]; |
| <i>Auxiliary variables of systems</i> | |
| P_e | total outdoor water input due to effective precipitation and outdoor water use [mm]; |
| $U_o(t)$ | Outdoor water use amount in month t [mm] |
| f_{sat} | Ratio of saturated area to pervious surfaces [%] |
| S_{smax} | Maximum storage capacity of shallow soil layer [mm]. |

pervious area. The roofs, the rainwater harvesting systems, and other impervious surfaces can generate impervious surface runoff when full. Their storages are depleted by evaporation (i.e., the roofs and other surfaces) or rainwater extraction (i.e., rainwater harvesting systems). Besides, the stormwater harvesting systems are supposed to collect runoff from the whole urban surface (i.e., the pervious and the impervious surfaces) for stormwater supply.

We assume that a UWM agent can supply surface water and groundwater by extracting from the river and the aquifer storage units. It also can access rainwater and stormwater collected by rainwater and stormwater harvesting systems. Indoor and outdoor demands are considered in the model. Following Mitchell et al. (2001) approach, indoor water use is divided into potable and non-potable water demands, and outdoor water use is regarded as non-potable. The potable water demand is assumed to be only satisfied by surface water and groundwater supply, and all water resource supplies can support the non-potable case.

Urban Surfaces: In the UWB-SM, we assume that precipitation is distributed evenly over the entire area and does not take urban spatial features into account due to the limited monthly impact on urban water management decisions. By the assumption, the amounts of rainfall on different urban surfaces can be calculated by ratios of relevant surface areas to the urban

Table C5. Underground and river-related variables and parameters of the UWB-SM

| | |
|--|--|
| <i>State variables of storage systems</i> | |
| $S_{ri}(t)$ | Store levels of river in month t [mm]; |
| <i>Drainage-related parameters of systems</i> | |
| P_s | Percolation in the shallow soil layer [mm]; |
| Q_b | Base flow in the aquifer [mm]; |
| S_{amin} | Minimum storage level of aquifer for generating base flow [mm]; |
| $Q_{ro}(t)$ | River outflow in month t [mm]; |
| <i>Evapotranspiration-related variables of systems</i> | |
| ET_s, ET_a | Evapotranspiration in the shallow soil layer and aquifer [mm]; |
| <i>Pipe network-related variables</i> | |
| L_d, L_w | Leakage of pipe network for water supply and wastewater drainage [mm]; |
| GI_w | Groundwater infiltration into wastewater pipe network [mm]; |
| Q_{wd}, q_{wd} | Wastewater drainage to river [mm, m ³]; |
| <i>Infiltration-related variables of systems</i> | |
| I_p | Infiltration on the pervious surfaces [mm]; |
| <i>Auxiliary variables of systems</i> | |
| f_{iw} | Ratio of submersed wastewater pipelines to total wastewater pipelines [%]. |

Table C6. ~~Variables and parameters~~ Parameters of the ~~IGWM-OM~~ Muskingum-Cunge routing model

| | |
|--|---|
| <i>Cost-related parameters of GI systems</i> | <i>Urban area-related parameters</i> |
| c_{ig}, c_{rg}, c_{sg} | A_u^i, A_u^{i+1} |
| c_{ig}, c_{rg}, c_{sg} | $Q_{ri}^{i+1}, q_{ri}^{i+1}$ |
| <i>Cost-related parameters of water supply and sewage drainage</i> | c_{ri}, c_{ri} |
| c_{amax}, c_{amin} | Q_{ro}^i, q_{ro}^i |
| c_{rw}, c_{sw} | $q_{ra}^i(t), q_{ra}^i(t-1)$ |
| TC_i | Note: [—] represents dimensionless. Parameters of the S-APSO |
| τ | Subscripts $t, f_{r1}^i, f_{r2}^i, f_{r2}^i$ |
| <i>Particle-assessment-related parameters</i> $Fitness[P_l(\tau)]$ The fitness value of the l th particle at the τ th iteration; <i>Particle-updating-related parameters</i> $P_l(\tau), V_l(\tau)$ The p | |

area’s multiple gross precipitations. Notice that the pervious surface receives input from effective precipitation, outdoor water use, and surface runoff from adjacent impervious areas. The effective precipitation is defined by the relevant gross precipitation minus the interception and evaporation on the plant cover area within the region. For the infiltration process, the infiltration and saturation excess are modeled to calculate the runoff and the infiltration according to the soil moisture conditions. The impervious and pervious surface runoff flows into the drains, collected by stormwater harvesting systems. The rest discharges into the river. The relevant terms and units of which are defined in Tab. C4. Taking the IGWM decisions of UWM agent i in month t as an example, the detail of the hydrologic process on the urban surface is formulated as follows;

1210 *Hydrologic process on the impervious roof surfaces:* The water mass balance equation for the impervious roof surfaces can be expressed as;

$$S_r(t) - S_r(t-1) = P_g(t) - E_{ir}(t) - Q_{rir}(t), \quad (C1)$$

where the roof area $A_r = r_r \cdot (A_u - A_p)$, $P_g(t)$ represents precipitation on the impervious roof surfaces, and evaporation can be calculated by $E_{ir}(t) = \max[E_{ismax} \cdot \frac{S_r(t-1)}{S_{rmax}}, E_p(t)]$ based on Mitchell et al. (2001) equation. And the storage levels is updated by a reservoir model; $S_r(t) = \min[S_r(t-1) + P_g(t) - E_{ir}(t), S_{rmax}]$.

1215 *Hydrologic process on the other impervious surfaces:* Similar to the impervious roof surfaces, the water mass balance formulation for the other impervious surfaces is shown as;

$$S_o(t) - S_o(t-1) = P_g(t) - E_{io}(t) - Q_{rio}(t), \quad (C2)$$

where the other impervious surfaces area A_o is equal to $(1 - r_r) \cdot (A_u - A_p)$, and the calculation of the evaporation is also dependent of Mitchell et al. (2001) method; $E_{io}(t) = \max[E_{ismax} \cdot \frac{S_o(t-1)}{S_{omax}}, E_p(t)]$. The update of relevant storage levels, $S_o(t)$ is equal to $\min[S_o(t-1) + P_g(t) - E_{io}(t), S_{omax}]$.

1220 *Hydrologic process for the rainwater harvesting systems:* In the rainwater harvesting systems, evaporation is ignored because of the assumption of that rainwater is collected rapidly and storage is sealed. We can draw its mass balance relationship as follows;

$$S_{gr}(t) - S_{gr}(t-1) = P_g(t) - W_{rr}^i(t) - Q_{rrr}(t), \quad (C3)$$

where $W_{rr}^i(t)$ is obtained from the unit conversion from $[m^3]$ to $[mm]$, which is equal to $\frac{w_{rr}^i(t)}{1000 \cdot RG_r^i}$, and the updated storage levels of the system $S_{gr}(t)$ is equivalent to $\min[S_{gr}(t-1) + P_g(t) - W_{rr}^i(t), S_{grmax}]$.

1225 *Hydrologic process on the non-effective area:* Hydrologic process on the non-effective area: For the simplicity of the model, it assumed that rainfall only generates runoff and evaporation on the non-effective area. This study calculates the corresponding runoff based on the following equation - $Q_{rin}(t) = r_n \cdot [\frac{A_r}{A_i} \cdot Q_{rir}(t) + \frac{A_r - RG_r}{A_i} \cdot Q_{rio}(t) + \frac{A_o - IG}{A_i} \cdot Q_{rrr}(t)]$, where the impervious area $A_i = A_u - A_p - IG$.

$$P_g(t) = Q_{rin}(t) + E_{in}(t). \quad (C4)$$

Hydrologic process on the pervious surfaces: The water mass conservation equation for the pervious surfaces is represented as follows;

$$Q_{rin}(t) + P_g(t) + U_o(t) = Q_{rp}(t) + E_{pi}(t) + I_p(t). \quad (C5)$$

1230 The right side of Eqs. C5 donates the inflow on the pervious surface, including runoff from the non-effective area, precipitation, and outdoor water use. The outdoor water use is the total amount of water supply minus indoor water demand - $U_o(t) = (1 - r_{dl}) \cdot [W_s^i(t) + W_g^i(t)] + W_{rr}^i(t) + W_{rs}^i(t) - \frac{d_{ip}(t) + d_{in}(t)}{1000 \cdot A_u^i}$, where $W_s^i(t)$, $W_g^i(t)$ and $W_{rs}^i(t)$ are obtained from the unit conversion from $[m^3]$ to $[mm]$, which are equal to $\frac{w_s^i(t)}{1000 \cdot A_u^i}$, $\frac{w_g^i(t)}{1000 \cdot A_u^i}$ and $\frac{w_{rs}^i(t)}{1000 \cdot RG_s^i}$.

The left hand side of Eqs. C5 represents outflow on the pervious surfaces, consisting of runoff, interception evaporation and infiltration, separately. Interception evaporation is calculated based on urban vegetation canopy area and associated features, following Van Dijk and Bruijnzeel (2001) approach - $E_{pi}(t) = \min[r_c \cdot r_{ie} \cdot P_g(t), E_{imax}]$. The calculation of infiltration is based on two hydrologic processes; saturated and infiltration excess (Viney et al., 2015). we assume that there would be no infiltration on the saturated area within the pervious surface, and its ratio $f_{sat}(t) = \max[\frac{S_a(t-1) - h_{ul}}{h_{uh} - h_{ul}}, 0]$ (See Fig. 3 B). For the other part - unsaturated area, an infiltration rate estimated by using an exponential function of storage levels of the shallow soil layer (Chiew and McMahon, 1999), which infiltration is minimum when the storage level is saturated and continuously increases to a maximum when the storage level is empty. Therefore, the formulation of infiltration is $I_p(t) = [1 - f_{sat}(t)] \cdot \max[I_{pmax} \cdot e^{-IF \cdot \frac{S_s(t-1)}{S_{smax}}}, P_e(t) + Q_{rin}(t)]$, where maximum storage capacity of shallow soil layer $S_{smax} = 1000 \cdot n \cdot h_s$ and total outdoor water input $P_e(t) = P_g(t) + U_o(t) - E_{pi}(t)$.

Hydrologic process for the stormwater harvesting systems: Similar to rainwater harvesting systems, stormwater harvesting systems is also hypothesized to have no evaporation. Its mass balance equation can be represented by:

$$S_{gs}(t) - S_{gs}(t-1) = Q_{ru}(t) - W_{rs}^i(t) - Q_r(t), \quad (C6)$$

where runoff that is available for collection is the sum of runoff from the effective impervious and the pervious surfaces - $Q_{ru} = Q_{rp}(t) + (1 - r_n) \cdot [\frac{A_r}{A_i} \cdot Q_{rir}(t) + \frac{A_r - RG_r}{A_i} \cdot Q_{rio}(t) + \frac{A_o - IG}{A_i} \cdot Q_{rrr}(t)]$. The relevant storage levels can be updated by: $S_{gs}(t) = \min[S_{gs}(t-1) + Q_{ru} - W_{rs}^i(t), S_{gsmax}]$.

Shallow Soil Layer: As shown in Fig. 3 (B), a non-linear reservoir model with the depth h_s is given to describe relevant hydrologic processes in the shallow soil layer. The shallow soil layer receives water from the urban surfaces by infiltration, and drains water by percolation into the aquifer and evapotranspiration to the atmosphere. Therefore, the water mass balance equation for the shallow soil layer can be written as:

$$S_s(t) - S_s(t-1) = I_p(t) - P_s(t) - ET_s(t) \quad (C7)$$

where percolation is assumed to occur according to the following Frost et al. (2016) equation for shallow soil layer - $P_s(t) = k_s \cdot [\frac{S_s(t-1)}{S_{smax}}]^2$. The evapotranspiration process occurs in the unsaturated portion of the shallow soil layer, and it can be given by using Frost et al. (2016) method: $ET_s(t) = [1 - f_{sat}(t)] \cdot F_{set} \cdot ET_p(t) \cdot \min[\frac{S_s(t-1) + I_p(t)}{S_{smax}}, 1]$.

Aquifer: In the UWB-SM, the only unconfined aquifer is considered as a linear reservoir model to simulate groundwater-related hydrologic dynamics (Mitchell et al., 2001), indicating that there is no deep seepage from the aquifer. The aquifer receives water from percolation, and leakage of water supply and wastewater pipelines, and discharges water in the manners of base flow, evapotranspiration, groundwater extraction for use and infiltration into wastewater pipelines (Ellis, 2001). Hence, the mass balance formulation of aquifer can be expressed as:

$$S_a(t) - S_a(t-1) = P_s(t) + L_d(t) + L_w(t) - GI_w(t) - W_g^i(t) - ET_a(t) - Q_b(t) \quad (C8)$$

where the leakage of water supply pipe networks is $L_d(t) = r_{dl} \cdot [W_{rr}^i(t) + W_{rs}^i(t)]$, and the calculation of the sewer pipelines infiltration and exfiltration (leakage) is by comparing the depth of wastewater pipelines with groundwater table (Wolf, 2006)

- groundwater would infiltrate into wastewater pipelines when the pipe is below the groundwater table, whereas wastewater would leak into the aquifer from pipelines when the pipe is above the level of the groundwater table. Fig. 3 (C) illustrates that the fraction of the sewer pipelines that is below the groundwater table is defined as $f_{iw}(t) = \max[\frac{S_a(t-1)}{1000 \cdot n} + h_{wp} - h_{ul}, 0]$, which is used to calculate the sewer pipelines infiltration $GI_w(t) = f_{iw}(t) \cdot I_{gi} \cdot F_{gi}$ via using Wolf (2006) method, and the associated exfiltration part of pipe networks $L_w(t) = r_{wl} \cdot (1 - r_{wc}) \cdot (1 - f_{iw}(t)) \cdot [\frac{d_{ip}(t) + d_{in}(t)}{1000 \cdot A_u}]$ though applying Mitchell et al. (2001) equation. The evapotranspiration in the aquifer occurs in the saturated portion of the shallow soil layer (Fig. 3 C), which can also be computed according to Frost et al. (2016) method: $ET_a(t) = f_{sat}(t) \cdot F_{set} \cdot ET_p(t)$. The amounts of base flow is assumed to be linearly proportional to the storage level of the aquifer (Fenicia et al., 2006) - $Q_b(t) = \max[k_r \cdot (S_a(t-1) - S_{amin}), 0]$, where $S_{amin} = 1000 \cdot n \cdot h_{ul}$.

River: We assume that the “River” component of the UWBv-SM includes all surface water bodies within an urban area. It accepts water from upstream inflow, runoff within the urban surfaces and base flow from the aquifer, and drains water to the adjacent downstream region. In addition, an urban area can withdraw water from the river, and discharge wastewater into it. So, the water mass conservation equation for a river can written as:

$$S_{ri}(t) - S_{ri}(t-1) = Q_{ri}(t) + Q_r(t) + Q_b(t) + Q_{wd}(t) - W_s^i(t) - Q_{ro}(t) \quad (C9)$$

where total wastewater drainage is calculated as the sum of indoor water drainage and sewer infiltration and sewer leakage have been subtracted: $Q_{wd} = (1 - r_{wc}) \cdot [\frac{d_{ip}(t) + d_{in}(t)}{1000 \cdot A_u}] + GI_w(t) - L_w(t)$. The outflow of the river is routed via a notional river store level, which can be controlled by a routing delay factor (k_{rd}) according to Frost et al. (2016) equation: $Q_{ro}(t) = (1 - e^{-k_{rd}}) \cdot [S_s(t-1) + Q_{ri}(t) + Q_r(t) + Q_b(t) + Q_{wd}(t) - W_s^i(t)]$.

1280 C3 ~~IGWM-optimization~~ Muskingum-Cunge routing model

~~Before model construction, the fundamental assumptions are given.~~

~~ASSUMPTION 1. Three types of GIs can only be built in specific urban areas.~~

~~ASSUMPTION 2. Four types of urban water demand need to be met via four types of water supply.~~

~~ASSUMPTION 3. All water resources for supply can only be withdrawn or collected in urban areas.~~

1285 ~~ASSUMPTION 4. The combined sewer system is considered in the urban system.~~

Some of these assumptions are imposed for the simplicity of the model. Assumption 1 describes urban land features and the space limitations for the development of three types of GIs, which is consistent with corresponding settings of the UWB-SM. Fig. 1 (B) illustrates the upstream-downstream hydrologic interaction between UWM agent i and $i+1$ in the associated river reach. A Muskingum-Cunge routing model is used to simulate changes in streamflow in the river reach connected with two adjacent urban areas (Garbrecht and Brunner, 1991; Weinmann and Laurenson, 1979). That is, taking the UWM agent $i+1$ in month t as an example (See Fig. 3 C). Assumption 2 is coherent with the associated hypothesis of the UWB-SM. Meanwhile, the irrigation demand of urban green space is also considered here. Assumption 3 indicates that inter-watershed water transfer schemes are not considered in the model for simplicity. Assumption 4 represents that the model would take the sum of stormwater and wastewater into account in the calculation of urban wastewater drainage cost. The relevant decision

1295 variables and parameters of the IGWM-OM are listed in Tab. B1 and B2, separately. Based on the above assumptions, using the UWM agent 1 B), its upstream inflow in month t can be expressed mathematical by outflow of the UWM agent i in month t and $t + 1$, as follows, Fig. 1 (B) illustrates the upstream-downstream hydrologic interaction between UWM agent i and $i + 1$ in the associated river reach. A Muskingum-Cunge routing equation is used to simulate changes in streamflow in the river reach connected with two adjacent urban areas (Garbrecht and Brunner, 1991; Weinmann and Laurenson, 1979). That is, taking the UWM agent $i + 1$ in month t as an example (See Fig. 1 B), its upstream inflow in month t can be expressed mathematical by outflow of the UWM agent i in month t and $t + 1$, as follows, the IGWM-OM model is formulated as a non-linear programming as follows:-

$$\min_{W, GI} TC_i = C_{gi} + C_{si} + C_{wi}$$

$$s.t. \left\{ \begin{array}{ll} C_{gi} = c_{ig} \cdot (IG^i)^{e_{ig}} + c_{rg} \cdot (RG_r^i)^{e_{rg}} + c_{sg} \cdot (RG_s^i)^{e_{sg}}, & (01) \\ C_{si} = \sum_{t=1}^{12} [c_{ri} \cdot w_s^i(t)^{e_{ri}} + [c_a(t)]_* \cdot w_g^i(t) + c_{rw} \cdot w_{rr}^i(t) + c_{sw} \cdot w_{rs}^i(t)], & (02) \\ C_{wi} = \sum_{t=1}^{12} c_{wd} \cdot [q_r(t) + q_{wd}(t)]^{e_{wd}}, & (03) \\ w_s^i(t) = 1000 \cdot A_u^i \cdot W_s^i(t), w_g^i(t) = 1000 \cdot A_u^i \cdot W_g^i(t), & \forall t \quad (04) \\ w_{rr}^i(t) = 1000 \cdot A_u^i \cdot W_{rr}^i(t), w_{rs}^i(t) = 1000 \cdot A_u^i \cdot W_{rs}^i(t), & \forall t \quad (05) \\ q_r(t) = 1000 \cdot A_u^i \cdot [Q_r(t)]_*, q_{wd}(t) = 1000 \cdot A_u^i \cdot [Q_{wd}(t)]_*, & \forall t \quad (06) \\ 0 \leq IG^i \leq r_{imax} \cdot A_o, 0 \leq RG_r^i \leq r_{rmax} \cdot A_r, 0 \leq RG_s^i \leq r_{smax} \cdot A_u, & (07) \\ 0 \leq W_s^i(t) \leq \max[0, \min([S_{ri}(t-1)]_* + Q_{ri}(t) - S_{minr}, WC_{ri})], & \forall t \quad (08) \\ 0 \leq W_g^i(t) \leq \max[0, \min([S_a(t-1)]_* - S_{mina}, WC_a)], & \forall t \quad (09) \\ 0 \leq W_{rr}^i(t) \leq [S_{gr}(t-1)]_* + \frac{RG_r^i}{A_u^i} \cdot P_g(t), & \forall t \quad (10) \\ 0 \leq W_{rs}^i(t) \leq [S_{gs}(t-1)]_* + \frac{RG_s^i}{A_u^i} \cdot [Q_{ru}(t)]_*, & \forall t \quad (11) \\ (1 - r_{dl}) \cdot [w_s^i(t) + w_g^i(t)] \geq D_{id}(t), & \forall t \quad (12) \\ (1 - r_{dl}) \cdot [w_s^i(t) + w_g^i(t)] + w_{rr}^i(t) + w_{rs}^i(t) \geq D_{id}(t) + D_{in}(t) + D_o(t), & \forall t \quad (13) \\ f_{sm} \cdot (1 - [f_{sat}(t)]_*) \cdot S_{smax} \leq [S_s(t)]_*, & \forall t \quad (14) \end{array} \right.$$

$$\left\{ \begin{array}{ll} q_{ri}^{i+1}(t) = f_{r1}^i \cdot q_{ro}^i(t) + f_{r2}^i \cdot q_{ro}^i(t-1) + f_{r3}^i \cdot q_{ri}^{i+1}(t-1), & (01) \\ q_{ro}^i(t) = 1000 \cdot A_u^i \cdot [Q_{ro}^i(t)]_*, & (02) \\ q_{ri}^{i+1}(t) = 1000 \cdot A_u^{i+1} \cdot Q_{ri}^{i+1}(t), & (03) \end{array} \right. \quad (C10)$$

1305 where $[-]_*$ represents that the parameter is from simulation results of the UWB-SM. Equation (C10) represents the objective function of the model, which aims to minimize the annual IGWM cost for the UWM agent. This cost is comprised of GI construction (C_{gi}), water supply (C_{si}), and wastewater drainage costs (C_{wi}). The calculation methods for these three costs are presented in the first to all parameters of the above notation are listed in Tab. C6. The first row of Eq. (C10) is the Muskingum-Cunge model for calculating the relevant river reach inflow of downstream agents. The second and third rows of Equation (B1b). The fourth to sixth rows of Equation B1b indicate the unit conversion process from millimeters (Eq. (C10))

1310 represent that the units for hydrological parameters were converted from $[mm]$ to cubic meters ($[m^3]$ to $[m^3]$ based on the
associated urban total areas. In addition, it should be noted that the Muskingum-Cunge approach is also applicable in the case
that there are branches in the main river reach (See UWM agents 1,2 and 3 in Fig. 1 A), which is essential for coupling the
UWB-SM (using the unit $[mm]$) with the IGWM optimization model (using the unit $[m^3]$). The seventh row of Equation (B1b)
establishes the constraints for GI construction. Meanwhile, can be solved by dividing the river reach into several sub-reaches
1315 based on intersections of the main river and associated branches, and then calculate them in sequence.

Appendix D: Details of the agent-based model for city scale IGWM

This appendix comprehensively elucidates the details of the relevant solution approach pertaining to the agent-based model for
city scale IGWM - simulation-based adaptive particle swarm optimization (S-APSO). It is meticulously described from various
aspects including the notation and the solution approaches pertaining to this model.

1320 D1 Notations

To facilitate the model presentation, some of the important notations used hereafter are summarized in Table D1.

Table D1. Parameters of the S-APSO

| <u>Subscripts</u> | |
|---|---|
| l | Index of the particle, where $l = 1, 2, \dots, L$; |
| τ | Index of the iteration, where $\tau = 1, 2, \dots, \Gamma$; |
| <u>Particle-assessment-related parameters</u> | |
| $Fitness[P_l(\tau)]$ | The fitness value of the l th particle at the τ th iteration; |
| <u>Particle-updating-related parameters</u> | |
| $P_l(\tau), V_l(\tau)$ | The position and the eighth to eleventh rows describe the water supply constraints for surface water, groundwater, rainwater, and stormwater withdrawal |
| PB_l | Personal best particle of the l th particle achieved so far; |
| GB | Global best particle among all the particles; |
| $EP(\tau)$ | Elite particle at the τ th iteration; |
| $\theta(\tau)$ | Inertia weight at the τ th iteration; |
| $c_p(\tau), c_s(\tau)$ | Personal and social acceleration coefficients at the τ th iteration; |
| r_p, r_s | The uniformly distributed random numbers generated within $[0, 1]$; |
| $\varepsilon(\tau)$ | The ratio for social learning at the τ th iteration; |

D2 Solution approach

Unlike traditional water management models (Loucks and Van Beek, 2017), it might be hard to solve the UWM-agent
model(Eq. B1)agent-based model, which consists of the IGWM-OM-agent-based model for UWM (Eq. B1) and UWB-SM,
1325 via using general methods, because of the non-linearity of its objective function and complexity of its solution space induced
by coupling with the UWB-SM. To solve complex water resources management problems, heuristic search-based techniques,

such as particle swarm optimization (PSO) that is a swarm-based intelligence method to search for globally optimal solutions via imitating swarm behavior in birds flocking (Kennedy and Eberhart, 1995), are widely applied and developed (Nicklow et al., 2010; Chang et al., 2013). Therefore, in this study, according to features of the UWM agent model, a simulation-based adaptive particle swarm optimization (S-APSO) is designed, and its flowchart diagram is illustrated in Fig. D1 (A). As shown in Fig. D1 (A), compared with particle initialization and evaluation for standard PSO, a coupling procedure proposed above for data exchange between IGWM-OM-agent-based model for UWM and UWB-SM is nested to make sure all particles feasible and measurable. Compared with the standard PSO updating mechanism, a Boltzmann selection operator and an evolutionary state-based parameter adaptation scheme are added to avoid premature convergence to improve algorithm performance; a simulation-based check & repair mechanism is introduced to guarantee all particles feasible during the particle updating process. These key features of the proposed S-APSO are explained as follows.

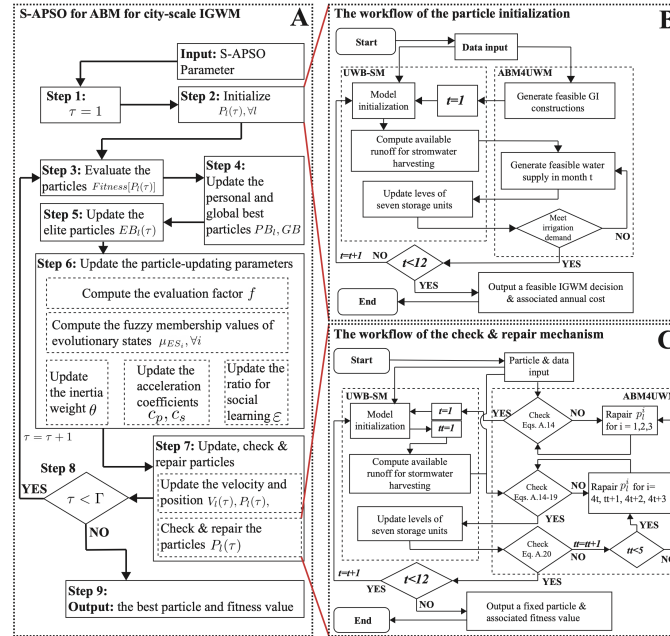


Figure D1. Flowchart diagram of the S-APSO for agent-based model for city-scale IGWM

Solution representation and particle performance calculation: In the S-APSO, a particle representing a feasible solution of the Eq. (B1) can be encoded as an array with 51 dimensions, which indicates 3 GI construction variables and 4×12 monthly water supply variables, respectively. It can be written as follows,

$$P_l(\tau) = [p_l^1(\tau), p_l^2(\tau), p_l^3(\tau), p_l^4(\tau), p_l^5(\tau), p_l^6(\tau), p_l^7(\tau), \dots, p_l^{51}(\tau)] \quad (D1)$$

$$\leftrightarrow [IG^i, RG_r^i, RG_s^i, W_s^i(1), W_g^i(1), W_{rr}^i(1), W_{rs}^i(1), \dots, W_{rs}^i(12)],$$

where the relevant parameters of the S-APSO are listed in Tab. D1 of Appendix D1.

To measure the performance of each particle, the objective function in the UWM agent model (Eq. C10) is regarded as the fitness function for particles, indicating that the value of the objective function for particles is used to represent their merits in a swarm, which, therefore, can be expressed as

$$Fitness[P_l(\tau)] = C_{gi} + C_{si} + C_{wi} \quad (D2a)$$

$$\begin{cases} C_{gi} = c_{ig} \cdot [p_l^1(\tau)]^{e_{ig}} + c_{rg} \cdot [p_l^2(\tau)]^{e_{rg}} + c_{sg} \cdot [p_l^3(\tau)]^{e_{sg}}, \\ C_{si} = \sum_{t=1}^{12} [c_{ri} \cdot p_l^{(4t)}(\tau)^{e_{ri}} + c_{gi} \cdot p_l^{(4t+1)}(\tau)^{e_{gi}} + c_{rw} \cdot p_l^{(4t+2)}(\tau) + c_{sw} \cdot p_l^{(4t+3)}(\tau)], \\ C_{wi} = \sum_{t=1}^{12} c_{wd} \cdot [q_r(t) + q_{wd}(t)]^{e_{wd}}, \end{cases} \quad (D2b)$$

Note that, as seen in Eq. D2, to complete a performance calculation for each particle in S-APSO is required by running the coupling procedure mentioned above.

Particle Initialization: The initial storage levels of the river, the aquifer, the rainwater, and the stormwater harvesting systems to determine the available amounts of four water sources and the runoff and the wastewater to calculate the costs of drainage. It means that generating a feasible solution of the IGWM-OM-agent-based model for UWM involves conducting the UWB-SM procedure many times. Furthermore, as shown in the UWB-SM, the solutions at one stage from the IGWM-OM-agent-based model for UWM will also be as input data of the UWB-SM to update urban hydrologic conditions-states for simulation at next stage. Therefore, the UWB-SM and the IGWM-OM-agent-based model for UWM are tightly coupled at the source code level, i.e., the routine of the UWB-SM is embedded into the algorithm for the IGWM-OM-agent-based model for UWM. The primary data exchanged and shared between the two models are 1) GI construction decision variables (i.e., construction areas for three types of GIs from IGWM-OM-agent-based model for UWM), 2) water supply decision variables (i.e., monthly water supply amounts for four kinds of water sources from IGWM-OM-agent-based model for UWM) 3) urban hydrological parameters (e.g., monthly storage levels of storage units from UWB-SM). The workflows of coupling two models for the generation of a feasible city-scale IGWM decision are shown in Fig. D1 (B):

~~Fig. D1 (B) illustrates a two-phase data exchange procedure between the UWB-SM and the IGWM-OM for a feasible solution of IGWM-OM. In Phase 1, internal data exchange between two models at a time for UWB-SM initialization. Initial data (e.g., urban water demand, land and water characteristic data, hydroclimatic data) are inputted into two models, respectively. Available construction areas for infiltration-based GI, rainwater, and stormwater harvesting systems are generated by the GIs construction constraints, all of which, as input data, will update the urban land features of the UWB-SM.~~

~~In Phase 2, internal data exchange between two models at the monthly scale generates a feasible water supply decision variable for a UWM agent month by month. In each month, the UWB-SM runs at least twice and exchanges data with the IGWM-OM, relying on the internal linkage between their modules, as detailed below: UWB-SM initializes the procedure to update urban hydrologic conditions based on the storage levels of seven storage units in the previous month and then computes available runoff for stormwater harvesting this month. Next, runoff along with storage levels of four storage units in the previous month (i.e., river, aquifer, rainwater, and stormwater harvesting systems) are used by IGWM-OM as part of the input to generate feasible monthly water supply decision variable for surface water, groundwater, rainwater and stormwater in this month by the water supply and demand constraints. After that, these decision variables are transferred to the UWB-SM procedure to simulate relevant urban hydrologic variables in this month (e.g., storage levels of seven storage units), and the~~

updated urban hydrologic variables (e.g., storage level of soil layer) then is sent back to the IGWM-OM for re-checking the feasibility of these decision variables using the irrigation demand constraints. These decision variables will be re-generated by the IGWM-OM if the check fails to pass. At the same time, they will be recorded to calculate relevant IGWM cost in this month through the IGWM cost objective function, and all updated storage units data will be used to initialize the UWB-SM procedure for simulating calculation in next month. At the end of this month, the time criteria t update to $t + 1$. Both UWB-SM and IGWM-OM continue to generate water supply decision variables in the next month until the termination criteria are satisfied. At the end of the simulation, the coupling procedure can generate a feasible IGWM decision variable for the UWM agent and associated annual cost.

Particle-updating mechanism: There is a shortage of standard PSO when dealing with problems with the complexity of solution spaces (Liang et al., 2006), such as Eq. (B1). It is easy to occur premature convergence, which hinders the search for global optima. The main reason behind the premature convergence seems to be that the particle-updating mechanism makes particles' information exchange frequency, which may result in fast clustering of particles (Riget and Vesterström, 2002). Therefore, to avoid premature convergence, the S-APSO applies two strategies - combination with auxiliary operators and control of algorithm parameters to modify traditional particle-updating equations. Specifically, for the introduction of auxiliary operators, a new particle, the so-called elite particle, is selected from all personal best particles so far via using a Boltzmann selection operator for each iteration. Then the linear combination of the global best and the elite particle is used to formulate the social learning components of the particle-updating equations. The improved particle-updating mechanism can be mathematically written as

$$V_l(\tau + 1) = \theta(\tau) \cdot V_l(\tau + 1) + c_p(\tau) \cdot r_p \cdot [PB_l - P_l(\tau)] + c_s(\tau) \cdot r_s \cdot \{\varepsilon(\tau) \cdot [GB - P_l(\tau)] + (1 - \varepsilon(\tau)) \cdot [EP(\tau) - P_l(\tau)]\}, \quad (D3a)$$

$$P_l(\tau + 1) = V_l(\tau + 1) + P_l(\tau), \quad (D3b)$$

where $EP_l(\tau)$ indicates an elite particle at τ th iteration, which is randomly selected from the current personal best particles pool (i.e., $\{PB_l, l = 1, 2, \dots, L\}$) via running the procedure for the Boltzmann selection operator. Instead of the standard social learning components - only learning from global best particle, there are two advantages in the modified particle-updating mechanism (Xu et al., 2016). The first is that the intervention of a random elite particle can, to some extent, prevent all particles from gathering around the global best particle prematurely, enhancing the exploration of the swarm at an early stage of the search process. The second is that the impact of elite particles on particle updating gradually declines with an increase in iterations due to the characteristics of the Boltzmann selection operator - the personal best particles close to the global best one are more likely to be chosen with time, which can guarantee the exploitation of the algorithm in end-stage. Therefore, this approach might be reasonable to balance the global and local search during a PSO process.

On the other hand, for the control of algorithm parameters, an evolutionary state-based adaptive parameter scheme, which is proposed by Zhan et al. (2009), is applied to manage automatically the parameters of the particle-updating equation (Eq. D3a) for each iteration - the inertia weight ($\theta(\tau)$), the personal and social acceleration coefficients ($c_p(\tau)$, $c_s(\tau)$) as well as the ratio for social learning ($\varepsilon(\tau)$). Each parameter is set in the parameter control scheme in terms of a well-defined index that characterizes the current swarm distribution. It is worth mentioning that we use a fuzzy logic system (Jang et al., 1997)

to adjust acceleration the coefficients and the ratio for social learning in each generation, and it can increase or decrease them intelligently following four defined evolutionary states - exploration, exploitation, convergence, and jumping out. By automatic control of the algorithm parameters in time, it can improve the search efficiency and convergence speed of the S-APSO.

Particle check & repair mechanism: In addition, to avoid a premature convergence of the PSO, it is another crucial factor in successful applications of the PSO to keep all particles feasible during the search process (AP, 2005), especially for this model with the complex solution space induced by integrated with the UWB-SM. Therefore, a check & repair mechanism is developed based on the above coupling strategy, which can examine and fix (if necessary) all updated particles to make sure that they are available. Note that, similar to the particle initialization, there are also many times data exchanges between IGWM-OM-agent-based model for UWM and UWB-SM in the process, indicating the reparation in the previous position of a particle might affect that in the subsequent positions, especially in case of fixing the first three positions of a particle that represents GI construction decision variables. It may cause failures of using general check & repair methods.

Therefore, the study uses a multi-round loop structure to check & repair different positions of a particle in terms of the features of the constraints (Eq. B1b), which permits modified particles to be feasible and also to keep the original characters as much as possible. Fig. D1 (C) illustrates the flow chart of the check & repair mechanism, which has a two phases data exchange procedure between the UWB-SM and IGWM-OM-for-agent-based model for UWM for examination and reparation of particles. As reflected in Fig. D1 (C), the first three positions of a particle that indicates GI construction variables in the Eq. B1 are checked and repaired (if necessary) in line with the constraint (7 in B1b) in Phase 1. In Phase 2, the 4 to 51 positions of a particle, which are related the constraints (8 in B1b) - (14 in B1b), are examined and fixed in a multi-round loop structure.

Appendix E: Details of the multiagent system for IGWM-at-an-inter-city scale IGWM

This appendix provides a comprehensive and detailed exposition of the multiagent system for IGWM at an inter-city scale. The various components of the system are thoroughly explained, encompassing aspects such as the ~~notation, the application of the Muskingum-Cunge routing equation, and the MAS-UWM framework. Additionally, the appendix delves into the multiagent system as well as the~~ relevant solution approaches associated with this ~~model~~ system.

E1 ~~Notations~~Multiagent system

~~To facilitate the model presentation, some of the important notations used hereafter are summarized in Table C6.~~

~~Parameters of the MAS-UWB~~Urban area-related parameters A_u^i, A_u^{i+1} Urban total area for UWM agent i and $i+1$ [m^2]; ~~Flow-related parameters~~ $Q_{ri}^{i+1}, q_{ri}^{i+1}$ Upstream river inflow for UWM agent $i+1$ in $[mm]$ and $[m^3]$; $q_{ri}^{i+1}(t), q_{ri}^{i+1}(t-1)$ Upstream river inflow for UWM agent $i+1$ in month t and $t-1$ [m^3]; Q_{ro}^i, q_{ro}^i River outflow for UWM agent i in $[mm]$ and $[m^3]$; $q_{ro}^i(t), q_{ro}^i(t-1)$ River outflow for UWM agent i in month t and $t-1$ [m^3]; ~~Model-related parameters~~ $f_{r1}^i, f_{r2}^i, f_{r2}^i$ Coefficient 1, 2 and 3 of the Muskingum-Cunge equation for river reach i [$dimensionless$].

E2 Muskingum-Cunge routing equation

1435 Fig. 1 (B) illustrates the up- and downstream hydrologic interaction between UWM agent i and $i + 1$ in the associated river reach. A Muskingum-Cunge routing equation is used to simulate changes in streamflow in the river reach connected with two adjacent urban areas (Garbrecht and Brunner, 1991; Weinmann and Laurenson, 1979). That is, taking the UWM agent $i + 1$ in month t as an example (See Fig. 1 B), its upstream inflow in month t can be expressed mathematical by outflow of the UWM agent i in month t and $t + 1$, as follows, Fig. 1 (B) illustrates the up- and downstream hydrologic interaction between UWM agent i and $i + 1$ in the associated river reach. A Muskingum-Cunge routing equation is used to simulate changes in streamflow in the river reach connected with two adjacent urban areas (Garbrecht and Brunner, 1991; Weinmann and Laurenson, 1979). That is, taking the UWM agent $i + 1$ in month t as an example (See Fig. 1 B), its upstream inflow in month t can be expressed mathematical by outflow of the UWM agent i in month t and $t + 1$, as follows,

$$\begin{cases} q_{ri}^{i+1}(t) = f_{r1}^i \cdot q_{ro}^i(t) + f_{r2}^i \cdot q_{ro}^i(t-1) + f_{r3}^i \cdot q_{ri}^{i+1}(t-1), & (01) \\ q_{ro}^i(t) = 1000 \cdot A_u^i \cdot [Q_{ro}^i(t)]_*, & (02) \\ q_{ri}^{i+1}(t) = 1000 \cdot A_u^{i+1} \cdot Q_{ri}^{i+1}(t), & (03) \end{cases}$$

1445 where all parameters of the above notation are listed in Tab. C6. The first row of Eq. (C10) is the Muskingum-Cunge equation for calculating the relevant river reach inflow of downstream agents. The second and third rows of Eq. (C10) represent that the units for hydrological parameters were converted from $[mm]$ to $[m^3]$ based on the associated urban total areas. In addition, it should be noted that the Muskingum-Cunge approach is also applicable in the case that there are branches in the main river reach (See UWM agents 1,2 and 3 in Fig. 1 A), which can be solved by dividing the river reach into several sub-reaches based on intersections of the main river and associated branches, and then calculate them in sequence.

E2 MAS-UWM

The basic assumptions for formulation of the [MAS-UWM multiagent system for inter-city scale IGWM](#) are shown as follows,

ASSUMPTION [5-1](#). *Hydrologically, all UWM agents are interconnected with each other only by a surface water system.*

ASSUMPTION [6-2](#). *Socially, all UWM agents are considered to be noncooperative.*

1455 To simplify the model, Assumption [5 demonstrates the hydrologic-1 demonstrates the river](#) connection among all UWM agents within the watershed, which [means that are a significant factor in the effect of GIs on urban and watershed hydrology concerning water resource allocation. So,](#) all UWM agents have to share surface water resources with others, and IGWM activities of upstream agents may affect that of downstream. In addition, we do not take the connection between urban areas' groundwater systems into account since it is assumed that its effect may be negligible in watershed-scale IGWM in the short term, comparing with that of the surface water system (Brannen et al., 2015). Besides, surface water-groundwater interaction processes induced by city-scale IGWM have been considered in the UWB-SM, which can, to some extent, reflect the associated effect via the connection in the surface water system. Assumption [6-2](#) exhibits the social relationship between UWM agents in the watershed; that is, each agent only pays attention to their local objectives and does not share information with the other agents (Giuliani and Castelletti, 2013). This assumption is reasonable for some watersheds, especially when urban areas within the watershed have to face competition for urban development in many aspects.

Therefore, the ~~MAS-UWM-multiagent system for UWMs~~ can be formulated by the integration of the ~~UWM-agent-model agent-based model for UWM~~ (Eq. B1), ~~the UWB-SM (Eqs. C1 - C9)~~ with the Muskingum-Cunge routing model (Eq. C10), depending on its feature of the Markov property. A special type of multi-stage decision system is employed to model the ~~MAS-UWM-multiagent system for UWMs~~ (Bellman, 1966) and the sequence of decisions-makings for each UWM agent -
 1470 city-scale IGWM - relies on associated spatial locations along with the river networks, which is in order from upstream to downstream. The hydrologic variable - upstream inflow of each UWM agent - is considered the state variable to describe interactions between UWM agents. It can be written as follows,

$$\begin{cases} \text{Eq. (B1),} & \forall i & (01) \\ \text{Eq. (C10),} & \forall i, t & (02) \\ q_{ri}^1(t) = Q_t^1, \text{ and } q_{ri}^i(0) = Q_0^i, & \forall i, t & (03) \end{cases} \quad (E1)$$

where the third row of Eq. (E1) are initial conditions for the ~~MAS-UWM-multiagent system for UWMs~~, and Q_t^1 and Q_0^i are the initial amounts of the upstream inflow for UWM agent 1 in month t and UWM agent i in month 0, respectively.

1475 E2 Solution approach

~~It~~ ~~To solve the multiagent system, it~~ is available to combine multiple S-APSO algorithms with the Muskingum-Cunge routing equation (~~Eq.-C10~~) to simulate the dynamics of the ~~MAS-UWM (Eq. E1)-multiagent system for UWMs~~ according to its Markovian property. That is, the optimal solutions for each UWM agent model are solved one by one in a specific order, which follows the sequence of the ~~MAS-UWM-multiagent system for UWMs~~ via using the associated S-APSO. Notice in particular
 1480 that the monthly outflow amounts for the optimal solution of each UWM agent model needs to be recorded during the S-APSO search process. They, as an input of the relevant Muskingum-Cunge equation, are used to calculate the monthly upstream inflow amounts in the associated downstream reach - an input data for the adjacent UWM agent model. In this way, the multi-S-APSO framework for simulation of the interactions of the ~~MAS-UWM-multiagent system for UWMs~~ is developed (See Fig. E1).

Appendix F: Details of ~~the~~ bi-level multiagent system for ~~IGWM-at-a-watershed-scale~~ ~~watershed-scale~~IGWM

1485 This appendix presents a thorough and comprehensive examination of the ~~bi-level~~ multiagent system for IGWM at a watershed scale. The diverse components of the system are meticulously elucidated, encompassing elements such as the ~~notation, the agent-based model for watershed management, the~~ extended agent-based model for UWM, ~~and~~ the bi-level multiagent system ~~. Furthermore, the appendix explores the~~ ~~as well as the~~ pertinent solution approaches associated with this ~~multiagent bi-level~~ system.

1490 F1 Notations

~~To facilitate the model presentation, some of the important notations used hereafter are summarized in Table B3.~~

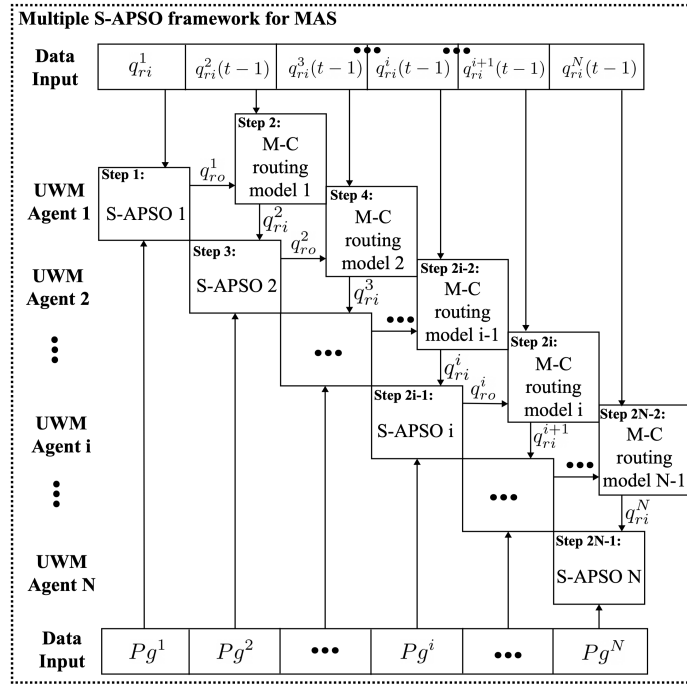


Figure E1. Flowchart diagram of the [MAS-UWM multi-S-APSO framework to multiagent system for inter-city-scale IGWM](#)

Parameters of the agent-based model for WM *Objective-related parameters* $Gini$ -Water allocation Gini-coefficient index; r_p Penalty rate in the watershed, $[\$/m^3]$; P_i Total annual penalty fees for the UWM-agent i $[\$]$; *Constraints-related parameters* $SQ^i_{min}(t), SQ^i_{max}(t)$ Minimum and maximum historical streamflow at checkpoint i in month t $[m^3]$.

1495 **F1 Agent-based model for watershed manager**

The ABM-WM is discussed in detail in the following. The relevant hypotheses for constructing the model are given.

ASSUMPTION 7. The flow of each urban catchment at the outlet is checked.

ASSUMPTION 8. Water withdrawal limit is not considered in the model.

Assumption 7 simplifies our models as WM set low flow thresholds of each urban area at the outlet. For Assumption
1500 8, computational complexity may be high in optimization of policy portfolio (setting water withdrawal limits and low flow thresholds) for a WM-agent model, especially when it is integrated into the MAS-UWM. Also, a policy limiting the water withdrawal of urban areas, as a mandatory regulation, generally relies on other water users' activities within a watershed, such as agriculture sectors, which is beyond the scope of this study. Therefore, this paper considers water withdrawal limits (i.e., the minimum storage levels of aquifer and river) as UWM-agent models' specific parameters (See the 8th and 9th rows of Eq.
1505 B1b).

As demonstrated in the above assumptions, a WM-agent model is used to describe how a WM set a watershed management policy—a streamflow penalty strategy—to regulate all UWM agents' decision behavior of IGWM in a watershed. That is, a WM limits water abstraction decisions of each UWM agent in the period via prescribing a series of low streamflow thresholds in associated hydrological stations based on hydrologic conditions; If streamflow in outlet for an urban area is below its threshold, a penalty fee will be imposed on the UWM agent. The strategy, in theory, can force UWM agents to recognize one or more of the externalities caused by IGWM, thereby adjusting their IGWM decisions because it can, to some extent, determine the cost of IGWM (Baumol et al., 1988). The WM can share fair water resources among urban areas in a watershed by setting a rational streamflow penalty strategy that affects all UWMs' decisions. Therefore, And details of the objective and constraints of the agent-based model for WM are illustrated as follows.

Equity objective: The Gini coefficient is widely used to assess resource allocation inequality (Gini, 1921; Nishi et al., 2015). Therefore, the WM agent model uses a water allocation Gini coefficient index proposed by Hu et al. (2016) and Xu et al. (2019)—the equitable sharing of the used water quantity for each unit of cost—to measure equity of water sharing in watershed-scale IGWM. Based on the definition of the index, to minimize the Gini coefficient means maximal fairness of water resources distributions in a watershed; accordingly, the minimization of the equity objective for the WM can be expressed mathematically as follows,

$$\min_{S_q^i} Gini = \frac{1}{2 \cdot N \cdot \sum_{i=1}^N \frac{\sum_{t=1}^{12} [w_s^i(t) + w_g^i(t) + w_{rr}^i(t) + w_{rs}^i(t)]}{TC_i}} \cdot \sum_{i=1}^N \sum_{j=1}^N \left| \frac{\sum_{t=1}^{12} [w_s^i(t) + w_g^i(t) + w_{rr}^i(t) + w_{rs}^i(t)]}{TC_i} - \frac{\sum_{t=1}^{12} [w_s^j(t) + w_g^j(t) + w_{rr}^j(t) + w_{rs}^j(t)]}{TC_j} \right|$$

Streamflow constraints: The WM specifies the low streamflow thresholds at each checkpoint, which should adapt to actual hydrologic conditions. Therefore, the low streamflow thresholds at each checkpoint cannot exceed the associated maximal historical streamflow and cannot be below the minimal one in each month:

$$SQ_{min}^i(t) \leq S_q^i \leq SQ_{max}^i(t), \quad \forall t, i$$

In short, the WM agent model is represented as follows:

$$\min_{S_q^i} Gini = \frac{1}{2 \cdot N \cdot \sum_{i=1}^N \frac{\sum_{t=1}^{12} [w_s^i(t) + w_g^i(t) + w_{rr}^i(t) + w_{rs}^i(t)]}{TC_i}} \cdot \sum_{i=1}^N \sum_{j=1}^N \left| \frac{\sum_{t=1}^{12} [w_s^i(t) + w_g^i(t) + w_{rr}^i(t) + w_{rs}^i(t)]}{TC_i} - \frac{\sum_{t=1}^{12} [w_s^j(t) + w_g^j(t) + w_{rr}^j(t) + w_{rs}^j(t)]}{TC_j} \right|$$

$$s.t. \left\{ \begin{array}{l} SQ_{min}^i(t) \leq S_q^i \leq SQ_{max}^i(t), \quad \forall t, i \end{array} \right.$$

F1 Extended agent-based model for UWM

Under the policy intervention from a WM, each UWM agent needs to make reasonable IGWM decisions to trade off the previous three types of costs (i.e., GIs construction, water supply, wastewater drainage) and the possible penalty fee set by

a WM to minimize their own total IGWM costs under the specified low streamflow thresholds. Therefore, the above UWM agent model will be extended - its annual IGWM cost function is converted as the sum of GIs construction, water supply, wastewater drainage costs, and penalty fees. Taking the UWM agent i as an example, the extended **UWM-agent-model-for city-scale-IGWM-agent-based model for UWM** under the streamflow penalty strategy is shown as follows,

$$\min_{W,GI} TC_i = C_{gi} + C_{si} + C_{wi} + P_i \quad (F1a)$$

$$s.t. \begin{cases} P_i = \sum_{t=1}^{12} r_p \cdot \left[\frac{[q_{ro}^i(t) - S_q^i(t)] + |q_{ro}^i(t) - S_q^i(t)|}{2} \right]; & (01) \\ \text{Eq. (B1b)}; & (02) \\ q_{ro}^i(t) = 1000 \cdot A_u^i \cdot [Q_{ro}^i(t)]_* \quad \forall t & (03) \end{cases} \quad (F1b)$$

where the first row of Eq. (F1b) indicates the annual penalty fee for the UWM agent i , and its calculation in detail shown as follows. The third row of Eq. (F1b) represents that the units for hydrological parameters were converted from $[mm]$ to $[m^3]$ based on the associated urban total areas.

Penalty fees: In the extended UWM agent model, a penalty fee must be imposed on UWM agent when the outflow in its urban catchment is below the specified low streamflow threshold at the corresponding checkpoint. It is assumed that the WM prescribes a constant penalty rate for the watershed and that a penalty fee is only imposed on out-of-threshold streamflow. Hence, for UWM agent i in month t , if the outflow at checkpoint i is not below the low streamflow threshold (i.e., $q_{ro}^i(t) \geq S_q^i(t)$), the penalty fee is 0; however, if it is below the quota (i.e., $q_{ro}^i(t) < S_q^i(t)$), a fee equal to $r_p \cdot [S_q^i(t) - q_{ro}^i(t)]$ is imposed. By integrating the above cases, the annual penalty fee for UWM agent i can be written as:

$$P_i = \sum_{t=1}^{12} r_p \cdot \left[\frac{[q_{ro}^i(t) - S_q^i(t)] + |q_{ro}^i(t) - S_q^i(t)|}{2} \right]. \quad (F2)$$

F2 Bi-level multiagent system

As mentioned above, a streamflow penalty strategy prescribed by a WM agent might change some UWM agents' decisions of IGWM - upstream UWM agents might have to adjust their IGWM decisions to increase outflow to avoid over high penalty fees for costs minimization, which is beneficial to the downstream agents. Such changes in UWM agents' behavior can, to some extent, shift the interactions in the **MAS-UWM-multiagent system for UWMs**, which might have a potential impact on the watershed environment that can be measured by the assessment index (i.e., water allocation Gini coefficient) set by the MW (See Fig. 1 (C)). Therefore, a WM agent can assess the effects of the policy on the watershed via checking the given index that reflects feedbacks of the **MAS-UWM-multiagent system for UWMs** and then gradually adjusts it to find the optimal one. This process is a WM-UWM agent interaction in watershed-scale IGWM under a water policy.

Fig. 1 (C) illustrates that the WM-UWM agent interaction is no longer determined only by the WM or the UWMs, and both of them try to optimize their objectives (i.e., equity vs. cost objectives for WM and UWMs) under the associated constraints (i.e., steamflow vs. GI construction, water supply and demand constraints) and reactions of the other party. Therefore, they follow a specific decision rule. That is, the WM agent first makes a decision, and then each UWM agent specifies a decision to optimize their own objectives with full knowledge of the WM's decision; the WM also optimizes its own objective based

on the rational UWMs' reactions. In economic theory, this process - the WM-UWM agent interaction - is a Stackelberg game
 1560 (Von Stackelberg, 2010).

Therefore, the WM-UWM agent interaction can follow a hierarchical decision rule for the leader - the WM agent and the multiple followers - the UWM agents (Dempe, 2002). Besides, for the followers, the UWM agents form a MAS-UWM multiagent system for UWMs (Eq. C10) that has a Markov property, which involves a special multi-stage decision-making process (Bellman, 1966). By integrating the WM (Eq. B4), the UWM (Eq. F1) agent model and the MAS-UWM-multiagent system for UWMs (Eq. C10) mentioned above, a BL-MAS-bi-level multiagent system for WM-UWM agent interaction can
 1565 be developed to describe the Stackelberg game between the WM and multiple UWM agents, and unique multi-stage system constructed to reflect the state transitions for the multiple WM-UWM agents, which can be formulated as follows:

$$\begin{aligned} & \text{Eq. (F1)} \\ & \left\{ \begin{array}{l} \text{Eq. (B4b);} \\ \text{where } W_i, GI_i \text{ solves} \end{array} \right. \\ & s.t. \left\{ \begin{array}{ll} \text{Eq. (F1);} & \forall i \\ \text{Eq. (C10);} & \forall i, t \\ q_{ri}^1(t) = Q_t^1, \text{ and } q_{ri}^i(0) = Q_0^i. & \forall i, t \end{array} \right. \end{aligned} \quad (F3)$$

where $[-]_*$ represents that the parameter is from simulating calculation of the UWB-SM.

F3 Solution approach

1570 In the BL-MAS-bi-level multiagent system (Eq. F3), ~~the UWM-agent-models-agent-based models for UWM~~ are converted to Eq. (F1) due to the introduction of a streamflow penalty strategy. Compared with the above UWM-agent-model-models (B1), only the objective function of the transformed model (F1a) is changed - adding a penalty fee. Therefore, to apply the proposed S-APSO to solve the UWM-agent-models-in-the-BL-MAS-agent-based models for UWM in the bi-level multiagent system, only the fitness function for particles needs to be adjusted. Besides, the above multi-S-APSO framework is also available
 1575 in simulating the interactions among all UWM agents in the BL-MAS-bi-level multiagent system under a given streamflow penalty strategy because of the features of its hydrologic connections - Markovian property.

For the ~~WM-agent-model-agent-based model for WM~~, the above S-APSO framework without the simulation-based initialization and the check & repair mechanism is available to look for the optimal solution due to its simple constraint conditions (B4b). However, there is a critical factor in the simulation of the BL-MAS-bi-level multiagent system that is how to deal
 1580 with the special decision rule between the WM ~~and the UWN-agent and the UWM~~ agents - a Stackelberg game, i.e., the WM agents'agent's best response is based on the associated reactions of all UWM agents (Von Stackelberg, 2010). In fact, it is challenging to obtain a Stackelberg solution to the BL-MAS-bi-level multiagent system using general solution methods because the bi-level model is an NP-hard problem, even in its simplest linear case (Dempe, 2002). To deal with the specific bi-level model decision rules, the study nests the multi-S-APSO framework for the MAS-UWM-multiagent system for UWMs mentioned
 1585 before into the particle performance measurement of the S-APSO for the WM~~agent~~, which can simulate the responses of the

MAS-UWM-multiagent system for UWMs to a given streamflow penalty strategy prescribed by the WM agent, thereby assessing the policies' effects accurately. By the nested structure, therefore, a nested S-APSO framework is proposed for searching for the optimal WM-UWN interactions in the **BL-MAS**-bi-level multiagent system under a streamflow penalty strategy. The flowchart diagram for the nested S-APSO is illustrated in Fig. F1(€).

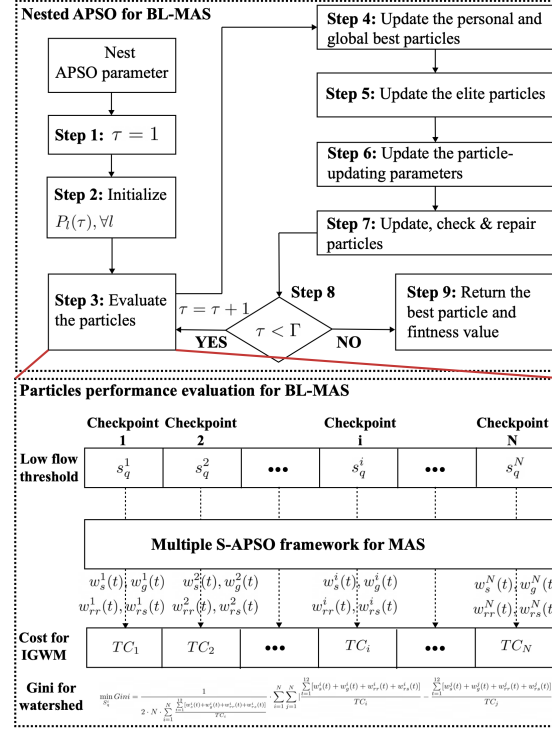


Figure F1. Flowchart diagram of the **BL-MAS**-nested S-APSO framework to bi-level multiagent system for watershed-scale IGWM

1590 *Author contributions.* MXZ designed the study, acquired the data, wrote the code, conducted the numerical experiments, analyzed the results, and prepared and revised the paper. TFMC contributed to the design of study framework, supervised the study, validated the results, and revised the paper.

Competing interests. The authors declare that they have no conflict of interest.

Acknowledgements. We thank the anonymous reviewers and editors for providing valuable suggestions and comments for improving the
1595 quality of this paper.

References

- Akhbari, M. and Grigg, N. S.: A framework for an agent-based model to manage water resources conflicts, *Water resources management*, 27, 4039–4052, 2013.
- AP, E.: *Fundamentals of computational swarm intelligence*, 2005.
- 1600 Archfield, S. A. and Vogel, R. M.: Map correlation method: Selection of a reference streamgage to estimate daily streamflow at ungaged catchments, *Water resources research*, 46, 2010.
- Askarizadeh, A., Rippey, M. A., Fletcher, T. D., Feldman, D. L., Peng, J., Bowler, P., Mehring, A. S., Winfrey, B. K., Vrugt, J. A., AghaKouchak, A., et al.: From rain tanks to catchments: use of low-impact development to address hydrologic symptoms of the urban stream syndrome, *Environmental science & technology*, 49, 11 264–11 280, 2015.
- 1605 Askew-Merwin, C.: *Natural Infrastructure’s Role in Mitigating Flooding Along the Mississippi River*, Northeast-Midwest Institute Report, 16 pp, 2020.
- Bach, P. M., McCarthy, D. T., and Deletic, A.: Can we model the implementation of water sensitive urban design in evolving cities?, *Water Science and Technology*, 71, 149–156, 2015.
- Baldwin, C. K. and Lall, U.: Seasonality of streamflow: the upper Mississippi River, *Water Resources Research*, 35, 1143–1154, 1999.
- 1610 Banks, S. C.: Agent-based modeling: A revolution?, *Proceedings of the National Academy of Sciences*, 99, 7199–7200, 2002.
- Barreteau, O. and Abrami, G.: Variable time scales, agent-based models, and role-playing games: The PIEPLUE river basin management game, *Simulation & Gaming*, 38, 364–381, 2007.
- Baumol, W. J., Baumol, W. J., Oates, W. E., Bawa, V. S., Bawa, W., Bradford, D. F., Baumol, W. J., et al.: *The theory of environmental policy*, Cambridge university press, 1988.
- 1615 Beielstein, T., Parsopoulos, K. E., and Vrahatis, M. N.: Tuning PSO parameters through sensitivity analysis, *Citeseer*, 2002.
- Bellman, R.: Dynamic programming, *Science*, 153, 34–37, 1966.
- Berger, T. and Ringler, C.: Tradeoffs, efficiency gains and technical change-Modeling water management and land use within a multiple-agent framework, *Quarterly Journal of International Agriculture*, 41, 119–144, 2002.
- Berger, T., Birner, R., McCarthy, N., Díaz, J., and Wittmer, H.: Capturing the complexity of water uses and water users within a multi-agent framework, *Water resources management*, 21, 129–148, 2007.
- 1620 Berglund, E. Z.: Using agent-based modeling for water resources planning and management, *Journal of Water Resources Planning and Management*, 141, 04015 025, 2015.
- Brannen, R., Spence, C., and Ireson, A.: Influence of shallow groundwater–surface water interactions on the hydrological connectivity and water budget of a wetland complex, *Hydrological Processes*, 29, 3862–3877, 2015.
- 1625 Chang, J.-x., Bai, T., Huang, Q., and Yang, D.-w.: Optimization of water resources utilization by PSO-GA, *Water resources management*, 27, 3525–3540, 2013.
- Chen, J., Liu, Y., Gitau, M. W., Engel, B. A., Flanagan, D. C., and Harbor, J. M.: Evaluation of the effectiveness of green infrastructure on hydrology and water quality in a combined sewer overflow community, *Science of the Total Environment*, 665, 69–79, 2019.
- Chiew, F. and McMahon, T.: Modelling runoff and diffuse pollution loads in urban areas, *Water Science and Technology*, 39, 241–248, 1999.
- 1630 Cooley, H., Phurisamban, R., and Gleick, P.: The cost of alternative urban water supply and efficiency options in California, *Environmental Research Communications*, 1, 042 001, 2019.

- Coutts, A. M., Tapper, N. J., Beringer, J., Loughnan, M., and Demuzere, M.: Watering our cities: The capacity for Water Sensitive Urban Design to support urban cooling and improve human thermal comfort in the Australian context, *Progress in physical geography*, 37, 2–28, 2013.
- 1635 Daigger, G. T.: Evolving urban water and residuals management paradigms: Water reclamation and reuse, decentralization, and resource recovery, *Water environment research*, 81, 809–823, 2009.
- Daigger, G. T. and Crawford, G. V.: Enhancing water system security and sustainability by incorporating centralized and decentralized water reclamation and reuse into urban water management systems, *Journal of Environmental Engineering and Management*, 17, 1, 2007.
- Dallman, S., Chaudhry, A. M., Muleta, M. K., and Lee, J.: The value of rain: benefit-cost analysis of rainwater harvesting systems, *Water*
- 1640 *Resources Management*, 30, 4415–4428, 2016.
- Dandy, G. C., Marchi, A., Maier, H. R., Kandulu, J., MacDonald, D. H., and Ganji, A.: An integrated framework for selecting and evaluating the performance of stormwater harvesting options to supplement existing water supply systems, *Environmental Modelling & Software*, 122, 104554, 2019.
- Darbandsari, P., Kerachian, R., Malakpour-Estalaki, S., and Khorasani, H.: An agent-based conflict resolution model for urban water re-
- 1645 *sources management*, *Sustainable Cities and Society*, 57, 102112, 2020.
- Dempe, S.: *Foundations of bilevel programming*, Springer Science & Business Media, 2002.
- Dierauer, J. R. and Zhu, C.: Drought in the twenty-first century in a water-rich region: modeling study of the Wabash River Watershed, USA, *Water*, 12, 181, 2020.
- Dietz, M. E.: Low impact development practices: A review of current research and recommendations for future directions, *Water, air, and*
- 1650 *soil pollution*, 186, 351–363, 2007.
- Du, E., Tian, Y., Cai, X., Zheng, Y., Li, X., and Zheng, C.: Exploring spatial heterogeneity and temporal dynamics of human-hydrological interactions in large river basins with intensive agriculture: A tightly coupled, fully integrated modeling approach, *Journal of Hydrology*, 591, 125313, 2020.
- Ebrahimian, A., Wadzuk, B., and Traver, R.: Evapotranspiration in green stormwater infrastructure systems, *Science of the total environment*,
- 1655 688, 797–810, 2019.
- Ellis, J. B.: Sewer infiltration/exfiltration and interactions with sewer flows and groundwater quality, in: *2nd International Conference Interactions between sewers, treatment plants and receiving waters in urban areas–Interurba II*, pp. 19–22, Citeseer, 2001.
- Ellis, J. B.: Sustainable surface water management and green infrastructure in UK urban catchment planning, *Journal of Environmental Planning and Management*, 56, 24–41, 2013.
- 1660 Endreny, T. and Collins, V.: Implications of bioretention basin spatial arrangements on stormwater recharge and groundwater mounding, *Ecological Engineering*, 35, 670–677, 2009.
- Ennenbach, M. W., Concha Larrauri, P., and Lall, U.: County-scale rainwater harvesting feasibility in the United States: Climate, collection area, density, and reuse considerations, *JAWRA Journal of the American Water Resources Association*, 54, 255–274, 2018.
- Esri: World Topographic Map, <http://www.arcgis.com/home/item.html?id=30e5fe3149c34df1ba922e6f5bbf808f> (accessed on February 19,
- 1665 2012), 2012.
- Fenicia, F., Savenije, H., Matgen, P., and Pfister, L.: Is the groundwater reservoir linear? Learning from data in hydrological modelling, *Hydrology and Earth System Sciences*, 10, 139–150, 2006.
- Fielding, K. S., Gardner, J., Leviston, Z., and Price, J.: Comparing public perceptions of alternative water sources for potable use: The case of rainwater, stormwater, desalinated water, and recycled water, *Water Resources Management*, 29, 4501–4518, 2015.

- 1670 Fletcher, T. D., Mitchell, V., Deletic, A., Ladson, T. R., and Seven, A.: Is stormwater harvesting beneficial to urban waterway environmental flows?, *Water Science and Technology*, 55, 265–272, 2007.
- Fletcher, T. D., Andrieu, H., and Hamel, P.: Understanding, management and modelling of urban hydrology and its consequences for receiving waters: A state of the art, *Advances in water resources*, 51, 261–279, 2013.
- Frost, A., Ramchurn, A., and Smith, A.: The bureau's operational AWRA landscape (AWRA-L) Model, Bureau of Meteorology Technical
1675 Report, 2016.
- Frydenberg, M.: The chain graph Markov property, *Scandinavian Journal of Statistics*, pp. 333–353, 1990.
- Garbrecht, J. and Brunner, G.: Hydrologic channel-flow routing for compound sections, *Journal of Hydraulic Engineering*, 117, 629–642, 1991.
- Gini, C.: Measurement of inequality of incomes, *The economic journal*, 31, 124–126, 1921.
- 1680 Giuliani, M. and Castelletti, A.: Assessing the value of cooperation and information exchange in large water resources systems by agent-based optimization, *Water Resources Research*, 49, 3912–3926, 2013.
- Glendenning, C., Van Ogtrop, F., Mishra, A., and Vervoort, R.: Balancing watershed and local scale impacts of rain water harvesting in India—A review, *Agricultural Water Management*, 107, 1–13, 2012.
- Golden, H. E. and Hoghooghi, N.: Green infrastructure and its catchment-scale effects: an emerging science, *Wiley Interdisciplinary Reviews: Water*, 5, e1254, 2018.
1685
- Goonrey, C. M., Perera, B., Lechte, P., Maheepala, S., and Mitchell, V. G.: A technical decision-making framework: stormwater as an alternative supply source, *Urban Water Journal*, 6, 417–429, 2009.
- Guo, Q.: Strategies for a resilient, sustainable, and equitable Mississippi River basin, *River*, 2, 336–349, 2023.
- Guo, T., Englehardt, J., and Wu, T.: Review of cost versus scale: water and wastewater treatment and reuse processes, *Water Science and Technology*, 69, 223–234, 2014.
1690
- Gupta, H. V., Sorooshian, S., and Yapo, P. O.: Status of automatic calibration for hydrologic models: Comparison with multilevel expert calibration, *Journal of hydrologic engineering*, 4, 135–143, 1999.
- Hardy, M., Kuczera, G., and Coombes, P.: Integrated urban water cycle management: the UrbanCycle model, *Water science and technology*, 52, 1–9, 2005.
- 1695 He, X.: Droughts and Floods in a Changing Environment Natural Influences, Human Interventions, and Policy Implications, Ph.D. thesis, Princeton University, 2019.
- Houle, J. J., Roseen, R. M., Ballesterio, T. P., Puls, T. A., and Sherrard Jr, J.: Comparison of maintenance cost, labor demands, and system performance for LID and conventional stormwater management, *Journal of environmental engineering*, 139, 932–938, 2013.
- Hu, Z., Wei, C., Yao, L., Li, L., and Li, C.: A multi-objective optimization model with conditional value-at-risk constraints for water allocation equality, *Journal of Hydrology*, 542, 330–342, 2016.
1700
- Hung, F. and Yang, Y. E.: Assessing adaptive irrigation impacts on water scarcity in nonstationary environments—a multi-agent reinforcement learning approach, *Water Resources Research*, 57, e2020WR029 262, 2021.
- Jang, J.-S. R., Sun, C.-T., and Mizutani, E.: Neuro-fuzzy and soft computing-a computational approach to learning and machine intelligence [Book Review], *IEEE Transactions on automatic control*, 42, 1482–1484, 1997.
- 1705 Jayasooriya, V. and Ng, A.: Tools for modeling of stormwater management and economics of green infrastructure practices: a review, *Water, Air, & Soil Pollution*, 225, 1–20, 2014.

- Kallis, G.: Coevolution in water resource development: The vicious cycle of water supply and demand in Athens, Greece, *Ecological Economics*, 69, 796–809, 2010.
- Kanta, L. and Zechman, E.: Complex adaptive systems framework to assess supply-side and demand-side management for urban water resources, *Journal of Water Resources Planning and Management*, 140, 75–85, 2014.
- Kennedy, J. and Eberhart, R.: Particle swarm optimization, in: *Proceedings of ICNN'95-international conference on neural networks*, vol. 4, pp. 1942–1948, IEEE, 1995.
- Kenway, S., Gregory, A., and McMahon, J.: Urban water mass balance analysis, *Journal of Industrial Ecology*, 15, 693–706, 2011.
- Khorshidi, M. S., Izady, A., Nikoo, M. R., Al-Maktoumi, A., Chen, M., and Gandomi, A. H.: An Agent-based Framework for Transition from Traditional to Advanced Water Supply Systems in Arid Regions, *Water Resources Management*, 38, 2565–2579, 2024.
- Kim, J. E., Humphrey, D., and Hofman, J.: Evaluation of harvesting urban water resources for sustainable water management: Case study in Filton Airfield, UK, *Journal of Environmental Management*, 322, 116 049, 2022.
- Kirshen, P. H., Larsen, A. L., Vogel, R. M., and Moomaw, W.: Lack of influence of climate on present cost of water supply in the USA, *water Policy*, 6, 269–279, 2004.
- Kling, H., Fuchs, M., and Paulin, M.: Runoff conditions in the upper Danube basin under an ensemble of climate change scenarios, *Journal of hydrology*, 424, 264–277, 2012.
- Kock, B. E.: Agent-based models of socio-hydrological systems for exploring the institutional dynamics of water resources conflict, Ph.D. thesis, Massachusetts Institute of Technology, 2008.
- Langevin, C. D., Hughes, J. D., Banta, E. R., Niswonger, R. G., Panday, S., and Provost, A. M.: Documentation for the MODFLOW 6 groundwater flow model, Tech. rep., US Geological Survey, 2017.
- Last, E. W.: City water balance: a new scoping tool for integrated urban water management options, Ph.D. thesis, University of Birmingham, 2011.
- Li, H., Ding, L., Ren, M., Li, C., and Wang, H.: Sponge city construction in China: A survey of the challenges and opportunities, *Water*, 9, 594, 2017.
- Liang, J. J., Qin, A. K., Suganthan, P. N., and Baskar, S.: Comprehensive learning particle swarm optimizer for global optimization of multimodal functions, *IEEE transactions on evolutionary computation*, 10, 281–295, 2006.
- Likas, A., Vlassis, N., and Verbeek, J. J.: The global k-means clustering algorithm, *Pattern recognition*, 36, 451–461, 2003.
- Lin, Z., Lim, S. H., Lin, T., and Borders, M.: Using agent-based modeling for water resources management in the Bakken Region, *Journal of Water Resources Planning and Management*, 146, 05019 020, 2020.
- Loucks, D. P. and Van Beek, E.: *Water resource systems planning and management: An introduction to methods, models, and applications*, Springer, 2017.
- Lu, E., Takle, E. S., and Manoj, J.: The relationships between climatic and hydrological changes in the upper Mississippi River basin: A SWAT and multi-GCM study, *Journal of Hydrometeorology*, 11, 437–451, 2010.
- Marquardt, D. W.: An algorithm for least-squares estimation of nonlinear parameters, *Journal of the society for Industrial and Applied Mathematics*, 11, 431–441, 1963.
- McArdle, P., Gleeson, J., Hammond, T., Heslop, E., Holden, R., and Kuczera, G.: Centralised urban stormwater harvesting for potable reuse, *Water Science and Technology*, 63, 16–24, 2011.
- McDonald, R. I., Weber, K., Padowski, J., Flörke, M., Schneider, C., Green, P. A., Gleeson, T., Eckman, S., Lehner, B., Balk, D., et al.: Water on an urban planet: Urbanization and the reach of urban water infrastructure, *Global environmental change*, 27, 96–105, 2014.

- 1745 Meng, X.: Understanding the effects of site-scale water-sensitive urban design (WSUD) in the urban water cycle: a review, *Blue-Green Systems*, 4, 45–57, 2022.
- Mitchell, V. G., Mein, R. G., and McMahon, T. A.: Modelling the urban water cycle, *Environmental modelling & software*, 16, 615–629, 2001.
- Montalto, F. A., Bartrand, T. A., Waldman, A. M., Travaline, K. A., Loomis, C. H., McAfee, C., Geldi, J. M., Riggall, G. J., and Boles, L. M.:
1750 Decentralised green infrastructure: the importance of stakeholder behaviour in determining spatial and temporal outcomes, *Structure and Infrastructure Engineering*, 9, 1187–1205, 2013.
- Moravej, M., Renouf, M. A., Lam, K. L., Kenway, S. J., and Urich, C.: Site-scale Urban Water Mass Balance Assessment (SUWMBA) to quantify water performance of urban design-technology-environment configurations, *Water Research*, 188, 116477, 2021.
- Motlaghzadeh, K., Eyni, A., Behboudian, M., Pourmoghim, P., Ashrafi, S., Kerachian, R., and Hipel, K. W.: A multi-agent decision-making
1755 framework for evaluating water and environmental resources management scenarios under climate change, *Science of The Total Environment*, 864, 161060, 2023.
- Müller, M. F., Müller-Itten, M. C., and Gorelick, S. M.: How Jordan and Saudi Arabia are avoiding a tragedy of the commons over shared groundwater, *Water Resources Research*, 53, 5451–5468, 2017.
- Nash, J. E. and Sutcliffe, J. V.: River flow forecasting through conceptual models part I—A discussion of principles, *Journal of hydrology*,
1760 10, 282–290, 1970.
- Nicklow, J., Reed, P., Savic, D., Dessalegne, T., Harrell, L., Chan-Hilton, A., Karamouz, M., Minsker, B., Ostfeld, A., Singh, A., et al.: State of the art for genetic algorithms and beyond in water resources planning and management, *Journal of Water Resources Planning and Management*, 136, 412–432, 2010.
- Nishi, A., Shirado, H., Rand, D. G., and Christakis, N. A.: Inequality and visibility of wealth in experimental social networks, *Nature*, 526,
1765 426–429, 2015.
- Nix, H. and Rouhi Rad, M.: Water Withdrawal Regulation in South Carolina, <https://lpress.clemson.edu/publication/water-withdrawal-regulation-in-south-carolina/>, 2022.
- Palla, A. and Gnecco, I.: Hydrologic modeling of Low Impact Development systems at the urban catchment scale, *Journal of hydrology*, 528, 361–368, 2015.
- 1770 Parsapour-Moghaddam, P., Abed-Elmdoust, A., and Kerachian, R.: A heuristic evolutionary game theoretic methodology for conjunctive use of surface and groundwater resources, *Water Resources Management*, 29, 3905–3918, 2015.
- Poustie, M. S., Deletic, A., Brown, R. R., Wong, T., de Haan, F. J., and Skinner, R.: Sustainable urban water futures in developing countries: the centralised, decentralised or hybrid dilemma, *Urban Water Journal*, 12, 543–558, 2015.
- Prior, C. H., Schneider, R., and Durum, W. H.: *Water Resources of the Minneapolis-St. Paul Area, Minnesota*, vol. 274, US Geological
1775 Survey, 1953.
- Ravazzani, G., Corbari, C., Morella, S., Gianoli, P., and Mancini, M.: Modified Hargreaves-Samani equation for the assessment of reference evapotranspiration in Alpine river basins, *Journal of irrigation and drainage engineering*, 138, 592–599, 2012.
- Reed, T., Mason, L. R., and Ekenga, C. C.: Adapting to climate change in the upper Mississippi river basin: exploring stakeholder perspectives on river system management and flood risk reduction, *Environmental Health Insights*, 14, 1178630220984153, 2020.
- 1780 Reeves, H. W. and Zellner, M. L.: Linking MODFLOW with an agent-based land-use model to support decision making, *Groundwater*, 48, 649–660, 2010.

- Riget, J. and Vesterstrøm, J. S.: A diversity-guided particle swarm optimizer-the ARPSO, Dept. Comput. Sci., Univ. of Aarhus, Aarhus, Denmark, Tech. Rep. 2, 2002, 2002.
- Rosegrant, M. W., Ringler, C., McKinney, D. C., Cai, X., Keller, A., and Donoso, G.: Integrated economic-hydrologic water modeling at the basin scale: The Maipo River basin, *Agricultural economics*, 24, 33–46, 2000.
- Rozos, E., Makropoulos, C., and Butler, D.: Design robustness of local water-recycling schemes, *Journal of Water Resources Planning and Management*, 136, 531–538, 2010.
- Sapkota, M., Arora, M., Malano, H., Moglia, M., Sharma, A., George, B., and Pamminger, F.: An overview of hybrid water supply systems in the context of urban water management: Challenges and opportunities, *Water*, 7, 153–174, 2014.
- Schewe, J., Heinke, J., Gerten, D., Haddeland, I., Arnell, N. W., Clark, D. B., Dankers, R., Eisner, S., Fekete, B. M., Colón-González, F. J., et al.: Multimodel assessment of water scarcity under climate change, *Proceedings of the National Academy of Sciences*, 111, 3245–3250, 2014.
- Sharma, S. K., Tignath, S., Gajbhiye, S., and Patil, R.: Use of geographical information system in hypsometric analysis of Kanhiya Nala watershed, *Int J Remote Sens Geosci*, 2, 30–35, 2013.
- Simaan, M. and Cruz, J. B.: On the Stackelberg strategy in nonzero-sum games, *Journal of Optimization Theory and Applications*, 11, 533–555, 1973.
- Sitzenfrei, R., Möderl, M., and Rauch, W.: Assessing the impact of transitions from centralised to decentralised water solutions on existing infrastructures—Integrated city-scale analysis with VIBe, *Water research*, 47, 7251–7263, 2013.
- Souto, S. L., Reis, R. P. A., and Campos, M. A. S.: Impact of Installing Rainwater Harvesting System on Urban Water Management, *Water Resources Management*, pp. 1–18, 2022.
- Steffen, J., Jensen, M., Pomeroy, C. A., and Burian, S. J.: Water supply and stormwater management benefits of residential rainwater harvesting in US cities, *JAWRA Journal of the American Water Resources Association*, 49, 810–824, 2013.
- U.S. Census Bureau, U.: Census Cartographic Boundary Files, 2018 vintage, <https://library.metatab.org/census.gov-boundaries-2018-1.2.8/index.html>, 2018.
- U.S. Geological Survey, U.: Watershed Boundary Dataset (WBD), <https://www.usgs.gov/national-hydrography/watershed-boundary-dataset> (accessed on July 20, 2021), 2021.
- Van Dijk, A. and Bruijnzeel, L.: Modelling rainfall interception by vegetation of variable density using an adapted analytical model. Part 1. Model description, *Journal of Hydrology*, 247, 230–238, 2001.
- Viney, N., Vaze, J., Crosbie, R., Wang, B., Dawes, W., and Frost, A.: AWRA-L v5. 0: Technical description of model algorithms and inputs, Publisher: CSIRO. doi: <https://doi.org/10.4225/08/58518bc790ff7>, 2015.
- Von Stackelberg, H.: Market structure and equilibrium, Springer Science & Business Media, 2010.
- Weinmann, P. E. and Laurenson, E. M.: Approximate flood routing methods: A review, *Journal of the Hydraulics Division*, 105, 1521–1536, 1979.
- Wolf, L.: Assessing the influence of leaky sewer systems on groundwater resources beneath the City of Rastatt, Germany Department of Applied Geology. Karlsruhe, University of Karlsruhe, Ph.D. thesis, PhD Thesis, 2006.
- Xu, J., Zhang, M., and Zeng, Z.: Hybrid nested particle swarm optimization for a waste load allocation problem in river system, *Journal of Water Resources Planning and Management*, 142, 04016014, 2016.
- Xu, J., Lv, C., Yao, L., and Hou, S.: Intergenerational equity based optimal water allocation for sustainable development: A case study on the upper reaches of Minjiang River, China, *Journal of Hydrology*, 568, 835–848, 2019.

- 1820 Yang, Y.-C. E., Cai, X., and Stipanović, D. M.: A decentralized optimization algorithm for multiagent system-based watershed management, *Water resources research*, 45, 2009.
- Zhan, W. and Chui, T. F. M.: Evaluating the life cycle net benefit of low impact development in a city, *Urban Forestry & Urban Greening*, 20, 295–304, 2016.
- Zhan, Z.-H., Zhang, J., Li, Y., and Chung, H. S.-H.: Adaptive particle swarm optimization, *IEEE Transactions on Systems, Man, and Cyber-*
1825 *netics, Part B (Cybernetics)*, 39, 1362–1381, 2009.
- Zhang, K. and Chui, T. F. M.: A review on implementing infiltration-based green infrastructure in shallow groundwater environments: Challenges, approaches, and progress, *Journal of Hydrology*, 579, 124 089, 2019.
- Zhou, Q.: A review of sustainable urban drainage systems considering the climate change and urbanization impacts, *Water*, 6, 976–992, 2014.